ISAS - INTERNATIONAL SCHOOL
FOR ADVANCED STUDIES

MARKARIAN GALAXIES

by

Cong Xu

A thesis submitted for the degree

of *Doctor Philosophiae*

Trieste – October 1988

Supervisers:

Prof. Gianfranco De Zotti

Prof. Dennis Sciama

SISSA - SCUOLA
INTERNAZIONALE
SUPERIORE
DI STUDI AVANZATI
TRIESTE
Strada Costiera 11

TRIESTE

MARKARIAN GALAXIES

by

Cong Xu

A thesis submitted for the degree

of *Doctor Philosophiae*

Trieste – October 1988

Supervisers:

Prof. Gianfranco De Zotti

Prof. Dennis Sciama

天長地久天地所以能長且
久者以其不自生故能長生

Heaven and earth last forever.
Why do heaven and earth last forever?
They are unborn.
So ever living.

Lao Tsu (6th B. C.): in *"Tao Te Ching"*

Contents

Acknowledgements

My greatest debt of gratitude is due to Gianfranco De Zotti, my supervisor, from whom I have learned how to do research. His excellent guidance was necessary for every achievement in this thesis.

Special thanks are due to Alberto Franceschini and Luigi Danese, for their help, and for a fruitful collaboration.

I am also very grateful to Dennis Sciama, George Ellis, Marek Abramowicz, Massimo Calvani, and John Miller, for their support, advice and encouragement.

I acknowledge Prof. M. Huck, and Prof. G. Sedmak, for allowing me to use the VAX computer in Osservatorio di Trieste.

I benefited from discussions with my colleagues and friends Gabriele Ghisellini, Ewa Szuszkiewicz, Vincenzo Antonuccio, and Roberto Scaramella.

The last and deepest thanks are owed to my wife, Yihong, who typed the greatest part of this thesis. Without her help and encouragement, especially at the most difficult times, the thesis could never have been completed.

This thesis is dedicated to the memory of my father.

Chapter 1
Introduction

1.1. The Markarian Survey

Beginning in the mid-1960s and continuing through 1978, the first large-scale objective prism survey for galaxies with blue and ultraviolet excess in their continuum radiation was conducted by Markarian, Lipovetskii and Stepanian (Markarian 1967, 1969; Markarian and Lipovetskii 1971, 1972, 1973, 1974, 1976a, 1976b; Markarian, Lipovetskii and Stepanian 1977a, 1977b, 1979a, 1979b, 1979c, 1981, here after Lists I—XV). The observations were obtained using primarily a 1°.5 objective prism with the 40—52 inch (1.0—1.3 m) Schmidt telescope of the Byurakan Astrophysical Observatory. Their setup produced an inverse dispersion of 2500 Å/mm at H_β (Markarian 1967). The low-dispersion objective-prism was used with Kodak II a-F plates to detect faint galaxies with relatively strong blue and ultraviolet continuum radiation. Although many of the selected galaxies also displayed visible emission lines on the plates, the primary selection criterion was the presence of the ultraviolet excess in the continuum. The complete Markarian Survey covers 15,200 square degrees (4.6 steradians) north of $-15°$ declination, excluding regions within 15°—20° of the Galactic plane. The results of the survey were reported in 15 lists (Lists I — XV), containing on the whole 1500 sources. Among them, 24 were identified as Galactic stars or probable stars (Mazzarella and Balzano 1986, here after MB86). Fig. 1.1 (taken from MB86) contains an all-sky Hammer-Aitoff projection of the entire Markarian survey in Galactic coordinates (l, b).

There is no well defined limiting magnitude to which the Markarian survey is complete. MB86 list two reasons for this. First, the limiting magnitude varies with the observing conditions and the emulsion densities of the objective-prism plates. Second, the types of objects discovered vary greatly in surface

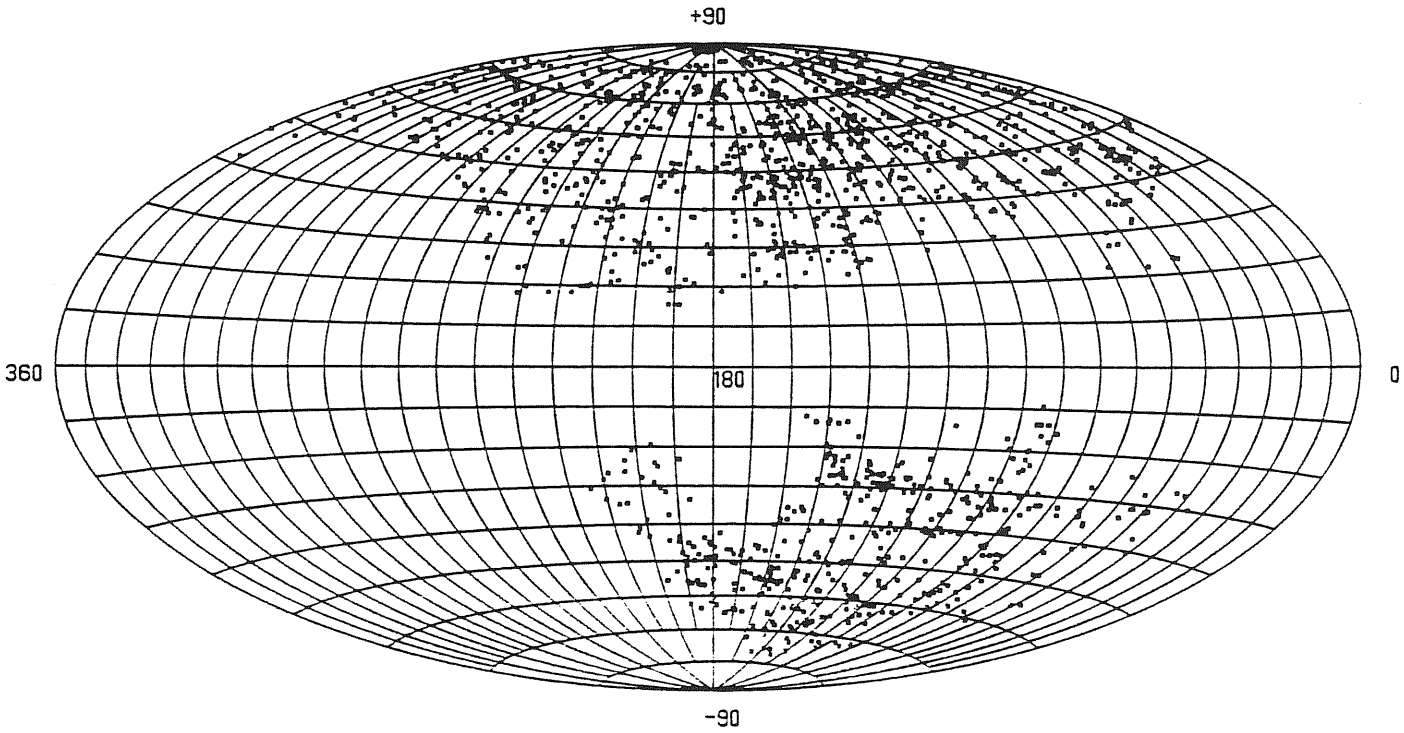

FIG. 1.—An all-sky Hammer-Aitoff projection of the Markarian objects in Galactic coordinates (l, b)

Fig. 1.1. Taken from Fig. 1. of MB86.

brightness, so the limiting magnitude varies with different types of objects in the lists. The second problem mentioned by MB86, however, might not be terribly serious. Although a wide range of galaxy types is represented in the Markarian survey, judging from Table 4 of Huchra (1977a, hereafter H77a), the dependence of blue surface brightness (BSB) of Markarian galaxies on galaxy type is significantly weaker than for normal field galaxies. From BSB data for 197 Markarian galaxies reported by H77a, I find a mean $BSB = 21.36 \pm 0.43\ mag/arcsec^2$. The dispersion is not very different from that for field disk galaxies (Freeman (1970) obtained a mean BSB of $21.65 \pm 0.30\ mag/arcsec^2$ for 27 disk galaxies, while Schweizer (1976) got $\langle BSB \rangle = 21.67 \pm 0.35\ mag/arcsec^2$ for 6 disk galaxies).

On the other hand, Xu et al. (1988) in their study of surface density of bright Markarian galaxies ($m_{Zw} \leq 14.5$) found a strong excess of low surface density sub-regions over expectations from a Poisson distribution. Such excess is most easily interpreted as due to poor coverage of some areas of the sky.

According to Markarian, Lipovetskii and Stepanian (1981), the limiting magnitude of the Markarian survey is roughly in the range 16.5—17.5 mag. However, the V/V_{max} test and the $d\log N/d\log S$ test carried out by MB86 revealed that the survey is complete only down to 15.2 mag (see also Xu et al. 1988). It must also recalled that most galaxies brighter than 13 mag were deliberately excluded from the Markarian Survey (Markarian 1967), partly because of the difficulty in distinguishing abnormal from normal cases, and partly because a list of bright galaxies with anomalous spectral features was published previously (Markarian 1963).

1.2. Markarian Objects

a. Content of the Markarian lists

A thorough study on the content of the 15 Markarian lists was done by MB86. Here I will summarized their main results.

As pointed out above, 24 of the 1500 sources listed in the 15 Markarian lists are stars or possible stars. There are three duplications among the remaining sources: Mkr 107 = Mkr 20, Mkr 1318 = Mkr 49, Mkr 590=Mkr 503. Of the 1473 extragalactic objects, 5 are classified, according to MB86, as QSO's (Mkr 132, 380, 586, 679, 992), 3 as BL Lac objects (Mkr 180, 421, 501), one 115 as Seyfert 1 (including intermediate types), and 43 as Seyfert 2 galaxies. In fact the Markarian survey turned out to be remarkably successful in finding Seyfert 1 galaxies. On the other hand, it has probably missed a large fraction of type 2 Seyferts, which have a relatively weak ultraviolet continuum (Lawrence 1986, and references therein).

Although the majority of Markarian objects still lack spectral classification, it has been established by early studies (see, in particular, Huchra 1977a) that those emitting significant non-thermal continua from their nuclei (QSO's, Seyferts, BL Lac's) comprise only $\simeq 10\%$ of the total. The strong blue and UV continua are mostly of thermal origin, as indicated by the narrow, low-ionization emission lines, and appear to be due to a large population of hot, young stars. It is estimated that $\simeq 40\%$ of Markarian galaxies are experiencing a short-lived outburst of star-formation confined to the nuclear region ('starburst galaxies': Weedman 1983; Balzano 1983). Galaxies with emission line spectra similar to HII regions and emission not necessary confined to the nucleus are usually referred to as 'HII galaxies' (French 1980). Fig. 1.2 (taken from MB86) displays the frequencies of the various types of Markarian galaxies for which spectral classification is available. It should be stressed that the quoted numbers may represent lower limits to the actual numbers of each type of galaxies in the entire Markarian survey, since most galaxies are still unclassified. While the bulk of QSO's, BL Lac objects and Seyfert galaxies have probably been identified in the 15 lists, the identification of starburst galaxies or HII region galaxies is still strongly incomplete.

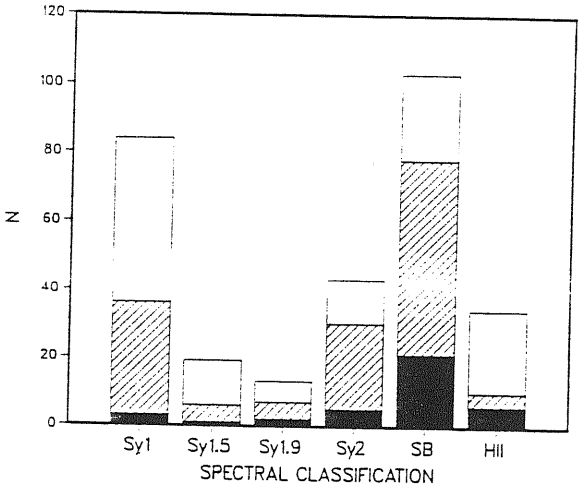

FIG. 7

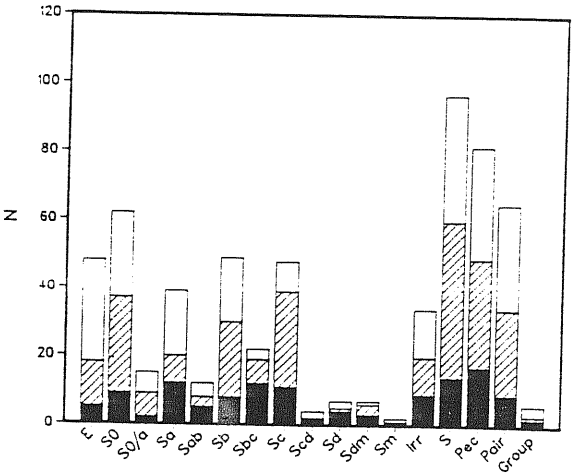

FIG. 8

FIG. 7.—Distribution of current spectral classifications in the catalog. These numbers are lower limits to the total number of each type of active galaxy in the Markarian sample because many objects have not been examined in detail. The third bar labeled "Sy1.9" represents the combined sample of 5 Seyfert 1.8 and 7 Seyfert 1.9 galaxies. The hatched region in each bar indicates the number of galaxies with tentative 60 μm *IRAS* detections, and the darkened region indicates the number with $S(60\ \mu\text{m}) > 2$ Jy.

FIG. 8.—Distribution of known morphological types. The hatched and darkened regions indicate the number of objects with 60 μm *IRAS* detections and the number with $S(60\ \mu\text{m}) > 2$ Jy, respectively.

Fig. 1.2. Taken from Fig. 7. of MB86.

Fig. 1.3. Taken from Fig. 8. of MB86.

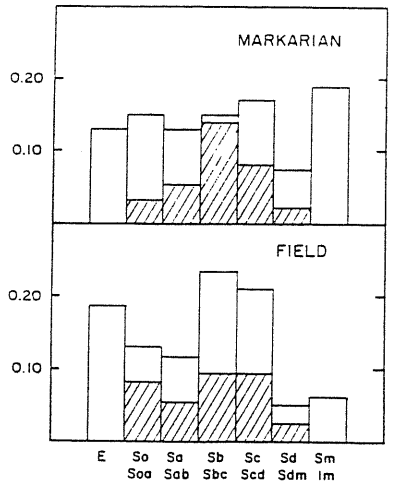

FIG. 6.—The distribution of morphological types of Markarian and field galaxies. Sample size has been normalized to unity.

Fig. 1.4.
Taken from Fig. 6 of H77a.

b. Morphological Distribution

The frequency of each morphological type among the classified Markarian galaxies is given in Fig. 1.3, again taken from MB86. The first 12 bars follow the Hubble sequence, and the remaining bars are for special types found to be very common in the survey. Among the non-stellar objects, 349 have well defined Hubble types, 97 are unclassified spiral galaxies, 379 are 'compact' in the sense of Zwicky (1971), 82 are peculiar, 65 seem to be close pairs, and six are tight groups of galaxies.

The above morphological distribution along Hubble types may be biased since it is not drawn from a complete sample. I would like to review another morphological study conducted by H77a, based on a complete sample comprising the 91 Markarian galaxies in the first 7 Markarian lists with apparent photographic magnitude $\leq$ 14.0. The morphological classification was made from a photographic survey plus available material from other sources. Seventy percent of the classifications have been made on the basis of large-scale ($15''.5/mm$) photographic plates taken with a 40mm ITT F4539 S20 image tube (10%) or a 90mm ITT F4092 S25 image tube (60%) in the bandpass between 6000 Åand 7500 Åwith 1.5m Palomar telescope. Twenty per cent have been classified on the basis of 1.2m Palomar Schmidt plates ($67''.5/mm$) taken mostly in the blue, and the remaining 10% have been classified using material in the Arp atlas (Arp 1966) or the Palomar Sky Survey plates, or classifications given in de Vaucouleurs and de Vaucouleurs (1964,) Kalloghlian (1971), and Borngen and Kalloghlian (1975). Fig. 1.4 (taken from Huchra 1977a) compares the resulting morphological distribution with that of 255 field-galaxies brighter than $m_{pg} = 11.75$ in the sample of Schechter (1973). The cross hatched areas in the S0 to Sdm bins indicate the fraction of barred galaxies. There is obviously an excess of late type galaxies in Markarian lists, compared with the normal field galaxy sample.

c. Redshift and Magnitude Distributions

The velocity distribution of extra-galactic Markarian objects with known redshifts is given in Fig. 1.5 (taken from MB86). The plotted redshifts are heliocentric. Of the 1228 objects with measured redshifts, the only objects with $Z > 0.1$ (not included in the distribution) are Mkr 64, 106, 132, 380, 679, 830, 992, 1014, and 1269. All these 9 objects are QSO's or Sy1's.

The distribution of apparent magnitudes for all 1473 non-stellar objects is given in Fig. 1.6 (taken from MB86). Among them, 843 are Zwicky magnitudes (Zwicky et al. 1961—1968, Zwicky 1971), 128 are photometric (B) magnitudes taken from the literature (MB86, and reference therein), and others (339) are eye-estimates by Markarian and his collaborators (lists I — XV). As mentioned above, the $\langle V/V_m \rangle$ test by MB86 found that the Markarian survey is no longer complete beyond $m = 15.2$. The peak in their apparent magnitude distribution is at about 15.5. Fig. 1.7 (taken from MB86) shows the absolute magnitude distribution of the 1228 objects with known redshifts.

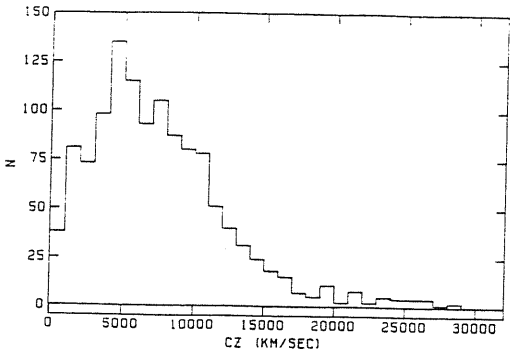

FIG. 2.—Velocity distribution of Markarian galaxies. The total number of available redshifts at the time of writing is 1228. There are only nine galaxies with $cz > 30{,}000$ km s^{-1}. See text.

Fig. 1.5. Taken from Fig. 2. of MB86.

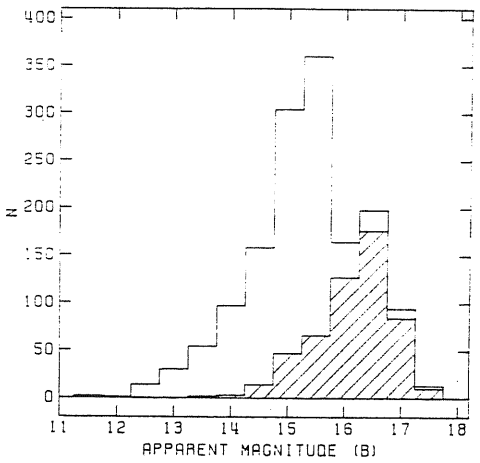

FIG. 3.—Distribution of apparent magnitudes. The unshaded distribution includes all magnitude types, and the hatched region indicates the distribution of the Markarian *et al.* magnitude estimates.

Fig. 1.6. Taken from Fig. 3. of MB86.

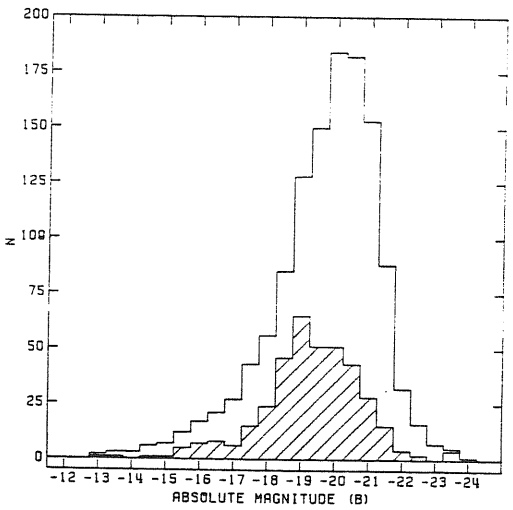

FIG. 5.—Distribution of absolute magnitudes. The unshaded histogram includes all magnitude types, and the hatched region indicates the distribution of the absolute magnitudes calculated using the Markarian *et al.* apparent magnitude estimates.

Fig. 1.7. Taken from Fig. 5. of MB86 ($H_0 = 75$).

Chapter 2
Non-Seyfert Markarian Galaxies

Markarian (1967) pointed out that the objects found in his survey formed a new category of galaxies with relatively blue central regions and spectral parameters similar to those of relatively early classes (A and F). Contrariwise, the cores of E to Sb galaxies are generally quite red and have spectra of the G and K types. He concluded that the diffuse galaxies in his lists are associations of stars and gas, but the 'stellar' objects—galaxies with bright nuclei—require a non-thermal energy source.

On the other hand, Weedman (1973) found that Markarian Seyferts and Markarian non-Seyfert galaxies (including 'stellar' objects) formed two separated distributions in the $U-B$ vs. $B-V$ diagram (Fig. 1.8). He suggested that different energy-input mechanisms were operating in Seyfert and non-Seyfert galaxies, and that strong non-thermal activity did not occur in non-Seyfert galaxies.

Huchra (1977a) carried out a comprehensive UBV photometric study of Markarian galaxies. His 'complete photometric sample' (91 objects) includes all galaxies in the first 7 Markarian lists with apparent photographic magnitude < 16.0 and absolute magnitude > -20.35. After correcting the photometric data for absorption within our own Galaxy and for aperture, he found that the Markarian galaxies (name given by Huchra to non-Seyfert galaxies in Markarian lists) locate, in the $U-B$ vs. $B-V$ diagram, in a region bluer than that occupied by ordinary field galaxies and have a larger dispersion. When Markarians are classified morphologically, he found that Markarian galaxies are generally blue for their type, with early type (elliptical, S0, Sa, Sb) Markarians falling in the region of the two-color diagram of field galaxies of the same morphological types, and late type (Sbc–Im) Markarians being consistently bluer than late

type field galaxies, although a significant overlap occurs. He concluded that there is no evidence for strong non-thermal sources in these objects; and their optical emission can be modeled with only stars and hot gas ionized by stars (Huchra 1977b).

The intrinsic difference between Markarian non-Seyfert galaxies and Seyferts was also noted by early spectroscopic studies. Two low resolution (190Å/mm) spectroscopic surveys of the first and second Markarian lists were carried out by Sargent (1970, 1972). Thirty objects in the first list were observed in the first survey. Emission lines were detected on the spectra of 26. Two of them were identified as Seyfert galaxies. Others showed sharp emission line spectra resembling those of galactic HII regions. He tentatively concluded that these objects were excited by hot stars, and most of them were not likely to have a Seyfert nucleus. The conclusion was confirmed by the second survey. Of the eighty objects, taken from the second Markarian list, that were observed, sixty-eight displayed emission lines. A sub-group of those exhibited particularly remarkable properties: they are dwarf galaxies with low absolute luminosities, strong and highly excited emission lines of very sharp profiles, and are free from absorption lines. As will be discussed below, these sources are now known as compact blue galaxies (CBG).

In an optical and infrared spectrophotometric study of 18 Markarian galaxies, Neugebauer et al. (1976) found that the 10 Markarian non-Seyfert galaxies in their sample show typical HII–region-like emission line spectra.

By now, it is well established that the strong emission lines showed in the vast majority of non-Seyfert Markarian galaxies are of thermal origin, and are indicative of violent outbursts of star-formations (French 1980; Thuan and Martin 1981; Feldman et al. 1982; Balzano 1983).

Non-Seyfert Markarians are usefully subdivided into 5 classes: (1) galaxies with 'starburst' nuclei ('starburst galaxies', Balzano 1983); (2) compact blue

galaxies (Thuan and Martin 1981), which are also referred to as 'extragalactic HII regions' (Sargent and Searle 1970); (3) clumpy irregulars (Heidmann et al. 1982); (4) interacting/peculiar galaxies; (5) others.

In the following we will summarize the main properties of each class.

2.1. Starburst Galaxies (SBG)

As mentioned in Section 1.2.a., the defining property of starburst galaxies is the presence of a large outburst of star-formation, confined to the nuclear region, resulting in the appearance of about 10^7—10^9 $M_\odot$ of hot, blue stars (Balzano 1983, hereafter B83). Their optical morphology is similar to that of Seyfert galaxies, with the dominant feature often being a bright, starlike nucleus. Balmer line luminosities are also in the same general range as those of Seyferts (B83). However they have spectral properties that allow to identify them as a well defined class. Their emission lines are very sharp and symmetric (with approximately Gaussian profiles). Usually the full width at half-maximum (FWHM) is less than 250 km/sec (B83); Feldman et al. (1982) found a median FWHM of 160 km/sec, corresponding to a median velocity dispersion $\sigma \simeq 68$ km/sec (σ = FWHM/2.35). A comparison with the median velocity dispersion of normal spiral nuclei (σ = 150 km/sec, Whitmore, Kirshner, and Schechter 1979; Whitmore and Kirshner 1981), suggests that the young star population is not in dynamical equilibrium with the original nuclear contents.

Using one of the diagnostics suggested by Baldwin et al. (1981), exploiting the line ratios $[NII]6584/H_\alpha$ vs. $[OIII]5007/H_\beta$, B83 showed that data points of most starburst galaxies locate in or close to the low-excitation end of the area specified by galactic HII regions, suggesting that photoionization by hot stars is very likely the primary energy-input mechanism. Starburst galaxies generally have $[OIII]5007/H_\beta < 3$ and $0.2 < [NII]6584/H_\alpha < 0.5$ (see also Shuder

and Osterbrock 1981). Their H_α luminosity is in the range $10^{40} < L(H_\alpha) < 6 \times 10^{42}\ erg/sec$ ($H_0 = 75$: B83).

From a study for a sample comprising 99 Markarian starburst galaxies plus three NGC starburst galaxies, Balzano (1983) found that, unlike Markarian galaxies on the whole which have a broad morphological distribution (H77a), Markarian starburst galaxies have a pronounced peak at the Sb/Sbc type ($\simeq$35%) with quite symmetric wings toward early (E) and late (Im) types. The fraction of barred galaxies as a function of morphological type is similar to that of Markarian galaxies in general. In particular, all Balzano's starburst galaxies of Sb–Sbc types are barred. As was noticed by H77a for Markarian galaxies on the whole, a strong excess, in comparison to normal field galaxies, of barred types also happens among Sb–Sc Markarian starburst galaxies. The fraction of barred galaxies for other morphological types is not significantly different from that of normal field galaxies. B83 estimated that ($\simeq$ 30%) of Markarian starburst galaxies show evidences of interactions with other objects and/or of mergers; this fraction is much higher than that found for normal galaxies ($\simeq$ 10%, H77a).

In the H77a sample of Markarian galaxies, I found 36 objects classified as starburst galaxies by B83. For them, the data reported by H77a give $\angle B-V\rangle = 0.60 \pm 0.12$ and $\langle U - B\rangle = -0.11 \pm 0.20$. These values are essentially equal to those for Markarian galaxies on the whole, $\langle B - V\rangle = 0.57$ and $\langle U - B\rangle = -0.11$ (H77a), but are slightly bluer than those of Markarian Sb/Sbc galaxies: $\langle B - V\rangle = 0.70$ and $\langle U - B\rangle = 0.06$. For comparison, the mean colors of field galaxies are $B - V = 0.79$ and $U - B = 0.23$ (H77a).

It has long been known that QSOs and Seyferts show near-infrared excesses, i.e. large $J - K$ (> 1.1: Rieke and Low 1972; Rieke and Lebofsky 1979; Balzano and Weedman 1981). Do starburst nuclei show similar properties?

The answer is no. B83 found that the distribution of $J-K$ and $J-H$ colors of starburst nuclei is very similar to that of nuclei of bright NGC galaxies and of normal E and S0 galaxies (Frogel et al. 1978): $\langle J-H\rangle = 0.70 \pm 0.06$, $\langle J-K\rangle = 1.02 \pm 0.12$. She concluded that for starburst nuclei, the near-infrared light comes primarily from a cool, old star population, as is the case for normal nuclei of galaxies. On the other hand, from the Fig. 6 of B83, I find that the distributions of $J-K$ of starburst nuclei has a slightly larger dispersion than that of normal galactic nuclei. A similar situation was found by Cutri and McAlary (1985) for interacting galaxies. This can be explained as a weak influence of the starburst activity on the near-infrared properties of nuclei, due either to radiation from dust, or to radiation from red supergiants.

A near-IR color criterion for distinguishing starburst nuclei from Seyfert nuclei was proposed by Balzano and Weedman (1981): most nuclei with $J-K < 1.1$ are starbursts, while those with $J-K > 1.1$ are mostly Seyferts (the mean $J-K$ of Seyferts is $\simeq 1.5$: Balzano and Weedman 1981).

Lawrence et al. (1985) carried out ground-based infrared observations (from 1 to 20 μm) of low-level active galactic nuclei (Seyfert 2's, star-forming galaxies, LINERs) in spiral galaxies. There are 6 starburst nuclei in the sample, all of which were found to have a mid-infrared spectrum similar to that of NGC 5461, a prototype extragalactic HII region in the nearby spiral galaxy M101. The very steep N-Q color index (10–20μm), corresponding to a spectral index $\alpha \sim 3$, of NGC 5461 is attributed to dust. The flattish JHK colors of SBG's can be explained by emission from an old stellar population plus recombination radiation.

A strong FIR excess, due to the re-radiation from dust surrounding the star-forming regions (Rieke et al. 1980; Telesco and Harper 1980), is an outstanding property of bursting galaxies.

Deutsch and Willner (1986, 1987), carried out a far-infrared (FIR) study of Markarian starburst galaxies, using data for the four IRAS bands (12μm,

$25\mu m$, $60\mu m$, and $100\mu m$) reported in the *IRAS Point Source Catalog*. Of 99 Markarian starburst galaxies in B83's sample, three (Mkr 44, 203, 1301) were not observed by IRAS; 78 have been detected in $60\mu m$ band; 18 have not been detected. Therefore the detection rate is 81.25%, comparable with that of bright ($m_{Zw} \leq 14.5$) Markarian galaxies (84% : Xu et al. 1988), but significantly higher than that of UGC disk galaxies (63% : Franceschini et al. 1988b). FIR ($10\mu m$ to ∞) luminosities were calculated from the IRAS fluxes assuming a Rayleigh-Jeans energy distribution beyond $100\mu m$. Six galaxies in the sample could not be uniquely identified as IRAS sources, and for these the calculated luminosities were considered upper limits. Galaxies surveyed by IRAS but not detected were also assigned upper limits based on the *IRAS Explanatory Supplement* (Perrson et al. 1985). All but four of the starburst galaxies are more luminous in FIR than in the blue (the exceptions are Mrk 13, 190, 430, and 743). The median ratio of FIR to blue luminosity is 2.45 for the sample, slightly larger than the mean FIR/blue luminosity ratio found by Xu et al. (1988) for the non-Seyfert Markarian galaxies on the whole ($L_{FIR}/L_B = 1.9 \pm 0.14$), if the difference in the definition of L_{FIR} is ignored (which, according to Soifer et al. 1986, corresponds to a uncertainty of order of 30%). The median value of the logarithm of FIR luminosity of the sample is $\log(L_{FIR}/L_\odot) = 10.16$ $(+0.18, -0.06)$ $(H_0 = 75)$, to be compared with $\log(L_{FIR}/L_{odot}) = 9.45$ $(+0.09, -0.18)$ found for a sample of Virgo spirals. The FIR, the nuclear H_α, and the blue luminosities (total and nuclear) of the Markarian starburst galaxies were all found to be correlated with each other. The far-infrared emission seems, however, better correlated with the blue (both total and nuclear) than with the nuclear H_α emission, possibly implying, as argued by Deutsch and Willner (1986), that the dust producing the far-infrared light is heated predominantly by B rather than by O stars.

Sekiguchi (1986) presented a study on IRAS colors of Markarian starburst galaxies. He found that their mean spectral indices (between IRAS bands) are

$\langle \alpha_{60\mu/25\mu} \rangle = 2.02 \pm 0.16$ and $\langle \alpha_{100\mu/60\mu} \rangle = 0.71 \pm 0.35$. The corresponding values for Markarians on the whole are (Xu and De Zotti 1988, cf. Chapter 5): $\langle \alpha_{60\mu/25\mu} \rangle = 2.2$ and $\langle \alpha_{100\mu/60\mu} \rangle = 1.1$, and the those for UGC spiral/irregular galaxies (Franceschini et al. 1988b): $\langle \alpha_{60\mu/25\mu} \rangle = 2.5$ and $\langle \alpha_{100\mu/60\mu} \rangle = 1.9$. Hence, the FIR spectra of starburst galaxies are not only warmer than those of normal spiral galaxies, but also warmer than the mean of non-Seyfert Markarians.

1.3 mm observations of Markarian galaxies have been reported by Krügel et al. (1988a, 1988b). Twenty-four Markarian galaxies brighter than 10 Jy at $100\mu m$ were observed with the 30m Millimeter Radio Telescope (MRT) (Baars et al. 1987) on Pico Veleta, Spain, using the bolometer System developed at the Max-Planck-Institut für Radioastronomie (MPIfR) (Kreysa 1985). The beam size was $11''$. The final sample contains eight Seyfert or possible Seyfert galaxies and nine starburst galaxies according to the classification in MB86. A mean spectral index between $100\mu m$ and $1300\mu m$, $\alpha_{1.3mm/100\mu}$, of 2.83 ± 0.26 was found. For the 9 starburst galaxies I derived a mean 100–1300 μm spectral index of 2.85 ± 0.27. Supposing a thermal origin for the sub-millimeter radiation from these galaxies, the mean of the corresponding dust temperatures (assuming a $\epsilon_\nu \propto \nu^2 B_\nu(T_d)$ dust emissivity) is $30.0 \pm 5.7K$. However, the $11''$ aperture used in the millimeter survey is much smaller than both the IRAS aperture at $100\mu m$ ($3'.0 \times 5'.0$: Neugebauer et al. 1984) and the optical sizes of the sources (H77a, Lists I—XV). The aperture correction might be unimportant if, as argued by Krügel et al. (1988a, b), the bulk of the FIR emission comes from the central compact nuclei. On the other hand, as pointed out by Xu and De Zotti (1988, see also Chapter 5), the $100\mu m$ flux is likely to come mainly from the cold dust associated with extended galactic disks. In that case the aperture correction must be taken into account. For example, let us assume a uniform distribution of the $100\mu m$ flux within galaxies. Using the optical sizes reported by Huchra (1977a), when available, or the size estimates given on the Lists

I—XV otherwise, I find that the aperture correction results in an appreciable flattening of the mean spectral index, which becomes $\alpha_{1.3mm/100\mu} = 2.09 \pm 0.36$ for Markarian starburst galaxies and $\alpha_{1.3mm/100\mu}$ of 2.12 ± 0.33 for all non-Seyfert Markarians in their sample.

Comparing the luminosity function of starburst galaxies with that of Markarians on the whole (Seyfert included, Huchra 1977a), Balzano (1983) estimated that 30—50% of Markarians in the absolute magnitude range -17.5 to -22.5 are starburst galaxies. Most Markarian galaxies (non-Seyfert) which had the comment 'data refers to nucleus' written in the note section, and many others which were given a 'S' (starlike appearance) classification by Markarian, turned out to be starburst galaxies.

2.2. Compact Blue Galaxies (CBG)

Thuan and Martin (1981) listed the following properties as defining compact blue galaxies (hereafter CBG): (1) low intrinsic luminosity ($M_B \geq -18$); (2) optical spectrum exhibiting strong narrow emission lines superposed on a blue continuum; (3) very compact optical images (≤ 1 *kpc* in diameter). They claimed that the criteria (2) and (3) ensure the presence of a very active star-formation, while criterion (1) ensures that the galaxies so classified do not vary too greatly in mass, and that stochastic star-formation (Geroia et al. 1980) is probably dominant within them, since the shock induced star-formation may be less important for low mass galaxies. 78 Markarian galaxies belonging to the first VIII Markarian lists are included in their list of CBG, which comprises 115 galaxies on the whole[†]. Ten of these Markarian CBG's (Mkr 13, 133, 140,

[†] Although Thuan and Martin (1981) claimed to have included only sources fainter than $M_B = 18$ and to have considered only the first VII Markarian lists, their catalog comprises many galaxies obeying criteria (2) and (3) but brighter than $M_B = -18$, as well as 4 galaxies from the Markarian list No. 8.

149, 158, 196, 206, 401, 409, and 449) are also identified by B83 as starburst galaxies.

CBG's appear to undergo intense bursts of star-formation, producing massive young blue stars in a localized compact region of size comparable to that of the nucleus of a starburst galaxy (Thuan and Martin 1981). Their emission line spectra, resembling that of HII regions in the outer part of Sc galaxies (Searle 1971), generally show higher ionization than starburst galaxies do (whose spectra are similar to those of HII regions in the inner arms of spiral galaxies). In the $[NII]6584/H_\alpha$ vs. $[OIII]5007/H_\beta$ diagram, CBG's lie in the high-ionization end of the area occupied by galactic HII regions, with $[OIII]5007/H_\beta > 3$ and values of $[NII]6584/H_\alpha$ in the same range, but mainly on the low-side, of those found for starburst galaxies (Neugebauer et al. 1976; French 1980; B83). To account for this relatively high ionization, a very high upper mass cut-off ($\sim 200 M_\odot$) for the IMF of CBG's has been proposed (Viallefond, 1985; Melnick 1985). The lines are very narrow, even narrower than those of starburst nuclei: a mean FWHM of 75 ± 4 km/sec was found by French for a sample of 11 CBG, a factor of 2 lower than the median FWHM of starburst nuclei found by Feldman et al. (1982) and B83.

On the other hand, from the HI data on Markarian CBG's reported by Thuan and Martin (1981), I found a mean FWHM of the HI line of 122 ± 80 km/sec. The difference between the widths of optical and 21 cm lines may indicate that either the space distributions of star-forming regions (HII regions) and of HI regions within CBG have different sizes, or they are not in dynamical equilibrium with each other. The former possibility was supported by several aperture synthesis studies of CBG's (Gottesman and Weliachew 1972; Balkowski et al. 1978; Lequeux and Viallefond 1980; Viallefond and Thuan 1983) which showed that the HI is always distributed with a core-halo structure with the core containing $\sim 50\%$ of the total HI mass, whereas the HII regions are always

within the core. The size of the HI region is always larger than the optical image of CBG (Brinks and Klein 1985).

From the data reported by Thuan (1983) for 13 Markarian CBG, I found a mean $U-B = -0.45 \pm 0.24$, and a mean $B-V = 0.40 \pm 0.14$. Hence CBG's appear to be significantly bluer than Markarian starburst galaxies and non-Seyfert Markarian galaxies on the whole (see section 2.1).

A remarkable property of CBG's is their significant metal deficiency: the interstellar gas in these galaxies is metal deficient by a factor of about 5 to about 10 as compared to the interstellar gas in the solar neighbourhood (Searle, Sargent and Bagnuolo 1973; O'Connell, Thuan and Goldstein 1978; Lequeux et al. 1979; French 1980; Kinman and Davidson 1981). They generally contain a large amount ($\sim 10^8$—$10^9 M_\odot$) of neutral hydrogen, which sometimes exceeds the mass in stars (Thuan 1983).

A long debated question has been whether CBG's are truly young systems where stars are just being formed, or are relatively old galaxies whose old stellar population is swamped by an ongoing starburst (Sargent and Searle 1970; Searle and Sargent 1972; Searle, Sargent and Bagnuolo 1973). Thuan (1983) carried out a near-infrared study to search for evidences of an underlying old stellar population. He observed 36 CBG's from the sample of Thuan and Martin (1981) at $J(1.2\mu m)$, $H(1.65\mu m)$, and $K(2.2\mu m)$ with the NASA 3m Infrared telescope Facility (IRTF) on Mauna Kea. Their NIR magnitudes are roughly in the ranges $12 \leq J \leq 16.5$, $11 \leq K \leq 16$, $10 \leq H \leq 15.5$, $10.5 \leq L \leq 16$. The mean NIR colors were found to be $J-H = 0.59 \pm 0.18$, $H-K = 0.23 \pm 0.12$, and $J-K = 0.83 \pm 0.16$, significantly bluer than those of starburst nuclei (B83). Dust and/or ionized gas emissions cannot account for these colors because they produce very different NIR spectra. A viable explanation could be stellar radiation. On the $J-H$ vs. $H-K$ diagram, the data for CBG's apparently locate in the region corresponding to red dwarfs and red giants, but away from that of red

supergiants. However, Thuan (1983) argued, before coming to any conclusion, the effect of metallicity must be examined, since CBG's are metal deficient and the above discussion is based on data for the solar neighborhood. He found that the linear regression of $J-K$ as a function of metallicity for CBG's agrees well with that for galactic globular clusters (Aaronson et al. 1978), whose NIR emission is mostly due to red giants. This is one of the reasons that prompted him to believe that the main contributors to the NIR radiation of CGB's is a population of red giants, although after the corrections for metallicity the data points moved to a region in the $J-H$ vs. $H-K$ diagram populated by both red giants and red supergiants. Two further arguments in that direction are: (1) In the case of Mrk 209=I Zw 36, the NIR observations were obtained in a position where there is no strong optical emission, thus the presence of supergiants there is very unlikely (Viallefond and Thuan 1983). (2) Galaxies with very high present star formation rates, such as II Zw 70, and galaxies with very low present star formation rates, such as II Zw 71 (O'Connell et al. 1978), show very similar near infrared fluxes.

Since the very blue UV-optical colors and the bright emission lines require a large amount of young massive stars in CBG's, while their very low metallicity constrains the age of the current massive star-formation event to be $\lesssim 5{\cdot}10^7\ yr$, Thuan (1983) concluded that there must be a pre-existent population of stars, to which the relatively old ($\gtrsim 10^8\ yr$) red giant stars belong, underlying the current starburst (as discussed below, this is not necessarily true for some CBG's such as II Zw 70).

Loose and Thuan (1985) carried out a morphological study with CCD observations. About 50 CBG's selected from the list of Thuan and Martin (1981) were observed in the B and R bands. Based on these observations, the following tentative classification scheme was proposed. (1) The iE galaxies[†].

[†] i reminds the irregularity of the nucleus; E denotes the elliptical outer isophote.

This type is the most common and the most characteristic one among CBG. The prototype objects are Mkr 86, Mkr 209, Mkr 297 and VII Zw 403. They show a complex structure with several centers of star-formation and irregular isophotes in the central regions. The brightest clumps are always found in the vicinity of the center of the outer elliptical isophotes but are not generally found at the exact central position. Viallefond and Thuan (1983) have also noted that the brightest star formation region in all CBG which have been mapped at 21 cm is always very near to the peak in the neutral hydrogen surface density but does not coincide with it. These observational facts may be clues for understanding how star-formation is triggered in CBG's.

(2) The nE galaxies. These galaxies have a distinct, single star formation region located in the nucleus with regular (circular or elliptical) isophotes. The prototypes are Haro 2=Mkr 33, Haro 20, Harol and II Zw 102.

(3)The iI galaxies. The star-formation zones in these galaxies are not located at or near the center of the outer isophotes. For some of them (e.g. Mkr 314), the irregularity is due to merging; for some others (e.g. Mkr 59, Arp 262), it may be due to the self-propagating star-formation which results in a chain of HII regions.

(4) The $i0$ galaxies. This class of galaxies does not show a faint outer structure visible in the Palomar Sky Survey plates. The i0 galaxies thus appear to lack an underlying older stellar population and are the best candidates for truly young galaxies, where the present burst of star formation is the first in the galaxy's lifetime. They are relatively rare among CBG's. The prototype is II Zw 70.

Since CBG's are intrinsically faint, they are not numerous in IRAS point catalog, as SBG's. However, for given limiting magnitude, the IRAS detection rates of the two galaxy types are not very different: In the bright Markarian galaxy sample of Xu et al. (1988), there are 33 objects which are on the list

of Thuan and Martin (1981). 24 of them were detected by IRAS at $60\mu m$, giving a detection rate of 73%. Nine of the 33 objects are also classified by B83 as starburst galaxies. of the remaining 24, 18 are detected by IRAS at $60\mu m$ (detection rate of 75%). A study of IRAS observations of CBG's has been presented by Kunth and Sévre (1985). They found a median $L_{FIR}/L_B \simeq 2$, also not very different from what Xu et al. (1988) found for Markarian galaxies on the whole. They failed to find significant evidence of correlations between: (1) $U-B$ and L_{FIR}/L_B; (2) $U-B$ and $F_{60\mu}/F_{100\mu}$; (3) $U-B$ and $F_{25\mu}/F_{60\mu}$; (4) metallicity and L_{FIR}/L_B. They argued that this may mean that CBG's generally have enough dust mass to convert a large fraction of ionizing flux into thermal emission. From their Fig. 3, it can be found that CBG's have quite warm $60\mu m$—$100\mu m$ colors: $F_{60\mu}/F_{100\mu} > 0.4$ with a median ~ 0.7, slightly warmer than the mean for Markarian galaxies (Chapter 5).

Probably all of Markarian galaxies fainter than $M_B = -18$ belong to this category. I have done a simple statistic using the complete sample of Markarian galaxies of Xu et al. (1988), which has a limiting apparent magnitude of $m_{Zw} = 14.5$. There are 176 non-Seyfert Markarian galaxies in the sample, of which 23 are fainter than -18 absolute photographic magnitude ($\sim 12.5\%$). All 14 galaxies belonging the first VIII Markarian lists are in Thuan and Martin's (1981) list of CBG's. Other 19 objects of the sample of Xu et al. (1988) brighter than $M_B = -18$, are on Thuan and Martin list†. Thus, excluding those (nine) objects identified as starburst galaxies, $\simeq 14\%$ of Markarian galaxies ($\simeq 18\%$ if Seyferts are excluded) can be classified as CBG's.

2.3. Clumpy Irregular Galaxies (CIG)

CIG's are Magellanic irregulars that are undergoing active star formation (Casini and Heidmann 1976a, 1976b; Benvenuti et al. 1979, 1980, 1981; Heidmann et al. 1982, Huchra et al. 1983b, Huchra 1987). Usually they are made

† See the footnote at the begining of this section.

up of a few (5—10) bright clumps loosely scattered in a common envelope, each clump being equivalent to 100 giant HII regions of the 30 Doradus type and being excited by some 10^5 early type stars (Benvenuti et al. 1979, 1980, 1981; Heidmann et al. 1982). Thus in clumpy irregular galaxies, star formation activity is proceeding vigorously over the whole of the galaxy, unlike in the ordinary irregular galaxies; for example, in LMC the very recent star-formation is centered on 30 Doradus. Other observational characteristics of CIG's include:

(1) Very strong UV excess which is due to a large population of massive young stars (Benvenuti et al. 1982). From the data reported by H77a, a mean $U - B = -0.40 \pm 0.03$ and a mean $B - V = 0.37 \pm 0.07$ have been found for 5 CIG's identified by Heidmann et al. (1982), much bluer than those of ordinary irregulars: $U - B = -0.23$ and $B - V = 0.46$ (H77a), but very close to those of Markarian irregular galaxies on the whole: $U - B = -0.36$ and $B - V = 0.41$ (H77a).

(2) Relatively high luminosity in comparison with normal irregulars. They are about 3—4 magnitude brighter than normal irregular galaxies: the median absolute photographic magnitude of CIG's is ~ -20 mag (Casini and Heidmann 1976a) while the absolute photographic magnitude of classical irregulars is ~ -16.5 mag (Balkowski, 1973).

(3) Large internal motions, with velocities ranging from 200 km/s to 500 km/s, (Casini and Heidmann 1976a), while for classical irregulars velocities are in the range 100—300 km/s.

(4) Large masses: the masses of CIG's are in the range of 10^{10}—$4 \cdot 10^{11} M_\odot$, while the masses of classical irregulars are in the range 2—$30 \cdot 10^6 M_\odot$ (Casini and Heidmann 1976a).

CIG's are strong FIR emitters. All six CIG's listed in Heidmann et al. (1982) have been detected by IRAS at $60\mu m$. Judging from the data for two

of them, Mkr 297 and Mkr 325, included in the study of Xu and De Zotti (1988; see Chapter 5), their $F_{60\mu}/F_{100\mu}$ flux ratio is relatively warm (~ 0.7), but $F_{25\mu}/F_{60\mu}$ flux ratio relatively cold (< 0.13).

CIG's were first identified from a morphological study of pairs of Markarian galaxies (Casini and Heidmann 1976a, b). The most comprehensive sample of CIG's is that by Heidmann et al. (1982), comprising six Markarian CIG's (Mkr 7, 8, 296, 297, 325, 523) for a centimeter wavelength radio study. Since CIG's are usually found in close pairs of galaxies, it has been suggested (Huchra et al. 1983b, Huchra 1987) that their intense star-formation is the result of recent mergers, or collisions with gas clouds or gas rich dwarf galaxies (Duflot-Augarde and Alloin 1982; Heidmann et al. 1982).

2.4. Interacting/peculiar galaxies (IPG)

There are overlaps between this subtype and those discussed above. As already mentioned, most CIG's belong to close interacting pairs, while Balzano (1983) claimed that $\simeq 30\%$ SBG's are numbers of binary systems or have double nuclei, indicative of merging. However, there are indeed some Markarian galaxies which show evidence of interactions and yet do not belong to any of the 3 previously discussed sub-classes, i.e. are not irregulars, nor compact galaxies, and don't have conspicuous nuclei. The prototype is the Mkr 171 (NGC 3690—IC 694) system. The morphology of the system is very complicated. Although the two galaxies NGC 3960 and IC 694 are sufficiently separated to have their own names, this system consists of two greatly distorted and partly overlapping spiral galaxies (Gehrz et al. 1983). Mkr 171 is the most luminous non-Seyfert Markarian galaxy in any sense: from UV (H77a), through infrared (Rieke and Low 1972; and IRAS catalog, cf. Xu et al. 1988) to radio (Sramek and Tovmassian 1976), and also for optical emission lines (Weedman 1972; Gehrz et

al. 1983). According to Gehrz et al. (1983), all of these extraordinary luminosities could be understood in terms of exceptional episodes of star formation occurring almost simultaneously in different zones all over the system. Augarde and Lequeux (1985), through a kinematical study, estimated that an order of $5 \cdot 10^7 M_\odot$ of stars ($\lesssim 10^{-3}$ of the total mass of the system), mainly O stars in the mass range of 20—$35 M_\odot$, have been formed since the beginning of the current starburst, $\simeq 1.5 \cdot 10^7$ yr ago.

Toomre and Toomre (1972), in a classical numerical study of tidal effects between pairs of galaxies, showed that interactions could result in a redistribution of substantial quantities of material into deeply plunging orbits in galaxies, which in turn could result in a rapid burst of star formation.

The interaction as a triggering mechanism of star formation was also proposed by several other authors (Searle and Sargent 1972; Searle, Sargent, and Bagnuolo 1973; van den Bergh 1975; Alloin, Bergeron, and Pelat 1977; Huchra 1977a, 1977b; Larson and Tinsley 1978). Some statistics available in the literature support this hypothesis, too. H77a found that approximately 20% of Markarian galaxies showed pecularities, indicative of interactions, while the corresponding percentage among NGC galaxies is only $\sim$ 7%. As mentioned above, B83 found a even higher percentage of starburst nuclei to be in interacting/merging systems: $> 30\%$. Direct evidence of burst of star formation triggered by interactions is provided by observations of interacting systems such as Mkr 171.

Larson and Tinsley (1978) compared the UBV colors of a sample of galaxies, selected from the "Atlas of Peculiar Galaxies" (Arp 1966), with the colors of normal galaxies. They found a significantly larger scattering in the color-color diagram of peculiar galaxies. Furthermore, after separating peculiar galaxies into interacting and noninteracting subgroups according to their morphological appearances, they found the scattering to be primarily due to interacting

galaxies, while the color-color distribution of non-interacting peculiar galaxies resembles that of normal galaxies. A remarkable difference between the UBV color distributions of interacting/peculiar galaxies and of Markarian galaxies (H77a) is that the former shows not only scatter toward the blue, as does the latter, but also scatter toward the red. The latter scatter was interpreted by Larson and Tinsley (1978) as a 'post-starburst' phenomenon, due to remnants of starbursts died some $10^8 yr$ ago, comprising many red giants (evolved moderate mass stars). The fact that the UBV color distribution of Markarian galaxies does not show scatter toward the red is obviously due to a selection effect.

The spectroscopic study of interacting spiral galaxies by Kennicutt and Keel (1984) and Keel et al. (1985) showed that interacting galaxies have: (1) significantly brighter emission lines, both in equivalent width and in luminosity; (2) more active and extensive nuclear star formation, irrespective of their Hubble type. An objective prism selected sample by Wasilewski (1983) showed that more than 30% of emission line galaxies are within interacting systems.

Joseph et al. (1984) have performed IR ($JHKL$) measurements for 28 Arp-atlas interacting pairs. Significant mid-infrared excess in the nuclear region (8–12$''$, the apertures of their survey) was found for some members of these pairs: half of the sources have $K - L > 0.5$, while for normal galactic nuclei the mean $K - L = 0.3 \pm 0.2$. They argued that this is due to an enhanced re-radiation by dust heated by massive stars, indicative a recent burst of star formation. They concluded that the interactions are extremely efficient in triggering starbursts, the efficiency apparently approaching 100%. An interesting result they found is that in no case had both galaxies in an interacting pair shown a $K - L$ excess. They interpreted this fact on the basis of the numerical studies of Toomre and Toomre (1972) and Wright (1972). The maximum tidal disruption and transfer of material occurs when the accreting galaxy orbits the 'victim' galaxy in the same plane and sense as the rotation of the 'victim'. Since

in any arbitrary interaction between two galaxies conditions close to these are more likely to be met for only one galaxy, it is not surprising that the burst of star formation preferentially appears in one member of the pair.

1 to 10 micron IR observations for a sample of 20 interacting galaxy systems were carried out by Lonsdale, Persson, and Matthews (1984). They found that interacting/merging galaxies as a class have substantially higher infrared luminosities than noninteracting spirals, and this emission is due to ongoing massive star formation, which is about 3 times higher than in normal cases. They also analyzed the results from the IRAS minisurvey, and found that a large fraction, perhaps as much as 30%, of all far-infrared emission from galaxies arises in starbursts triggered by interactions. However, contrary to Joseph et al. (1984), they estimated that only 50% of interacting/merging galaxy systems are undergoing a starburst.

Sanders et al. (1987) found that the fraction of interacting galaxies increases monotonically with increasing luminosity in the bright IRAS galaxy sample for $L_{FIR} > 3 \cdot 10^{10} L_{\odot}$ ($H_0 = 75$), with interacting and close pairs of galaxies accounting for one fourth of the galaxies with $L_{FIR} \sim 3 \cdot 10^{10} L_{\odot}$, for two thirds of the galaxies at $L_{FIR} \sim 10^{11} L_{\odot}$, and for all of the galaxies with $L_{FIR} > 5 \cdot 10^{11} L_{\odot}$.

On the other hand, an investigation on the environment of IRAS galaxies by Lawrence et al. (1986) led to quite different conclusions. Sixty-eight IRAS galaxies having measured redshifts were analyzed. Only 6% of them were found to have neighbors within 40 kpc, 15% with neighbors within 100 kpc. The average distance between IRAS galaxies and their neighbors is 765 kpc, close to the typical separation for spirals in small groups (Gott and Turner 1977). Lawrence et al. (1986) argued that galaxy interactions are not important for general IRAS galaxies; and, judging from the FIR activity, interaction is neither a sufficient nor a necessary condition for starbursts.

In the sample of Xu et al. (1988), I find 16 objects belonging to this category among sources in the first VII Markarian lists, which have relatively good morphological data (MB86). Fourteen of them were detected by IRAS at $60\mu m$, giving a detection rate of 87.5%, not much higher than that for the whole bright Marakarian sample.

2.5. Others

There are still some Markarian galaxies which can not be classified into the above 4 categories, i.e., they are neither compact, nor irregulars, nor show any evidence of star-like nuclei or of interactions. Table 2.1 lists 15 such galaxies which I picked up from Huchra's morphological sample (H77a). Galaxies with emission lines and without emission lines are sorted into two groups. Those which have emission lines also show some other evidences of enhanced star-formation activity. They have been all detected by IRAS regardless of their morphological type and have relatively high F_{FIR}/F_{op} ratios, where

$$F_{FIR} = C \cdot 1.26 \cdot 10^{-11} \cdot (2.58 \cdot F_{60\mu} + F_{100\mu}) \qquad (erg/cm^2/sec), \qquad (2.1)$$

$F_{60\mu}$ and $F_{100\mu}$ are IRAS fluxes in Jansky, and $C = 1.8$ (Xu and De Zotti 1988); and

$$F_{op} = 2.52 \cdot 10^{-5} \cdot 10^{-0.4 \cdot (V - B.C.)} \qquad (erg/cm^2/sec), \qquad (2.2)$$

where V is the apparent visual magnitude, $B.C.$ is the bolometric correction (Xu and De Zotti 1988). On the other hand, for those which have no detected emission lines, I can't find any evidence of enhanced star-formation activity: their UBV colours are not bluer than average for normal galaxies of their morphological type (H77a); they are either undetected by IRAS, or have relatively low $F_{60\mu}$ and F_{FIR}/F_{op}. Thus I conclude that they are likely to be normal galaxies included in the Markarian lists by chance. Another glance to these

Table 2.1. Non-seyfert Markarian galaxies without any feature (see text)

Mkr	type	z	$^{**}M_{Zw}$	$B-V$	$U-B$	$F_{60\mu}$ (Jy)	$^{\dagger}\left(\frac{L_{FIR}}{L_{op}}\right)$	$^{\ddagger}H_{\alpha}$	ref
*101	S0	0.0158	-20.8	0.57	-0.02	0.93	1.13	Y	3
321	Sc	0.0319	-22.5	0.62	-0.05	2.67	2.70	Y	7
323	Scd	0.0145	-20.7	0.73	0.07	2.98	4.00	Y	7
336	E5	0.0170	-20.9	0.74	0.16	1.31	1.77	Y	7
531	S0/E	0.0120	-20.3			4.71	4.07	Y	4
555	Sd	0.0137	-21.1			3.89	2.38	Y	1
558	S0	0.0129	-19.9			1.47	2.31	Y	1
626	E0	0.0131	-20.1	0.66	-0.01	1.00	1.30	Y	5
85	E	0.0117	-20.0	0.82	0.30	>0.6		N	1
179	SBbc	0.0110	-19.9	0.67	0.11	0.99	1.16	N	3
249	S0	0.0090	-19.2	0.84	0.30	>1.5		N	2
*386	SBb	0.0120	-20.0	0.88	0.40	0.73	1.13	N	7
389	S0/a	0.0156	-21.0	0.83	0.32	0.74	0.80	N	3
656	E0	0.0190	-21.3			>1.5		N	6
669	S0/E	0.0177	-20.6	0.94	0.46	>1.5		N	3

Table 2.2. Interacting/peculiar Markarian ellipticals

Mkr	type	z	$^{**}M_{Zw}$	$B-V$	$U-B$	$F_{60\mu}$ (Jy)	$^{\dagger}\left(\frac{L_{FIR}}{L_{op}}\right)$	$^{\ddagger}H_{\alpha}$	ref
341	E3	0.0152	-21.1	0.73	0.13	0.85	1.02	Y	7
607	S0/a	0.0089	-19.0			2.33	3.03	Y	1
452	S0	0.0177	-20.5	0.95	0.45	>1.5		N	3
*608		0.0091	-19.3			>0.6		N	8
616	S0/a	0.0119	-19.7			>1.5		N	6

* Superposed by a galactic star (ref. 3).

** Taken from MB86 ($H_0 = 75$).

† See text for the defination of L_{FIR} and L_{op}.

‡ Y: detected; N: undetected.

References for H_{α} data

1. Kopylov et al. (1974).
2. Ulrich (1971).
3. Huchra (1977a).
4. Markarian et al. (1984).
5. Denisyuk and Lipovetskii (1974).
6. Denisyuk et al. (1976).
7. Arakelyan et al. (1972).
8. Huchra (1988, private communication).

galaxies tell us that the majority of them (5/7) are E/S0 galaxies. I was stimulated, by this fact, to check the properties of other Markarian E/S0 galaxies, especially of those classifiead as interacting/peculiar galaxies, in view of the argument that interactions are not a sufficient factor for triggering starbursts (Lawrence et al. 1986, MB86). In Huchra's morphological sample, five E/S0 galaxies are in pairs or close groups, or show evidence of peculiarity (Table 2.2). A quite similar situation is found here as showed in Table 2.1: those (2 out of 5) which show optical emission lines are also detected by IRAS and have bluer optical colors than normal ellipticals. The three which do not show emission lines, are also undetected by IRAS and have rather normal optical colors.

In Huchra's morphological sample there are 15 E/S0 galaxies which are not Seyfert or BL Lac objects, and are not classified as SBG's or CBG's. According to above analysis, eight of them are very likely normal galaxies.

2.6. The relative abundances of subtypes

The most reliable estimates of the relative frequency of the various subtypes are obviously those based on a complete morphological sample, like that by H77a.

Huchra's 'complete morphological sample' contains 91 Markarian objects on the whole. Ten of them are Seyferts or possible Seyferts, and two are BL Lac's. Of the remaining 79 objects, 28, i.e. $\simeq$ 35% are starburst galaxies, in good agreement with the estimate of B83[†].

Thirteen are compact blue galaxies (Thuan and Martin 1981), excluding those CBG's (seven) classified as SBG by B83. The corresponding percentage

[†] Mkr 332 is not on Balzano's list, but is classified as a starburst galaxy by MB86

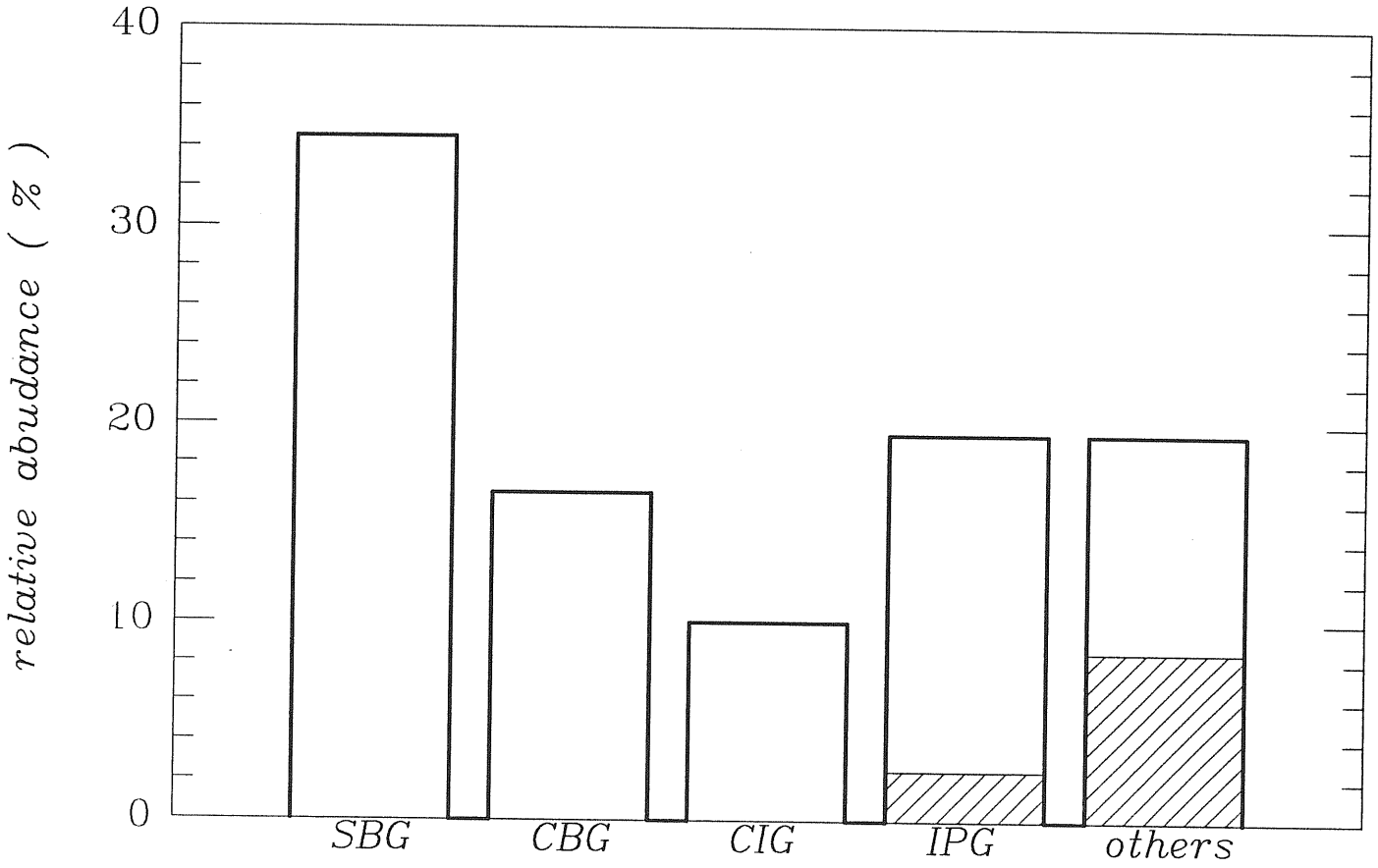

Fig. 2.1.

Note: shadowed areas represent 'normal' galaxies (see text).

is 16.5, in good agreement with the estimate based on an analysis of the sample of Xu et al. (1988) (see 2.2).

The identification of CIG's in Markarian lists is far from complete. It is, thus, hard to estimate their abundance. However, in Huchra's sample there are eight Markarian irregulars not identified as SBG's (B83) nor included in Thuan and Martin's (1981) catalog of CBG's. If these eight galaxies are all CIG's, given the fact that Markarian irregulars have same mean optical colors as those of CIG's (Section 2.3), these objects are $\simeq 10\%$ of Markarian galaxies.

Fifteen sources, which do not belong to any of the above subtypes, are in pairs or in close groups. Among them, 4 are normal spirals, 4 are barred spirals, 5 are E/S0 galaxies, one is a Sc+Im system (Mkr 171), and another is a Sc+SBab system (Mkr 271).

Of the remaining 15 galaxies not belonging to the previous classes, 8 have optical-UV emission lines, and were detected by IRAS; seven without detected emission lines show no evidence of being galaxies with any activity rather than normal galaxies. Five of them are E/S0 galaxies.

The percentages of non-Seyfert Markarians in the above sub-classes are summarized in Fig. 2.1.

2.7. Summary

(1) The Majority ($\simeq 90\%$) of non-Seyfert Markarian galaxies show evidences of enhanced star-formation activity ('starbursts'). We will refer to them as Markarian star-forming galaxies.

(2) Depending on the scale and on the location of the violent star-formation region (regions) relative to the host galaxy, Markarian star-forming galaxies can be divided into four main subtypes:

a). *Starburst galaxies* (SBG) are generally disk galaxies with starburst nuclei.

b). *Compact blue galaxies* (CBG) are generally compact galaxies with a starburst swamping the old underlying stellar population.

c). *Clumpy irregular galaxies* (CIG) are massive Magellanic irregulars with several (~ 5) violent star-formation regions all over the galaxy. They are generally interacting irregular galaxies.

d). *Interacting/peculiar galaxies* (IPG) have similar properties to CIG, except that they are not irregulars. Some of them (Mkr 171, 271) are examples of the most active star-forming galaxies showing evidences of a starburst extended over the whole system.

(3) About 10% of non-Seyfert Markarian galaxies are likely normal galaxies. The majority of them are ellipticals. The probability for a Markarian elliptical galaxy to be a normal one is more than 50%.

Chapter 3
Radio and X-ray Properties

3.1. Radio

Only the first 7 Markarian lists (Mkr 1–700) have been systematically observerd in radio band. Forty-two of the sources in these lists were found having $S(6cm) \geq 30$ mJy (Sramek and Tovmassian 1975; Sulentic 1976; Bieging et al. 1977; Kojoian et al. 1980; Biermann et al. 1980). Ten of them are Seyferts, and 3 are BL Lac objects. Of the remaining 29 objects, 15 out of 16 with morphological classifications are spirals (Mkr 11 is an E5/S0 galaxy: H77a).

Another analysis can be done using the complete UGC radio sample by Dressel and Condon (1978). They observed, at 2.4 GHz (12.6 cm) with a detection limit of 15 mJy, 2095 UGC (Nilson 1973) galaxies, 2018 of which make up a complete sample defined by $|b| > 10°$, $0° < \delta < 37°$, $m_p \leq 14.5$ (or $m_p \leq 14$ if $11^h30^m < \alpha < 13^h$). One hundred and seven non-Seyfert Markarian galaxies are included in the sample, 41 of which were detected above 15 mJy, giving a detection rate of $\simeq 40\%$, significantly higher than that for the whole UGC sample ($\simeq 21\%$, Dressel and Condon 1978; Toffolatti et al. 1988). The mean value of the logarithm of the monochromatic radio (2.4 GHz) to blue luminosity ratio ,$R_{2.4} = \log S_{2.4} + (m_z - 12.5)/2.5$ (Franceschini et al. 1988a), is 1.56 ± 0.04, higher by about 0.3 than that of UGC spiral galaxies (Franceschini et al. 1988a), and quite close to that of UGC Seyferts. Forty-two galaxies in this sample have been classified according to the scheme in Sect. 2.7. The detection rates for the represented subtypes are: 57% (16/28) for starburst galaxies (B83); 57% (4/7) for compact blue galaxies (Thuan and Martin 1981); 43% (3/7) for interacting/peculiar galaxies.

Klein et al. (1984) carried out a 6.3cm survey of 52 compact blue galaxies, of which 22 are Markarian CBG's, down to 1 mJy (3σ limit) using the Effelsberg 100m radio telescope. They found that, on the average, CBG's have about 10 times higher radio to optical luminosity ratios than normal spirals. There is evidence that the relation between radio and optical luminosity of CBG's is different from that for normal spirals. The average radio continuum spectrum of CBG's is significantly flatter ($\langle\alpha\rangle = -0.33 \pm 0.05$) compared to that of normal spirals ($\langle\alpha\rangle = -0.72 \pm 0.03$, Gioia et al. 1982), suggesting that an important, and even dominant, contribution comes from bremsstrahlung emission of hot electrons in HII regions. In view of the high rate of massive star formation of CBG's, and of the correspondingly large supernova rate, the relatively low fraction of synchrotron radiation may be surprising and may suggest that magnetic fields in these objects are relatively weak.

A sample of 33 bright spiral galaxies, that are relatively strong radio sources with high radio-to-optical flux ratio (R) was observed by Condon et al. (1982) at 4885 MHz (6.1cm) and/or 1413 MHz (21cm). VLA maps show evidence that the majority (28) of them, nearly all having nearby companions, are extended. Among them there are 4 Markarian interacting galaxies (IPG, cf. section 2.4): Mkr 38, Mkr 171, Mkr 533, Mkr 1376. Condon et al. (1982) argued, that, if the high radio emission of these galaxies is due to starbursts, supernova production rates as high as 1 yr^{-1} are required.

Sulentic (1976) found that the optical luminosity and the radio luminosity of Markarian galaxies are fairly well correlated (the correlation coefficient is about 0.7 for a sample containing 36 objects, including 8 Seyferts). This can be understood since the optical emission of star-burst galaxies is dominated by very bright O,B stars, while their radio emission is made up by bremsstrahlung from ionized gas and by non-thermal emission from relativistic electrons; O,B stars, ionized gas and relativistic electrons are all related to the star formation rate.

Twenty-one cm neutral hydrogen studies by Bottinelli et al. (1973) and Bottinelli et al. (1975) showed that Markarian galaxies contain a neutral hydrogen mass in the range of 10^7–10^8 $M_\odot$, corresponding to a mass fraction of a few percent.

3.2. X-ray

Fabbiano, Feigelson and Zamorani (1982) reported Einstein results for a sample of 33 peculiar galaxies, 3 of which are Markarian objects (Mkr 59, 131, 297). There is no uniform, well defined selection criterion for this sample, but most galaxies are in Arp's catalogue (Arp 1966), and many of them lie in groups and interacting pairs. In the $U-B$ vs. $B-V$ diagram, these galaxies are located in the same region of Markarians (Huchra 1977a), so they are believed to be actively star-forming galaxies. Thirteen objects were detected at 3σ level with soft X-ray (0.5—3 KeV) fluxes in the range $2—17 \times 10^{-13}\, erg/cm^2/sec$. The corresponding luminosities range from 1×10^{39} to $2.3 \times 10^{42}\, erg/sec$ ($H_0 = 50$). The galaxies with higher photon counts show evidences of extended or multiple emission regions. Population I binary X-ray sources and young supernova remnants are suggested to be the most important contributors. Since there are more O,B stars ($\sim 10^5$) in star-forming galaxies (Benvenuti et al. 1979) than in normal galaxies (e.g., in our own Galaxy, there are $\sim 10^4$ OB stars, ven den Heuvel 1980), more X-ray binaries exist, and the supernova explosion rate is higher. A SNR rate of $\sim 0.2 yr^{-1}$ and 200 X-ray binaries will produce an X-ray luminosity $\sim 10^{40}$–$10^{42}\, erg/sec$ (while in our own galaxy, the SN rate is $\sim 0.05\, yr^{-1}$ (Clark and Stephenson 1982), and there are $\sim$ 20 X-ray binaries (ven den Heuvel 1980)). Fabbiano et al. (1982) found that the X-ray luminosity is correlated with both radio luminosity and optical luminosity. The correlation is stronger with radio luminosity ($\sim 7\sigma$ level) than with optical luminosity ($\sim 3\sigma$ level).

Weedman et al. (1981) reported a single soft X-ray (0.25—3.5 KeV) observation for Mkr 538=NGC 7714 with the IPC on the Einstein Observatory (Giaconni et al. 1979). The exposure time was 2091 seconds on 1979 December 20. In a region of 2′ centered upon the nucleus of the galaxy, 17.7 ± 6.1 excess counts relative to the back ground were detected, corresponding a luminosity $L_x(0.25—3.5\ KeV) \simeq 6 \times 10^{40}\ erg/sec$ for $H_0 = 75$, or $L_x(0.25—3.5\ KeV) \simeq 1.4 \times 10^{41}\ erg/sec$ for $H_0 = 50$, consistent with the results of Fabbiano et al. (1982).

Using the relationship between X–ray and radio luminosities derived by Fabbiano et al. (1982) and their model for evolution of actively star-forming galaxies, Danese et al. (1987) estimated a contribution of these sources to the X–ray background at 2 keV in the range 5 to 11%.

On the other hand, the results of Fabbiano et al. (1982) were derived using a sample not well defined in a statistical sense and rely on soft X–ray data.

Persic et al. (1988) exploited the HEAO 1 A-2 data-base (Piccinotti et al. 1982) to investigate the hard X-ray properties of several samples of galaxies. Given the limited sensitivity of the A2 experiment, their could not study sources on an individual basis but adopted a statistical approach. Their method consisted in comparing the distribution of counting rates from positions coincident with the sources under study with that found for a large number of randomly chosen positions in the sky (control fields).

No statistically significant signal was found for a sample of 67 UGC starburst/interacting galaxies (S/I galaxies, Danese et al. 1987; Francheschini et al. 1988a, 1988b), comprising non-Seyfert Markarian galaxies, Zwicky blue compact galaxies, and galaxies classified by Nilson (1973) as peculiars, distorted, interacting or in close multiple systems, brighter than $m_{z_w} = 13.5$. However,

when the sample was subdivided by optical luminosity into three equally populated parts, Persic et al. (1988) found that the counting rates for high and intermediate luminosity sources tend to be systematically larger than those for control fields, although the difference is significant only at the 5.5×10^{-3} level (i.e. the probability of finding just by chance a difference with control fields equal to that observed is 5.5×10^{-3}). Even though the A2 data do not allow to reliably estimate the mean X–ray to optical luminosity ratio for these sources, the results by Persic et al. (1988) may suggest that such ratio might be increasing with optical luminosity, rather than decreasing as implied by the relationship derived by Fabbiano et al. (1982). Also, the A2 data turn out to be compatible with a mean X-ray to optical luminosity ratio for actively star-forming galaxies an order of magnitude larger than for normal galaxies. Such a possibility was suggested by Bookbinder et al. (1980), who pointed out that the former sources might be highly luminous in X–rays due both to bremsstrahlung emission during a hot wind phase powered by supernovae, and to hard X–ray binaries, which may be overabundant in metal poor systems.

Persic et al. (1988) also analyzed in a similar way a sample of 74 Markarian starburst nuclei (B83). No significant difference with the distribution of counting rates for control fields is found for these optically weaker sources, neither for the full sample nor subdividing it by H_α luminosity.

Rieke (1988) used the HEAO 1 A-1 ($\sim$ 3 times more sensitive than HEAO 1 A-2, Wood et al. 1984) data base to search for hard X-ray fluxes (2–10 Kev) from bright, ultraluminous infrared galaxies. In a sample of 15 such galaxies (3 are Markarian galaxies: Mkr 231, Mkr 273, Mkr 331) with far-infrared luminosity $\geq 10^{11}\ L_\odot$ ($H_0 = 75$: Soifert et al. 1987b) and $F_{60\mu}+F_{100\mu} \geq 30\ Jy$, drawn from the list of Soifer et al. (1987b), only the previously known hard X-ray source NGC 7469 (Sy1) is clearly detected. An additional weak detection of Mkr 331 is consistent with the number of detections expected from source confusion. The

uniformly low X-ray luminosities of these galaxies are inconsistent with the suggestion of Sanders et al. (1988) that they contain dust-embedded QSO's. Some alternatives are suggested: (1) the infrared galaxies may contain a form of X-ray quiet active nucleus; (2) the X-ray sources in active nuclei cannot turn on until after any circumnuclear gas is cleared up; (3) the bulk of the infrared luminosity in these galaxies may be generated by intense circumnuclear star formation.

Chapter 4
A Review of Theoretical Models

Given the fact that the majority of Markarian non-Seyfert galaxies have an intense star-formation activity (Chapter 2), all theoretical models for them in the literature have tried to build links between observational data and the following fundamental parameters of the 'starburst' (cf. Huchra 1987): (1) The duration and/or the age of the burst; (2) its *Initial Mass Function* (IMF), especially as a function of environment, e.g. metallicity, parent galaxy luminosity, galaxy-galaxy interaction rate, location of the burst, etc.; (3) the strength or the magnitude of the burst b, which is usually defined as the ratio between the mass involved in the burst and the mass of the underlying galaxy (Larson and Tinsley 1978).

4.1. Huchra's photometric models

Huchra (1977b) investigated 3 classes of evolutionary models: old galaxy models, young galaxy models, and 'composite' galaxy models, to explain the differences between the UV-optical colors and the H_β equivalent widths of Markarian galaxies and those of normal field galaxies.

He assumed that the emission from galaxies is a mixture of the integrated contribution from stars at different points of their lifetimes and of the contribution from interstellar gas. The data for stellar evolution was taken from literature (assuming a normal composition $x = 0.70$, $z = 0.02$):

(a) The low mass models ($m < 1.0 M_\odot$) were taken from an unpublished compilation by Caldwell et al. (1974). These models were assumed not to evolve on the time scales of interest.

(b) Models of 1—9 $M_\odot$ were taken from Iben (1965, 1966a,b, 1967a,b) with corrections and additions to the relatively low mass (1–3 $M_\odot$) red-giant evolution, following Tinsley (1972).

(c) High mass models ($\geq 10M_\odot$) were taken from Iben (1966c), Robertson (1972), Ziólkowsky (1972), Barbaro et al. (1973), Barbaro et al. (1972), and Chiosi and Summa (1970).

The majority of galaxy models contained only stars of 30 $M_\odot$ or less; the IMF was integrated between 0.05 and 30 $M_\odot$. The high-mass stars (35, 40, and 60 $M_\odot$) were included in a small number of galaxy models in order to examine the effects of increasing the upper mass limit.

The contribution from interstellar gas to the galaxy continuum radiation includes free-free emission, recombination of H^+, He^+, and He^{++}, and two-photon emission (Brown and Methews 1970). For simplicity, Huchra assumed that the galaxy contained sufficient gas so that HII regions are ionization-bounded. The adopted UBV colors of the ionized gas are $U - B = -0.95$, $B - V = -0.02$, and the absolute V magnitude due to one ionizing stellar photon is $M_V = 116.31$.

The three sets of galaxy models are characterized by different star-formation histories. 'Old' galaxies are defined as systems which started forming stars $\sim 10^{10}$ years ago, while 'young' galaxies are systems that started forming stars relatively recently compared with the age of the universe— $\lesssim 10^9$ years ago. For both old and young galaxies, the rate of star formation is monotonically decreasing with time. The simple parameterization of the stellar birth rate function

$$\Psi(m,t) \approx m^\alpha \exp(-\beta t/t_0) \tag{4.1}$$

of Searle, Sargent, and Bagnuolo (1973) is used. The IMF is a power law of slope α, with low mass cutoff at $m_{min} = 0.05M_\odot$ and high mass cutoff at

$m_{max} = 30$—$60 M_{\odot}$ (see discussion above). The integrated (over stellar mass) star formation rate as a function of time t is, therefore, taken to be exponential: t_0 is the age of the galaxy, β is the exponential decay rate. It was found that old galaxy models fit the observed colors and H_β emissions of Markarian galaxies only if they have sufficiently flat ($\alpha \leq 1.35$) IMF or, for somewhat steeper IMFs, nearly constant rate of star-formation. Models with these parameters predict relatively high metal abundances, but observations do not support this prediction.

The predicted UBV colors by all young galaxy models with different IMF, without reddening, do not fall within the envelope confining observed data of Markarian galaxies. Although models having flat IMF (the power index $\alpha < 2.35$) extinguished by ~ 1 *mag* internal visual extinction can account for the UBV data of compact blue galaxies, which are the bluest among non-Seyfert Markarians and the best candidates for being truly young galaxies, such amount of extinction is not supported by the observations of CBG's (see table 5 and 6 of Huchra 1977b) †.

The UBV colors of Markarian starburst galaxies (B83), judging from Fig. 6 of Huchra (1977b), can be accounted for by young galaxy models with normal IMF ($\alpha \sim 2.35$) reddened by $A_V \simeq 1$ *mag* internal extinction. On the other hand, the average A_V inferred from the Balmer decrement of the starburst nuclei (B83) is $\simeq 1.5$ *mag*. Nevertheless, the NIR observation reported by B83 revealed an old population, in direct contradiction with the young galaxy hypothesis.

A 'composite' galaxy is a system consisting of an old galaxy, as defined above, plus a burst of recent star formation. Simple models for the burst have been computed. A power-law IMF (within the same mass range as for old

† Thuan (1983) estimated a typical $A_V \simeq 0.25$ for CBG's.

galaxy models) was again used. The star-formation rate was taken to be a step function of time, constant for an interval of 1, 2.5, 5, or 10 $\times 10^7$ years and zero otherwise. These intervals are similar to observed cluster-formation times (Hartmann 1970; Schlesinger 1972). Smoothing the step function to a Gaussian did not significantly affect the colors as a function of time. For bursts of duration $\leq 5 \times 10^7$ yr and $\alpha \leq 2.35$, the colors and their evolution are almost independent of the duration and of α, the power index of adopted IMF of starbursts; in other words, they are only sensitive to their relative strength and to their age.

The UBV colors of Markarian galaxies can be accounted for, without any need of reddening, by some sets of composite models, either comprising starbursts of different strength at their brightest stage, or representing the evolution sequences of some 'composite' systems along the life-time and post-life-time of their starburst component. Besides, the looped evolution of these models in the H_β vs. $(U-B)$ plane (due to the different ages of ionizing and non-ionizing massive stars) helps explaining the observational evidence that some of the relatively red Markarian galaxies show strong Balmer emissions, and some relatively blue ones show weak Balmer emissions.

Huchra (1977b) concluded that the composite models fit best the optically observed properties of Markarian galaxies. The contribution of starbursts to the V band light of Markarian galaxies is estimated in the range of 20—50%, corresponding to starburst strengths $b < 0.01$ for the IMF of $\alpha = 2.35$, or $b < 0.001$ if $\alpha = 1.35$.

4.2. Biermann and Fricke's model for optical photometry and radio luminosity

Biermann and Fricke (1977) presented a study on the origin of the radio and optical radiation from Markarian non-Seyfert galaxies. They assumed an

underlying galaxy with $U-B=0.14$, $B-V=0.76$, and $S/L_B=0.128$, where S is the radio flux density (in mJy) at 5GHz, scaled to a standard distance of 20 Mpc; and L_B is the blue light in units of $10^9 L_\odot$. This corresponds to the model 4 of Biermann (1976), which fits the parameters (gas content, M/L_B ratio, deuterium and metal abundances, radio flux and supernova rate) of our Galaxy within a factor of two or better, according to the author.

The Salpeter IMF from 0.1 to 100 $M_\odot$ was used for the starburst, which was assumed to be a step function of time (cf. Huchra 1977b) with a duration of 10^7 yr. With the above assumptions, the only two free parameters are the relative strength of the burst b, given by the ratio of the peak blue light of the burst to the blue light of the galaxy, and the age of the burst t. The influence of the burst was calculated with a time step of 5 10^5 years for the first 10^8 years.

The model for the UV-optical colors of the burst was based on the work of Tinsley (1972), and is not very different from that of Huchra (1977b).

The radio emission was assumed (Biermann 1976) to come either from HII regions (thermal) or from relativistic charged particles originating in supernova remnants (non-thermal). The properties of HII regions were calculated using the model of Mezger and Henderson (1967) with an electron temperature of 8000 K. A total differential output at 5 GHz per SNR of 0.1 Jy-years seen from 20 Mpc distance ($\simeq 6.22 \cdot 10^{34}$ erg/Hz) was adopted, consistent with the results of Clark and Caswell (1976). All supernova remnants were assumed to be equal, although differences associated to different masses of progenitor stars and to different conditions of the outside gas are very likely (Gull 1973; Henning and Wendker 1975). The adopted mass range for supernova progenitors is $< 6.5 M_\odot$. The difference between supernova types I and II was ignored.

Models constructed with different values of the two parameters, b and t, fit the $U-B$ vs. $B-V$ diagram of Markarian galaxies reasonably well. A difference

between the evolution curves of composite models of Huchra (1977b) and those presented here can be found on the $U-B$ vs. $B-V$ diagram: after the death of the burst, the former return directly to the the points representing old host galaxies, while the latter form looped curves. The difference is probably due to the fact that Huchra (1977b) ignored the contribution from red supergiants.

On the other hand, judging from their Fig. 2a, the model provides a poor fit to the $\log(S/L_B)$ vs. $B-V$ diagram of Markarian galaxies. On one hand, most of the data points very far apart from the model loops now turn out to be Seyfert galaxies (e.g. Mkr 1, 3, 6, 231), for which the models are obviously inapplicable (Ulvestad 1982; Wilson 1983). On the other hand, starbursts strong enough to contribute more than 95% to the B light of the galaxies are required to account for the $\log(S/L_B)$ vs. $B-V$ data of non-Seyfert Markarians, in conflict with the results from fits of the UBV colors in the same work (see also the conclusion of Huchra 1977b). This problem could be a consequence of having ignored the non-thermal radiation associated with galactic disks, which, according to Helou et al. (1985), could be more than 10 times stronger than that coming directly from individual SNR's.

4.3. Struck-Marcell and Tinsley's model and the optical-NIR photometry of CBG's

Struck-Marcell and Tinsley (1978) pointed out that $V-K$ colors are in principle much more sensitive than UBV colors to the age of galaxies, an important parameter especially to understand the nature of compact blue galaxies (Searle, Sargent, and Bagnoulo 1973). Furthermore, when a starburst is superposed on an old galaxy model, a much more extended region is covered by loci of models, characterized by different starburst strength b and burst age Δt_b, in the $U-B$ vs. $V-K$ diagram than in the $U-B$ vs. $B-V$ diagram. It is easy to distinguish in a $U-B$ vs. $V-K$ diagram the systems with burst of 10%

strength from the truly young systems ($b \rightarrow \infty$), while this can hardly be done with a UBV diagram.

The models of Struck-Marcell and Tinsley (1978) rely on the galactic evolution code of Tinsley (1972) with a few modifications. The local (solar neighborhood) IMF, based mainly on the studies by Wielen (1974) and Burki (1977), was used. The mass range of the IMF is from 0.1 $M_\odot$ to 30 $M_\odot$. While stars more massive than 30 $M_\odot$ contribute negligibly to the total luminosity and to the UBV colors (Larson and Tinsley 1978, hereafter LT78), the choice of the lower mass limit affects only the calculated mass to light ratios. Actually, the resulting M/L ratios (LT78) had to be multiplied by a factor of two to fit the observational data (Nordsieck 1973). The contribution of red supergiants are estimated from observational data (Harris 1976). No contribution from emission of ionized gas and dust to near-IR emission was taken into account.

$U - B$ and $V - K$ colors of models in which starbursts superposed on a normal galaxy with $U - B = 0.56$ and $V - K = 3.22$, corresponding to the old galaxy model with a single flash of star formation lasting $10^7 yr$ and that occurred $10^{10} yr$ ago (see also LT78), were reported. The starburst was assumed to have a duration of $2 \times 10^7 yr$ and to have the same IMF of the old galaxy. The whole domain of the two parameters, the burst intensity b ($0 \leq b \leq \infty$) and the burst age Δt_b was fully explored. The results showed, for example, that while the difference of $B - V$ of models with $b = 0.1$ and with $b = \infty$ is only 0.04 (LT78), the difference of their $V - K$ is as large as 1.50.

The above models were employed by Thuan (1983) in his optical-NIR study of compact blue galaxies (cf. section 2.3). After a careful investigation of the JHK diagram of his sample, he ruled out significant contributions from re-radiation of dust and from transitions in ionized gas to the NIR emission of CBG's, and concluded that the emission is of stellar origin, consistent with the assumption of Struck-Marcell and Tinsley (1978).

Thuan (1983) found also that the range of predicted $U-B$ vs. $V-K$ colors match well the observed ones. Meanwhile, two points were made:

(1) all CBG's in his sample except for one (Haro 23) lie above the $\Delta t_b = 5\times10^7 yr$ (Δt_b is the age of the starburst) line predicted by models. This might indicate that the majority of the bursts within CBG's observed now have occurred less than $5\times10^7 yr$ ago, consistent with studies of individual CBG's (e.g. Viallefond and Thuan 1983 for Mkr 209). If so, there is not enough time for the stars made in the present burst to evolve into the K and M giants, which are very likely the main contributors to the NIR emission of CBG's (cf. Section 2.2). Thus, *most CBG's must have experienced previous star-formation.*

(2) It can be seen from his Fig. 5 that the data points encompass models with b ranging from ~ 1 (the mass of stars made in the present burst is about equal to that in older stars) to ~ 0.001. Metallicity and internal reddening effects will not change this range much since the metallicity and reddening vectors are nearly parallel to lines at constant b. There seems to be no galaxy blue enough in Thuan's sample to be truly 'young' in the sense that its entire stellar mass was made in the present burst ($b=\infty$), in agreement with the argument based on the age of the burst and stellar main-sequence lifetimes (point (1)). The several galaxies with $b \gtrsim 1.$ are also the most metal-deficient ones in the sample, such as I Zw 18 (with $Z \sim Z_\odot/25$).

As discussed in Section 2.2, the second point made above is not necessarily true in general, since some CBG's, like II Zw 70 and I Zw 18, indeed show evidences of being 'truly young' galaxies in the sense that their present bursts of star formation are the first in their lifetime (Loose and Thuan 1985). The failure of the models in predicting their starburst strengths is likely due to the possibility that their NIR emission comes really from red supergiants.

4.4. A model for optical photometry and FIR luminosity

Markarian galaxies turn out to be remarkably luminous in the FIR (see Chapter 2). Since the FIR radiation is interpreted as thermal emission of dust heated by starlight (Soifer et al. 1987a), it has been proposed that a large FIR luminosity is the result of a high present star formation rate (cf. Chapter 5). A simple photometric model, which permits the computation of the UBV colors and of the FIR luminosities, together with the L_{FIR}/L_B ratios, the H_α equivalent widths ($EW(H_\alpha)$), and the infrared excesses (IRE) of star-forming galaxies, has been developed by Belfort et al. (1987).

The model contains two components: an underlying galaxy and a burst of star-formation. The old galaxy component is based on another model by Mochkovitch and Rocca-Volmerange (1984). The adopted IMF is from Kennicutt (1983):

$$\phi(M) = \phi_0 M^{-1.4} \qquad for \quad 0.1 \leq M < 1 M_\odot \tag{4.2a}$$

$$\phi(M) = \phi_1 M^{-2.5} \qquad for \quad 1 \leq M \leq 100 M_\odot. \tag{4.2b}$$

Different extinction laws were used for massive stars and low mass stars (Mochokovitch and Rocca-Volmerange (1984):

$$E_1(B-V) = e \qquad (M < 20 M_\odot), \tag{4.3}$$

$$E_2(B-V) = e + e' \qquad (M \geq 20 M_\odot), \tag{4.4}$$

where e and e' are free parameters of the model. The FIR luminosity can be calculated from re-radiation from dust heated by stellar UV photons as well as by optical photons, assuming that a $(1-f)$ fraction of Lyman continuum photons are directly absorbed by dust. For $(1-f)$, e, and e', the values to be 0.5, 0.05, and 0.35, respectively, were adopted.

A starburst of duration $\tau = 2 \times 10^7 yr$ was assumed. The IMF for the burst was taken to be equal to that for the underlying galaxy, although there

is some evidence suggesting anomalous IMF's for starbursts (Rieke et al. 1980; Augarde and Lequeux 1985). The burst is defined by its strength b and its age Δt, defined as the time past since its beginning (LT78). The M/L ratio of the burst takes on its minimum value $M/L = 0.005(M_\odot/L_\odot)$ at the end of the burst ($\Delta t = \tau = 2 \times 10^7 yr$), and increases with the age of the burst. The extinction law in the burst $E(B-V)_b$, assumed to be identical for all stellar masses, is a parameter for the models.

In the extreme cases when $E(B-V)_b \geq 3$, no contribution from the burst is added to the optical light of the galaxy, but all to the FIR light. If $b = 1\%$, the possible extreme value for Markarian non-Seyfert galaxies (Huchra 1977b), L_{FIR}/L_B can be ≥ 20 for red underlying galaxies ($(B-V) \sim 1$), but ≤ 10 for blue galaxies ($(B-V) \lesssim 0.6$).

Belfort et al. (1987) applied their model to a sample of active star-forming galaxies, which contained 10 Markarian starburst galaxies and 5 Markarian compact blue galaxies. Rather than giving 'exact' values of b and $E_b(B-V)$, which have probably little meaning in view of the various uncertainties of the study, they simply defined three groups of starburst strength b [small ($b \leq 0.005$), intermediate ($0.005 < b < 0.01$), and large ($0.01 \leq b$)], and indicated an order of magnitude for $E_b(B-V)$. They found 2 Markarian starburst galaxies with 'small' bursts, 5 with 'small to intermediate', 'intermediate', or 'large to intermediate' bursts, and 3 with 'large' bursts. On the other hand, all of Markarian CBG's, together with other CBG's, were found having values of starburst strength of a few percent (very 'large').

A comment on the model is that the emphasis on the effect of internal extinction of starbursts complicates the whole problem. As a consequence, the models can make very few definite predictions. On the other hand, different classes of star-forming galaxies appear to display different amounts of internal

extinction; it would be interesting to study them separately. For example, judging from the data of Balzano (1983), starburst nuclei usually have intermediate internal reddening ($E(B-V) \sim 0.5$); CBG's have rather low internal reddening (French 1980), and active interacting galaxies are quite heavily extinguished (e.g. M82). Markarian non-Seyfert galaxies on the whole, given their relatively bluer colors in comparison to the field galaxies of the same morphological type (Huchra 1977a), are unlikely to have, in general, large internal extinction.

4.5. Sramek and Weedman's model for thermal and non-thermal radio emission

Little can be inferred about the IMF of the starburst from models described above, because optical and NIR colors, emission line equivalent widths, and FIR to optical luminosity ratios are all more sensitive to other parameters such as the strength and the age of the burst, the properties of the underlying galaxies, and so on. Sramek and Weedman (1986) suggested a way to estimate the IMF of the starburst through radio observations. They argued that the thermal radio luminosity arises as a consequence of the total ionizing flux from these stars, and is thereby related to their total mass, while the non-thermal radio luminosity relates the number of supernova remnants, so scales with the number of massive stars. Knowing the total mass and total number of stars within a given mass range specifies the shape of any IMF that is a power law.

Sramek and Weedman (1986) constructed models for thermal and non-thermal radio emission of Markarian galaxies based on the following assumptions: (1) The bursts of star-formation are in progress, so no age effect of the burst needs to be taken into account. (2) The HII regions associated with the burst are ionization bounded, and the absorption of ionizing photons by dust can be ignored (optically thin for *Lyc* photons), thus the total *Lyc* photon production rate by all ionizing stars, UV, is related to the observed thermal radio

flux by $UV = 8.5 \times 10^{49} d^2 f_\nu(4885, T)$ (Osterbrock 1974), d being the distance in Mpc, and $f_\nu(4885, T)$ the thermal radio flux by ionized gas of temperature T at 4885 MHz, in the unit of mJy. (3) Ulvestad's (1982) relation between the non-thermal radio flux and the number of supernova remnants, R, holds:

$$f(1465, NT) = 5.6 \cdot (1465/408)^{\alpha_{NT}+0.75} (d/100)^{-2} R. \tag{4.5}$$

The spectral index α_{NT} of non-thermal radiation is in the range of -0.9——-0.5.

The total *Lyc* production rate UV can be related to the total stellar mass through the formula:

$$UV = N_0 \int_{m(l)}^{m(u)} uv(m) m^{-\beta} \tau(m)\, dm, \tag{4.6}$$

where $uv(m)$ is the *Lyc* production rate by a star of mass m, and $\tau(m)$ is the lifetime over which this emission occurs. Both of $uv(m)$ and $\tau(m)$ can be estimated through stellar evolution models for massive stars. N_0 is in units of yr^{-1} and is the normalizing constant for the star-formation rate. The lower and upper mass limits $m(l)$ and $m(u)$ and the power index β specify the IMF. With the same notation, the supernova rate R (yr^{-1}) is related to the number of massive stars

$$R = N_0 \int_{m(l)}^{m(u)} m^{-\beta}\, dm. \tag{4.7}$$

The sample of starburst regions of Sramek and Weedman (1986) comprises six Markarian starburst nuclei (Mkr 52, 357, 603, 1089, 1259, 1344), two compact blue galaxies (Mkr 59, II Zw 40), and eight giant HII regions in the nearby galaxies M33 and M101. They found that the starburst nuclei can all be interpreted using an initial mass function of the same form, having a conventional slope (in the range 1.5—2.5) and mass limits ($m(l) \sim 6M_\odot$ and $m(u)$ in the

range ~25—40 $M_\odot$). On the other hand, a general deficiency of non-thermal radiation from CBG's and from giant HII regions is found, which, in Sramek and Weedman's (1986) scheme, means a deficiency of supernova remnants in these objects. For CBG's, the result is consistent with that of Klein et al. (1983) and might be interpreted by relatively low magnetic fields (Klein et al. 1983), or as due to very high upper mass cutoffs (see Section 2.2), which in turn may result in high UV/R ratios.

An obvious shortcoming of the model is the neglect of dust absorption of *Lyc* photons. As discussed in Chapter 5, almost all giant HII regions and starburst nuclei show quite substantial UV extinctions. Thus the predicted monochromatic luminosity at 4885 MHz should be significantly lower than the results of Sramek and Weedman (1986), indicating (see their Fig. 7) that the IMF's of starbursts are either flatter than predicted by them (power index $\alpha = 1.5$–2.5), or have higher ($> 40 M_\odot$) upper mass cutoffs.

4.6. Summary

(1) The observational properties (optical and near-IR photometry, radio and FIR luminosity, emission line strength, etc.) of non-Seyfert Markarian galaxies can all be accounted for by a class of models comprising an underlying galaxy superposed by a burst of star-formation.

(2) The duration of the starburst is in the range $1—10 \times 10^7$ yr. Except for very metal deficient CBG's (e.g. I Zw18=Mkr 118), the starburst strength of non-Seyfert Markarian galaxies is generally < 0.01.

(3) Although the maximum effect of a starburst on the observational properties of its host galaxy happens at about its end, significant influence can still show up until $\sim 10^8$ yr after its death.

(4) The IMF of starbursts might be conveniently described by a power law ($\alpha = 1.5$—2.5) with reasonable lower and upper cutoffs.

Chapter 5
A Model for FIR Emission of Markarian Star-forming Galaxies

5.1. Introduction

The *Infrared Astronomical Satellite* (IRAS) survey, with its essentially uniform coverage of almost the whole sky at 12, 25, 60, and 100 μm, has presented a new view of the Universe. One important outcome was the demonstration that most galaxies, and especially spirals and irregulars are strong far-infrared (FIR) emitters (Rowan-Robinson et al. 1984). It has been known from early studies of some prototype star-forming galaxies (NGC 253, M 82, Mrk 171, NGC 7714) that a strong FIR excess is an outstanding property of these sources (Rieke and Low 1975 ; Rieke et al. 1980; Weedman et al. 1981; Gehrz et al. 1983).

The FIR properties of Markarian galaxies have been widely studied in literature, since they have provide the largest, as well as the most homogeneous, pre-IRAS sample for selecting active star-forming galaxies. Xu et al. (1988) found that the IRAS detection rate of non-Seyfert Markarians is as high as $\sim$ 84%, while the detection rate for a complete sample of UGC spiral/irregular galaxies with the same limiting optical magnitude, $m_{Zw} = 14.5$, studied by Franceschini et al. (1988) is 63%. It was also found that most ($\sim$ 90%) Markarian galaxies are more luminous in FIR than in the blue. The mean value of $\log(L_{60\mu m}/L_B)$ (L_B being the luminosity at $0.43\mu m$) turned out to be 0.28 ± 0.03, to be compared with $\log(L_{60\mu m}/L_B) \sim -0.4$ found by de Jong et al. (1984) for Shapley-Ames galaxies.

Optical and FIR luminosities of Markarian galaxies were shown to be tightly correlated: the linear correlation coefficient between ($\log L_B$) and

$\log(L_{60\mu m}$ is $r = 0.85 \pm 0.03$. There is also strong evidence that more luminous Markarians tend to have relatively larger percentages of their output in the FIR. The correlation coefficient between $\log(L_{60\mu m}/L_B)$ and $\log L_{60\mu m}$ for the sample of Xu et al. is 0.66 ± 0.04; the slope of the linear regression is 0.25 ± 0.02.

Three mechanisms may contribute to the FIR radiation in bright extragalactic sources: (1) photospheric emission from stars, (2) synchrotron emission from relativistic electrons spiraling in the sources' magnetic fields, and (3) emission by dust. The dust reradiation is held responsible for the FIR emission of non-Seyfert disk galaxies (Soifer et al, 1987a). The observational evidences supporting this hypothesis include (a) the extended emission in those sources where sufficient resolution can be achieved, (b) the large FIR excesses over the expected photospheric emission or a reasonable extrapolation from the radio spectrum, and (c) the shape of the FIR continuum energy distributions generally quite like that of our own Galaxy, for which a dust-emission origin is well established (Cox et al. 1986).

Here we present a two-component model for FIR emissions of non-Seyfert Markarian galaxies. The warm component is assumed to comprise the emission of dust associated to star-forming regions, heated by the ultraviolet light from young massive stars. The cold component is due to dust dwelling in a galactic disk, heated by the general interstellar radiation field (ISRF). For both components, the contribution from 'very small grains', or rather molecules (Léger and Puget 1984), has been taken into account.

The model is compared with data for the sample of non-Seyfert Markarian galaxies, defined by Xu et al. (1988), as well as for three other samples: (1) the compact blue galaxies (CGB) of Kunth and Sévre (1985), (2) the IRAS selected galaxies of Smith et al. (1986), and (3) the nearby disk galaxies of Hawarden et al. (1986). The reason we consider the 3 additional samples is threefold: (a)

CBG's constitute an important subclass of non-Seyfert Marakarians. They are very likely a class of relatively young and metal deficient star-forming galaxies whose emission is dominated by young massive stars (Kunth et al. 1985). (b) It has been proposed that majority of bright IRAS selected galaxies are star-forming galaxies (Soifer et al. 1985), and the IRAS survey seems to be a very powerful tool for selecting objects of this kind, not hampered by dust extinction, unlike the Markarian survey. It is therefore interesting to compare the FIR properties of sources from the two surveys. (c) A FIR study of similarities and differences between 'normal' disk galaxies and Markarian galaxies will help to understand better the nature of the latter and the star-burst phenomenon.

The model is presented in Section 5.2. The samples used in this work are described in Sect. 5.3. The main results are given in Sect. 5.4. The last section, 5.5, is devoted to a discussion of the model in several astrophysical contexts.

5.2. The model

(1) *The grain model*

The grain model adopted here is a simplified version of that worked out by Mathis et al. (1977, here after MRN77) and refined by Draine and Lee (1984, hereafter DL84).

First, we ignore the difference between the optical properties of graphite and silicates, i.e. we deal with only one component. DL84 found that the difference between the optical properties of the two grain consituents is much smaller than predicted by MRN77 (see also Mathis, Mezger, and Panagia 1983, here after MMP83). Judging from the Fig. 11 of DL84 (the diagram of the Planck averaged emissivity $\langle Q(a,T)\rangle$ vs. temperature T), the $\langle Q(a,T)\rangle$ of graphite and silicates are strongly different from each other only in a relatively narrow range

around $T = 300\,K$. DL84 found only a $\sim 15\%$ difference between the local graphite ($\sim 20\,K$) and silicate ($\sim 17\,K$) temperatures, much smaller than the difference (graphite temperature $\sim 19.2\,K$ and silicate temperature $\sim 10.2\,K$) found by MMP83 using MRN77 model.

Second, we assume a unit absorption efficiency, Q_{UV}, for UV photons radiated by massive stars. The absorption efficiency for optical light Q_λ is approximated as $X_\lambda/(1+X_\lambda)$, where $X_\lambda = \frac{2\pi a}{\lambda}$, a is the grain radius, and λ is the photon wavelength. Thus, when $2\pi a >> \lambda$, $Q_\lambda \sim 1$, and when $2\pi a < \lambda$, $Q_V \simeq \frac{2\pi a}{\lambda}$. For grains' FIR absorption efficiency, (based on the results in Figs. 4b and 5b of DL84) we adopt the expression:

$$Q_{FIR}(\lambda) = \begin{cases} 0.065 \cdot a \cdot \lambda^{-1.7}, & (\lambda \leq 130.9\mu m) \\ 0.065 \cdot a \cdot (\frac{\lambda}{130.9\mu})^{-0.3} \lambda^{-1.7} & (\lambda > 130.9\mu m), \end{cases} \tag{5.1}$$

where λ and a are both in the unit of cm. The corresponding specific FIR cross section of grains per H-atom, is approximated as (cf. DL84's Fig. 9):

$$\sigma_{FIR.H}(\lambda) = \begin{cases} 2.63 \cdot 10^{-28} \cdot \lambda^{-1.7} & (\lambda \leq 130.9\mu m) \\ 2.63 \cdot 10^{-28} \cdot (\frac{\lambda}{130.9\mu})^{-0.3} \cdot \lambda^{-1.7} & (\lambda > 130.9\mu m), \end{cases} \tag{5.2}$$

where $\sigma_{FIR.H}$ is in the unit of cm^2/H-atom. We use MRN77's grain size distribution:

$$p(a) \propto a^{-3.5}. \qquad (a_1 \leq a \leq a_2), \tag{5.3}$$

where $a_1 = 50\mathring{A}$ and $a_2 = 2500\mathring{A}$.

Useful derived quantities are the mean absorption cross section (averaged over the grain size distribution) and the specific cross sections (per H-atom) for UV photons and V-photons ($\lambda = 5500\mathring{A}$):

$$\langle \sigma_{UV} \rangle = \frac{\int_{a1}^{a2} \pi a^2 \cdot a^{-3.5}\, da}{\int_{a1}^{a2} a^{-3.5}\, da} = 3.37 \cdot 10^{-12} \quad (cm^2); \tag{5.4}$$

$$\langle\sigma_V\rangle = \frac{\int_{a1}^{a2} \frac{X_\lambda}{1+X_\lambda}\pi a^2 a^{-3.5}\,da}{\int_{a1}^{a2} a^{-3.5}\,da} = 7.527\cdot 10^{-13} \quad (cm^2), \tag{5.5}$$

$$\begin{aligned}\sigma_{UV,H} =& n_{g,H}\langle\sigma_{UV}\rangle = \langle\sigma_{UV}\rangle\frac{\sigma_{FIR,H}(\lambda)}{\langle\sigma_{FIR}\rangle(\lambda)} \\ &= 1.14\cdot 10^{-21} \quad (cm^2/\text{H-atom});\end{aligned} \tag{5.6}$$

$$\sigma_{V,H} = n_{g,H}\langle\sigma_V\rangle = 2.55\cdot 10^{-22} \quad (cm^2/\text{H-atom}), \tag{5.7}$$

where $\langle\sigma_{FIR}\rangle$ is the size-averaged FIR absorption cross section of grains:

$$\begin{aligned}\langle\sigma_{FIR}(\lambda)\rangle &= \frac{\int_{a1}^{a2} Q_{FIR,\lambda}\cdot\pi a^2\cdot a^{-3.5}\,da}{\int_{a1}^{a2} a^{-3.5}\,da} \\ &= \begin{cases} 7.75\cdot 10^{-19}\cdot\lambda^{-1.7} & (cm^2) \quad (\lambda \le 130.9\mu m) \\ 7.75\cdot 10^{-19}\cdot\lambda^{-1.7}(\frac{\lambda}{130.9\mu})^{-0.3} & (cm^2) \quad (\lambda > 130.9\mu m), \end{cases}\end{aligned} \tag{5.8}$$

and

$$n_{gr,H} = \frac{\sigma_{FIR,H}}{\langle\sigma_{FIR}\rangle} = 3.39\cdot 10^{-10} \qquad (\text{H-atom})^{-1}, \tag{5.9}$$

is the specific number of grains per H-atom. Our $\sigma_{UV,H}$ and $\sigma_{V,H}$ are in excellent agreement with DL84's results (cf. Fig. 7 of DL84).

(2) *The PAH model*

Several evidences suggest that very small grains, which can be transiently heated by single UV or visual photons to temperatures as high as 1000K, are responsible for most of the MIR emission of galaxies. The existence of these small grains has been indicated by the high color temperature of the MIR emission from reflection nebulae (Sellgren 1984) and galactic cirrus (Boulanger et al. 1985), by the 'unidentified features' at 3.3μ, 6.2μ, 7.7μ, 8.6μ, 11.3μ observed in a wide variety of astronomical objects: reflection nebulae, planetary

nebulae and active galaxies (Léger and d'Hendecourt 1987; Allamandola 1984; Willner 1984), and by the anti-correlation between IRAS colors $F_{12\mu}/F_{25\mu}$ and $F_{60\mu}/F_{100\mu}$ of galaxies (Helou 1986). By a spectroscopic study, Léger and Puget (1984) identified them as polycyclic aromatic hydrocarbon (PAH) molecules. Now it is widely accepted that PAH molecules are the main contributors to the MIR emission of galaxies (Cox et al. 1986; Draine and Anderson 1985; Puget et al. 1985; Désert 1986; Helou 1986).

We have adopted the PAH model suggested by Puget et al. (1985). Although there are arguments against the presence of PAH's in HII regions, in view of the possibily that they are destroyed either by UV photons or by interaction with ionized gas (Puget 1987; Ghost and Drapatz 1987), Léger and d'Hendecourt (1987, see also Désert 1986) concluded that, since the majority of PAH are big molecules (consisting of more than 50 atoms), they are strong enough to withstand destruction. Following them, we assume that PAH molecules are present both in HII regions and in the disk.

Following Puget et al. (1985) and Désert 1986, we adopt for PAH's a power-law size distribution with the same slope used for grains but with an amplitude larger by a factor of three, and confined to the range $4\mathring{A}$—$15\mathring{A}$:

$$p_{PAH}(a) \propto a^{-3.5}, \qquad (4\mathring{A} \leq a \leq 15\mathring{A}). \tag{5.10}$$

Since Puget et al. (1985) reported the absorption rate of PAH's only at 700 Å, 2200 Å, and 1 μm, we have chosen the absorption rate at $700\mathring{A}$ as the representative value within HII regions†. From their Fig. 1, we deduce a relation between the cross section at $700\mathring{A}$ and the molecular radius a:

$$\sigma_{PAH}(\lambda = 700\mathring{A}) = 0.043a^2. \tag{5.11}$$

† 700 Åis a good approximation for the mean wavelength of ionizing photons, often taken as half the wavelength of Lyman limit (Mezger 1979).

With the above size distribution, we can compute the average absorption cross section

$$\begin{aligned}\langle\sigma_{PAH}\rangle(\lambda = 700\mathring{A}, a) &= 0.043\frac{\int_{a1}^{a2} a^{-1.5}\,da}{\int_{a1}^{a2} a^{-3.5}\,da} \\ &= 1.725\cdot 10^{-16} \qquad (cm^2)\,,\end{aligned} \tag{5.12}$$

and the specific absorption cross section per H-atom:

$$\begin{aligned}\sigma_{PAH.H}(700\mathring{A}) &= n_{PAH.H}\cdot\langle\sigma_{PAH}\rangle_{700\mathring{A}} \\ &= 9.3\cdot 10^{-23} \qquad (cm^2/\text{H-atom})\,,\end{aligned} \tag{5.13}$$

where $n_{PAH.H}$ is the specific number density of PAH per H-atom.

Puget et al. (1985) didn't report the absorption rate of V-photon by PAH's. However, it is reasonable to assume that the absorption efficiency of PAH for V-band photons is‡.

$$Q_{V.PAH} \propto \frac{a}{\lambda}\,, \tag{5.14}$$

30% of of absorption within galactic disks is attributed to PAH's (Draine and Anderson 1985, Puget 1987, Léger and d'Hendecourt 1987).

The specific emissivity per H-atom of PAH molecules is

$$\begin{aligned}4\pi\epsilon_{PAH,\nu} = \int\int S(\nu',\nu,a)\frac{\pi I_{\nu'}}{h\nu'}2\sigma_{PAH}(\nu',a)n_{PAH.H}p(a)\,d\nu'\,da \\ (erg/sec/\text{H-atom}),\end{aligned} \tag{5.15}$$

where:

‡ from the dipole approximation of Mie's theory in the case of $a/\lambda \lesssim 0.1$, DL84

- $S(\nu', \nu, a)$ is the differential power (in unit of erg/sec/Hz) radiated by a PAH of radius a heated by a photon $h\nu'$.

- $\sigma_{PAH}(\nu', a)$ is the absorption cross section; the factor of 2 takes into account the two surfaces of a molecule.

- $I_{\nu'}$ is the intensity of the heating radiation. For the case of HII regions, we approximate it as a delta function

$$I_{\nu'} = I_w \delta(\nu' - 4.3 \cdot 10^{15}), \tag{5.16}$$

where the frequency $4.3 \cdot 10^{15}$ corresponds to $\lambda = 700\mathring{A}$. For the radiation in the disk,

$$I_{\nu'} = I(r)\delta(\nu' - 5.5 \cdot 10^{14}), \tag{5.17}$$

where the frequency $4.3 \cdot 10^{15}$ corresponds to $\lambda = 5500\mathring{A}$, and I(r) is the intensity of ISRF in the ring of radius r.

We take into account only the contribution from NIR-MIR emission features of PAH's, i.e. we neglect their continuum radiation (Puget et al. 1985). The emitted flux density S can be expressed as

$$S(\nu', \nu, a) = \sum_i \delta_{\nu,\nu_i} \frac{A_i(a)}{\Delta\lambda_i} \int_{T_{min}}^{T_{max}(\nu', a)} \frac{2\pi B_{\nu_i}(T)}{F(T, a)} C(T, a)\, dT, \tag{5.18}$$

where

- ν_i is the effective frequency of the feature i;

- δ_{ν,ν_i} is a step function

$$\delta_{\nu,\nu_i} = \begin{cases} 1 & (\nu_i - 0.5\Delta\nu_i \geq \nu \leq \nu_i + 0.5\Delta\nu_i) \\ 0 & elsewhere. \end{cases}$$

- $A_i(a)$ is the integrated absorption cross section ($A_i = \sigma_i \Delta\lambda_i$) of the feature at ν_i, given by Léger and d'Hendecourt (1987);

○ $\Delta\lambda_i$ is the effective width of the feature;

○ $F(T,a) = \sum_i 2\pi B_{\lambda_i}(T) A_i(a)$ is the power released by a PAH molecule at temperature T, the factor 2 takes into account the two surfaces of a molecule;

○ $C(T,a)$ is the specific heat of PAH, derived from (Léger and d'Hendecourt 1987)

$$C(T,a) = \begin{cases} 3(N_t(a)-2)k(T/1300K), & \text{T¡1300K} \\ 3(N_t(a)-2)k, & \text{T¡1300K} \end{cases}$$

where $N_t(a)$ is the number of atoms contained in a PAH of size a (Puget et al. 1985; Léger and d'Hendecourt 1987):

$$N_t(a) = 2.5 \cdot 10^{16} a^2;$$

○ $T_{max}(\nu', a)$ is the maximum temperature of a PAH molecule of radius a heated by a photon $h\nu'$. It can be derived from

$$h\nu' = \int_{T_{min}}^{T_{max}(\nu',a)} C(T,a)\, dT. \tag{5.19}$$

The derived T_{max} is essentially independent of the choice for T_{min}. In actual calculations we take $T_{min} = 5K$.

The PAH contributions to IRAS fluxes are confined to the 12μ band, which encompasses three PAH emission features (those at $7.7\mu m$, $8.8\mu m$, and $11.3-11.9\mu m$). The predicted intensities of the latter have been convolved with the IRAS response function (IRAS Explanatory Supplement, 1986).

(3) *Warm dust*

Warm dust associated with HII regions is heated by massive stars. Mezger et al. (1979) and Cox et al. (1986) have argued that the main contribution to

the warm FIR radiation of our own Galaxy comes from the dust associated with 'extended HII regions', which correspond to type V/VI HII regions in Israel's classification scheme (Habing and Israel 1982), with typical density of ~ 10 H-atoms/cm^3 (see also Mezger et al. 1982). Their results are consistent with current scenarios for the evolution of HII regions (Smith et al. 1978; Habing and Israel 1979; Güsten and Mezger 1982; Mezger et al. 1982), implying that massive stars spend most ($\sim 90\%$) of their lifetime within extended HII regions; correspondingly 'compact HII regions' ($n_e \gtrsim 10^4$ H-atom/cm^3, type I/II of Israel) and 'radio HII regions' ($n \sim 50 \div 1000$ H-atoms/cm^3, Smith et al. 1978; type III/IV of Israel) are much rarer.

On the other hand, the observed correlation between blue and FIR luminosities, found for Markarians and optically selected galaxies in general, constitutes a direct proof that the bulk of FIR emission of these objects cannot come from compact HII regions, which are characterized by a large visual extinction. Therefore we will concentrate, in following, on dust associated with extended HII regions.

First of all, we assume that the radiation field within such regions is uniformly distributed. That this is a reasonable assumption is indicated by their modest intrinsic visual extinction ($\approx 0.3 mag$, see Cox et al. 1986). Independent, albeit sparse, data confirm that the mean free path of Lyman continuum (Lyc) photons within extended HII regions is of the order of, or smaller than, the average separation of heating stars. Mezger et al. (1982) found an average density of 12 H-atoms/cm^3 for the galactic extended HII regions. The cross section of grains for Lyc photons is $\approx 2 \cdot 10^{-21} cm^2$/H-atoms (DL84). So the mean free path is $r_\tau = 1/(12 \cdot 2 \cdot 10^{-21})\ cm \doteq 13 pc$. In the Orion Aggregate, star counts by Sharpless (1952, see also Reddish 1978) gave about 50 ionizing stars over an area of $100\,pc^2$. Given the size of the aggregate $\sim 100\,pc$, the mean density is $5 \cdot 10^{-3}/pc^3$, corresponding to an average separation of $\sim 6\,pc$. On

the other hand, Balzano(1983) found a typical mass $\approx 10^8 M_\odot$ within starburst nuclei with typical size of about 600 pc. Again, for reasonable choices of the average mass of young massive stars, their average separation turns out to be $\leq 10pc$.

The temperature of a grain in an extended HII region is derived from the energy balance:

$$\pi I_w 4\pi a^2 = \int \pi B_\nu(T^w_{gr}(a)) \cdot Q_{FIR}(a,\nu) \cdot 4\pi a^2 \, d\nu. \qquad (5.20)$$

As discussed above, the UV absorption efficiency of grains has been set to unity. Optical emission lines and the ISRF light are neglected, since both their intensity and their absorption efficiency are much smaller than those for the UV light within HII regions.

The specific emissivity (per H-atom per frequency interval) of warm grains associated with extended HII regions is

$$4\pi\epsilon^w_{FIR,\nu}(\nu) = n_{gr,H} \int_{a_1}^{a_2} \pi B_\nu(T^w_{gr}(a)) Q_{FIR}(a,\nu) \cdot 4\pi a^2 \cdot p(a)\, da, \qquad (5.21)$$

where again $n_{gr,H}$ represents the specific number density of grains per H atom, and $p(a)$ the normalized grain size distribution.

Since the FIR spectrum of our warm component (equation 5.21) depends only on the temperature distribution of warm dusts, which in turn is fully determined by I_w, the UV radiation field within HII regions (cf. equation 5.20), the only parameter for our warm component is I_w.

(4) *Cold dust*

Cold dust is associated with disks of galaxies, and is heated by the ambient interstellar radiation field (ISRF). Following Jura (1982), we assume that both the radiation field and the optical depth of dust follow an exponential law:

$$I = I_0 \exp(-r/r_i); \tag{5.22}$$

$$\tau = \tau_0 \exp(-r/r_\tau). \tag{5.23}$$

For our own Galaxy, MMP83 found both r_τ and r_i (for the disk star component of ISRF) to be $\approx 4pc$. Thus, for simplicity, we assume $r_i = r_\tau = r_0$, in general. I_0, τ_0 and r_0 are free parameters of our model.

The heating rate, $\int \pi I_\lambda Q_\lambda(a) \cdot 4\pi a^2 \, d\lambda$, for dust in the disk is estimated assuming for ISRF photons an effective wavelength $\lambda = 5500\mathring{A}$. This is obviously a crude approximation, but it is hard to do much better in view of the uncertainties on both the ISRF (Mezger et al. 1982; MMP83) and on the physical properties of grains. Thus, the temperature $T(a,r)$ of a dust grain of size a located in the disk at a distance r from the center can be estimated from:

$$\pi I(r) Q_V(a) \cdot 4\pi a^2 = \int \pi B_\nu(T^c_{gr}(a,r)) \cdot Q_{FIR}(a,\nu) 4\pi a^2 \, d\nu, \tag{5.24}$$

where:

$$I = I_0 \cdot \exp(-r/r_0), \tag{5.25}$$

$$Q_V(a) = \frac{X_V}{1+X_V}, \qquad X_V = \frac{2\pi a}{5500\mathring{A}}. \tag{5.26}$$

The differential FIR luminosity, in the unit of erg/sec/Hz, from the disk is

$$\begin{aligned} L^{cd}_{FIR,\nu} &= \int\int \pi B_\nu(T^c_{gr}(a,r)) \cdot Q_{FIR}(a,\nu) \cdot 4\pi a^2 \cdot n_{gr}(r) p(a) \cdot Z(r) \cdot 2\pi r \, da \, dr \\ &= \int\int \pi B_\nu(T(a,r)) Q_{FIR}(a,\nu) 4\pi a^2 \frac{\tau(r)}{\langle \sigma_V \rangle} p(a) \cdot 2\pi r \, da \, dr, \end{aligned} \tag{5.27}$$

where $n_{gr}(r)$ is the number density (per cm^3) of grains, $p(a)$ is the normalized grain size distribution (cf. equation 5.3); $Z(r)$ is the disk thickness at r; and

$$\tau_V(r) = Z(r) \cdot n_{gr}(r) \cdot \langle \sigma_V \rangle = \tau_0 \cdot e^{-\frac{r}{r_0}}, \tag{5.28}$$

is the opacity of the disk at r (cf. equation 5.23), and $\langle \sigma_V \rangle$ is the size-averaged V-band absorption cross-section of grains (cf. equation 5.5).

A glance to equation (5.27) tells us that the *shape* of the FIR spectrum of the cold dust component does not depend on the value of τ_0, nor of r_0 because both appear only as constant multipliers ($T(a,r)$ and τ depend only on r/r_0). Letting $x = r/r_0$, the equation (5.44) can be rewritten as

$$L^{cd}_{FIR,\nu} = r_0^2 \int\int \pi B_\nu(T(a,x)) Q_V(a) 4\pi a^2 \frac{\tau(x)}{\langle \sigma_V \rangle} p(a) \cdot 2\pi x \, da \, dx, \tag{5.29}$$

which clearly shows that the form of the FIR spectrum of the cold dust is determined by only one parameter, I_0.

5.3. The samples

(1) *Markarian galaxies*

Xu et al. (1988) have constructed a complete sample comprising all Markarian galaxies brighter than $m_{zw} = 14.5$ falling in the sky region $|b^{II}| \leq 30°$ and $\delta \leq -2°$. It contains 176 non-Seyfert Markarian galaxies, all having measured redshift. Ten of these galaxies are out of the sky region covered by IRAS; 139 have been detected by IRAS at 60 μm. In Table 5.1 we list the 66 galaxies which have been detected at least at 25 μm, 60 μm and 100 μm; 22 of these were detected in all four IRAS bands. Mkr313 has been excluded since it is

extended at 60 μm (Xu et al. 1988). All FIR data have been taken from the second version of the IRAS point source catalog.

(2) *Compact blue galaxies*

Kunth and Sévre (1985) compiled photometric, spectroscopic, IRAS, and some HI measurements for the 'most studied' compact blue galaxies, taken from various sources. They also collected IRAS data for a sub-sample of blue compact galaxies observed by Klein et al. (1984) at 6.3 cm. We picked from their two samples 26 galaxies detected by IRAS at 25μ, 60μ, and 100μ; 8 of them were detected in all four IRAS bands (Table 5.2).

(3) *IRAS selected galaxies*

From the complete sample of 72 IRAS selected galaxies brighter than $F_{60\mu} = 2$ Jy, defined by Smith et al. (1987, hereafter S87), we have selected the 51 objects which have been detected by IRAS at 25 μm, 60 μm, and 100μm, and show no evidence of being extended at any of these bands (S87). 13 have been detected also at 12 μm (Table 5.3).

(4) *Nearby disk galaxies*

The nearby disk galaxy sample of Hawarden et al. (1986, see also Puxley et al. 1988) comprises 186 galaxies in the Revised Shapley-Ames Catalog of Bright Galaxies (Sandadge and Tammann 1981) with morphological classifications in the Second Reference Catalogue of Bright Galaxies (de Vaucouleurs, de Vaucouleurs and Corwin 1976) between S0/a and Scd (inclusive), excluding Seyfert galaxies and LINERs listed in the catalog of Veron-Cetty and Veron

Table 5.1. The sample of Markarian galaxies.

Mrk	m_{Zw}	E(B-V)	z	$F_{12\mu}$(Jy)	$F_{25\mu}$(Jy)	$F_{60\mu}$(Jy)	$F_{100\mu}$(Jy)
12	12.7	0.03	0.014	0.247	0.325	3.202	7.144
18	14.3	0.03	0.011	<0.250	0.231	2.079	3.180
33	13.2	0.00	0.005	<0.260	0.969	4.786	5.488
35	12.9	0.00	0.004	<0.250	0.923	5.183	6.646
52	12.4	0.01	0.007	<0.349	1.081	4.660	6.126
59	12.8	0.00	0.003	<0.250	0.387	1.836	2.388
86	11.7	0.04	0.001	<0.250	0.296	3.193	6.516
111	13.9	0.04	0.013	<0.250	0.321	2.837	5.894
119	14.1	0.03	0.010	<0.250	0.290	2.182	4.182
133	12.8	0.03	0.007	<0.357	0.539	3.034	5.680
158	13.0	0.01	0.007	0.430	1.189	8.525	12.23
161	13.4	0.00	0.020	<0.250	0.375	2.475	4.116
169	14.2	0.00	0.005	<0.250	0.680	3.614	4.790
171	11.8	0.00	0.010	3.710	21.51	105.8	111.2
188	12.6	0.00	0.007	0.391	0.473	4.811	11.39
190	13.1	0.00	0.003	<0.250	0.438	2.669	5.462
201	13.0	0.00	0.009	0.857	4.357	22.79	25.94
207	13.5	0.01	0.008	<0.250	0.206	2.217	4.204
213	13.2	0.00	0.010	0.248	0.677	3.916	6.843
256	13.2	0.02	0.011	<0.250	0.346	2.878	5.689
281	12.5	0.00	0.008	0.344	0.643	5.287	13.07
286	13.9	0.02	0.027	0.265	0.739	4.431	6.661
297	14.1	0.03	0.016	0.243	0.873	7.042	10.10
307	13.7	0.05	0.019	<0.250	0.223	1.841	4.409
319	14.0	0.06	0.028	<0.314	0.562	4.265	7.302
321	13.5	0.06	0.033	<0.283	0.295	2.684	6.136
323	13.7	0.06	0.015	0.265	0.318	3.014	8.678
325	12.7	0.05	0.012	<0.250	0.505	5.250	6.978
326	13.9	0.05	0.013	0.279	0.755	3.895	6.140
332	12.7	0.03	0.009	0.321	0.636	5.059	10.03
353	14.2	0.01	0.017	<0.310	0.586	3.953	6.195
401	13.6	0.00	0.005	<0.250	0.595	2.537	3.828
404	12.0	0.00	0.004	0.653	1.342	11.85	23.92
432	14.0	0.00	0.011	<0.250	0.416	3.625	6.706
439	12.3	0.00	0.004	0.272	0.718	5.988	11.58
446	14.2	0.00	0.024	<0.250	0.280	1.458	2.617
480	14.2	0.00	0.019	<0.250	0.207	1.807	3.168
496	14.0	0.01	0.029	0.297	1.180	6.491	9.983
531	13.5	0.03	0.013	<0.250	0.510	4.798	7.197
534	13.2	0.03	0.018	0.504	1.149	7.412	9.856

Table 5.1 (continued)

Mrk	m_{Zw}	E(B-V)	z	$F_{12\mu}$(Jy)	$F_{25\mu}$(Jy)	$F_{60\mu}$(Jy)	$F_{100\mu}$(Jy)
538	13.1	0.01	0.010	0.496	2.801	11.230	11.29
545	12.5	0.03	0.016	0.468	1.140	9.151	16.27
582	14.0	0.00	0.019	<0.291	0.536	5.033	9.374
589	14.3	0.01	0.011	<0.250	0.448	2.708	3.542
602	13.2	0.06	0.010	<0.250	0.688	3.604	5.781
691	13.2	0.02	0.011	<0.250	0.536	4.098	7.600
703	13.3	0.03	0.012	<0.297	0.583	4.026	7.009
708	14.0	0.02	0.006	0,307	0.769	5.473	8.281
731	13.4	0.01	0.004	<0.428	0.686	3.046	4.756
759	12.5	0.02	0.007	0.283	0.527	4.202	9.532
761	14.3	0.01	0.014	<0.353	0.531	5.408	11.13
769	12.3	0.01	0.005	<0.375	1.036	8.691	12.40
799	12.7	0.01	0.011	0.518	1.639	10.40	20.49
814	14.4	0.01	0.013	<0.250	0.194	1.538	2.658
839	13.8	0.06	0.013	0.289	0.911	5.194	7.870
861	14.5	0.01	0.015	<0.250	0.249	1.347	2.005
1002	13.5	0.02	0.011	<0.321	0.852	4.944	6.566
1027	14.4	0.03	0.030	<0.316	0.620	5.380	8.476
1101	14.3	0.00	0.034	<0.250	0.248	1.861	3.541
1104	13.6	0.00	0.007	<0.270	0.274	1.461	1.859
1134	14.3	0.06	0.017	<0.288	0.464	4.826	1.031
1224	14.3	0.01	0.050	<0.250	0.535	4.433	7.262
1233	13.9	0.02	0.016	<0.250	0.312	2.834	4.811
1304	13.7	0.01	0.018	<0.250	0.850	3.886	4.508
1365	14.1	0.00	0.018	<0.250	0.710	3.896	5.817
1466	13.1	0.01	0.004	<0.402	1.208	5.979	10.96
1485	12.4	0.00	0.008	<0.637	0.342	2.254	8.597

Table 5.2. The sample of compact blue galaxies.

Name	m_{Zw}	*D(Mpc)	$F_{12\mu}$(Jy)	$F_{25\mu}$(Jy)	$F_{60\mu}$(Jy)	$F_{100\mu}$(Jy)
IIZw40	16.3	10.1	0.46	1.92	6.49	5.68
He2-10	13.0	8.72	1.10	6.55	23.8	25.7
NGC3690	12.5	40.8	3.73	21.6	105.4	110.0
NGC4214	11.1	6.4	0.40	1.76	14.24	24.75
NGC6764		32.0	0.38	1.34	6.41	11.47
IIZw102	15.4	25.0	0.58	1.03	8.98	18.28
NGC7714	13.2	40.0	0.50	2.81	11.1	10.9
Haro1	12.5	50.3	0.44	0.94	8.41	13.23
Mrk1089	13.8	53.0	<0.30	0.70	4.0	5.43
Mrk8	14.2	41.0	<0.30	0.41	2.37	3.82
Mrk33	13.5	21.6	<0.30	0.98	4.73	5.25
Mrk35	13.5	14.5	<0.30	0.93	5.13	6.37
Mrk162	14.6	86.1	<0.30	0.35	1.31	1.58
Mrk1304	14.5	73.0	<0.30	0.86	3.81	4.34
Mrk432	14.1	45.6	<0.30	0.42	3.58	6.44
11924-416		12.0	<0.40	0.51	1.61	1.34
IVZw149	13.9		<0.30	0.55	5.18	6.71
IIIZw107	15.0	73.7	<0.30	0.33	1.49	1.73
Mrk59	15.1	10.6	<0.30	0.42	1.83	2.29
Mrk71	13.8	3.6	<0.30	0.73	3.28	4.38
Mrk86	12.6	7.0	<0.30	0.42	3.15	6.26
Mrk169	14.5	17.4	<0.30	0.68	3.59	4.58
Mrk313	13.2	30.8	<0.30	0.44	3.12	6.55
Mrk401	13.70	22.2	<0.30	0.62	2.49	3.67
Haro2	13.17	20.5	<0.30	0.98	4.73	5.25
Haro3	13.15	13.9	<0.30	0.93	5.13	6.37

* Distances in Mpc ($H_0 = 75$).

Table 5.3. The sample of IRAS selected galaxies.

PSC Name	m_{Zw}	*Vr	$F_{12\mu}$(Jy)	$F_{25\mu}$(Jy)	$F_{60\mu}$(Jy)	$F_{100\mu}$(Jy)
08001+2331	14.2	4647	0.31	0.65	4.05	8.31
08111+2401	15.3	6052	0.24	0.52	3.00	6.61
08322+2838	12.9	2126	0.28	0.39	2.46	6.77
†08323+3003	18.0	17885	<0.11	0.16	3.24	4.75
08327+2855	15.3	7621	0.19	0.37	2.39	3.67
†08354+2555	14.4	5508	0.40	2.20	25.6	27.9
09028+2538	12.7	2670	<0.21	0.63	4.24	8.63
09120+2956	13.8	6313	0.29	0.44	2.22	5.94
09273+2945	13.6	1678	0.27	0.69	2.63	3.99
09534+2727	14.3	1236	0.30	0.50	3.79	7.95
10078+2439	14.6	6365	0.29	0.88	3.78	4.15
10245+2845	12.0	1370	0.17	0.20	2.34	4.22
10369+2659	15.1	5844	0.32	0.43	3.43	6.69
10460+2619	15.7	7687	0.16	0.70	2.32	2.48
†10565+2448	16.0	12926	0.25	1.56	12.8	16.4
11004+2814	11.8	1530	1.45	4.37	23.4	39.3
†11069+2711	17.0	21080	<0.10	0.14	2.56	4.59
11085+2859	14.7	8556	<0.16	0.70	4.38	8.22
†11102+3026	16.0	8788	<0.09	0.12	2.39	4.43
11474+2645	13.0	1737	0.27	0.49	3.48	7.67
11555+2809	14.0	3402	0.23	0.50	3.92	7.72
11561+2743	13.5	3432	0.22	0.20	2.35	6.15
11598+3008	14.4	3174	0.37	0.34	3.89	8.50
12031+3120	15.1	6910	<0.11	0.33	2.19	2.79
12099+2926	14.2	4034	0.38	0.58	5.79	2.78
12159+3005	13.7	3876	0.50	1.71	4.00	5.04
12200+3010	11.6	1004	0.25	0.54	3.96	9.12
12289+2924	14.1	4572	0.28	0.52	3.29	7.62
12341+2442	14.9	6920	0.27	0.45	4.06	5.72
12422+2641	15.3	4544	0.15	0.50	3.39	5.59
12428+2724	13.4	1051	0.15	0.38	3.08	5.25
12590+2934	15.0	7044	0.38	1.59	6.45	7.99
13086+2950	15.3	7252	<0.16	0.23	2.28	4.49
†13126+2452	14.8	3878	<0.11	1.77	19.0	19.1
13387+2331	15.11	8186	0.26	0.89	4.85	7.18
13408+3035	14.5	10407	0.20	0.42	2.59	5.99
13532+2517	15.5	8856	<0.17	0.44	2.26	2.75
14026+3058	15.5	7578	<0.13	0.40	2.97	5.14
†14158+2741	16.0	20902	<0.10	0.14	2.60	4.37
14165+2510	15.3	5278	0.25	0.43	3.57	8.16

Table 5.3 (continued)

PSC Name	m_{Zw}	*Vr	$F_{12\mu}$(Jy)	$F_{25\mu}$(Jy)	$F_{60\mu}$(Jy)	$F_{100\mu}$(Jy)
14221+2450	14.5	5087	0.35	0.95	5.40	9.02
14280+3126	13.4	3582	0.84	1.61	11.9	25.1
14356+3041	15.0	10408	0.20	0.57	2.52	3.46
14547+2448	14.6	10166	0.33	0.57	7.04	16.7
†15018+2417	16.5	20685	<0.11	0.38	3.05	4.16
15327+2849	13.2	2021	0.14	0.25	2.66	5.74
†15327+2340	14.4	5563	0.70	11.0	111.	126.
15373+2506	15.1	6869	0.14	0.71	2.38	3.39
15566+2657	14.9	4265	0.20	0.95	3.26	3.43
16403+2510	15.4	6873	<0.15	0.37	2.91	5.26

* Recession velocities in the units of km/sec.
† Ultraluminous IRAS galaxies (see text).

(1985). These galaxies have been detected by IRAS in all four bands. Extended sources and cirrus-contaminated sources have been excluded by the authors.

5.4. Results

Figures 5.1*a* and 5.1*b* compare the FIR color-color diagrams predicted by our model, with the observational data for Markarian galaxies. The filled squares correspond to detections, the triangles to upper limits at $12\mu m$.

For all figures we have used the disk model specified by $I_0 = 10I_{local}$, where I_{local} is the intensity of the ISRF in the solar vicinity (MMP83). Its color temperatures ($T_c(25\mu$—$60\mu) = 25.4$K and $T_c(60\mu$—$100\mu) = 23.2$K) agree very well with the results found by Sodroski et al. (1987) for the disk of our Galaxy.

Table 5.4. Models for the cold component (see text).

$\frac{I_0}{I_{local}}$	$\log \frac{F_{12\mu}}{F_{25\mu}}$	$\log \frac{F_{25\mu}}{F_{60\mu}}$	$^{\dagger}T_c(25\mu$–$60\mu)$	$\log \frac{F_{60\mu}}{F_{100\mu}}$	$^{\dagger}T_c(60\mu$–$100\mu)$
5	3.73	-4.48	(22.8)	-0.883	(20.9)
*10	2.85	-3.83	(25.4)	-0.688	(23.2)
15	2.40	-3.49	(27.0)	-0.583	(24.6)
20	2.10	-3.25	(28.3)	-0.512	(25.7)

* The model used in this paper.
† The color temperature, assuming ν^2 dependence for dust emisivity.

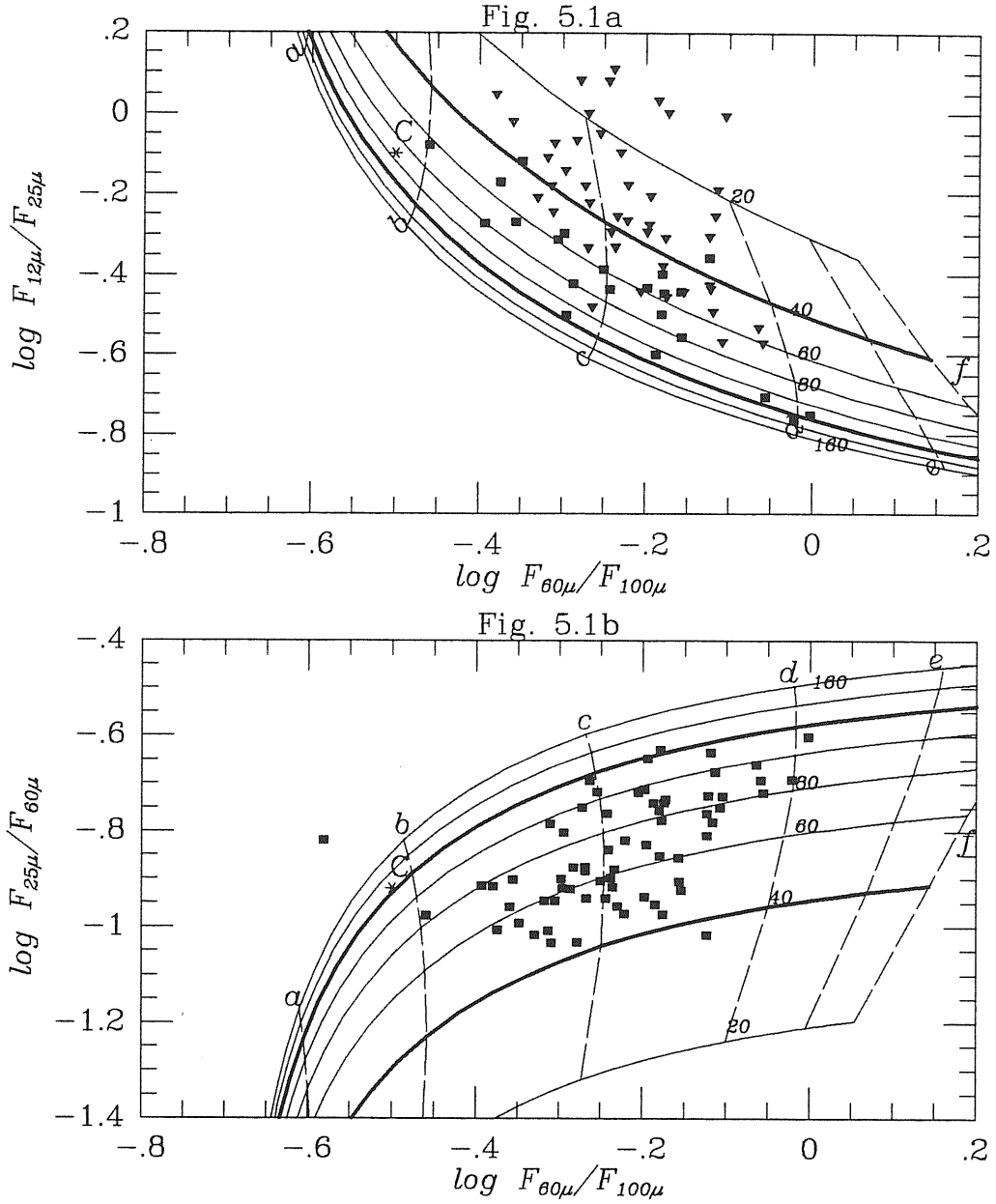

Fig. 5.1a. *The* $\log L_{12\mu}/L_{25\mu}$ vs. $\log L_{60\mu}/L_{100\mu}$ *diagram of Markarian galaxies*

Fig. 5.1b. *The* $\log L_{25\mu}/L_{60\mu}$ vs. $\log L_{60\mu}/L_{100\mu}$ *diagram of Markarian galaxies*

Solid squares are detected data; solid triangles are upper limits. Point C (the star) is the 'warm cirrus' (Boulanger et al. 1985). Solid lines are models with fixed I_w; from top to bottom for Fig. 5.1a., and from bottom to top for Fig. 5.1b.: I_w = 20, 40, 60, 80, 100, 120, 140, 160 × I_{local}. Dashed lines are models with fixed $R_{w/c}$; line *a*: $R_{w/c} = 0.1$; line *b*: $R_{w/c} = 0.3$; line *c*: $R_{w/c} = 1$; line *d*: $R_{w/c} = 3$; line *e*: $R_{w/c} = 10$; line *f*: $R_{w/c} = \infty$.

Some other disk models (Table 5.4) are investigated. Their color temperatures are not very different with each other. Our results are only weakly sensitive to different choices for I_0.

The solid lines are model families with constant I_w, the intensity of the radiation field within HII regions, but different relative contributions from the disk component and from the warm component, measured by the FIR luminosity ratio

$$R_{w/c} = \frac{L_{FIR}^{wd}}{L_{FIR}^{cd}}$$

where L_{FIR}^{wd} and L_{FIR}^{cd} are the total FIR luminosities (from 10 μm to 1000 μm) of the warm component and of the disk (cold) component (the MIR emission from PAH molecules associated to them is included), respectively. The dashed lines are model families of constant $R_{w/c}$.

It is very interesting to notice that the lines of constant $R_{w/c}$ correspond to almost constant $F_{60\mu}/F_{100\mu}$, when the latter ratio is < 1 (Fig. 5.1a), as a consequence of the fact that the cold component peaks around $100\mu m$, and the warm component peaks around $60\mu m$. Hence $F_{60\mu}/F_{100\mu}$ is a direct measure of $R_{w/c}$.

On the other hand, the $F_{25\mu}/F_{60\mu}$ ratio depends both on I_w and $R_{w/c}$. The falling-down of the predicted $F_{25\mu}/F_{60\mu}$ when $F_{60\mu}/F_{100\mu}$ is small (Fig. 5.1b) is due to the growing contribution from the cold component, relative to the warm component, to the $60\mu m$ flux.

The fast rise of the predicted $\log F_{12\mu}/F_{25\mu}$ when $\log F_{60\mu}/F_{100\mu}$ decreases (Fig. 5.1a) is a direct result of our assumption that the dominant contribution to $12\mu m$ flux comes from the emission lines of PAH molecules (Puget et al. 1985; Désert 1986).

Almost all Markarian galaxies locate in a region bounded by $-0.5 \leq \log R_{w/c} \leq 0.5$ (i.e. between the two dashed lines labelled b and d), and $40 \geq I_w/I_{local} \geq 120$ (i.e. between the two heavy continuous lines). Outside this region are only detected data points of three galaxies. One is Mkr 1485=NGC 5350†, whose anomalous colors may be due to contamination by other sources in the same galaxy group (around NGC 5353: MB86; Markarian et al. 1981). The other two are Mrk 538 (on the right hand side both in Fig. 5.1a and in Fig. 5.1b) and Mrk325 (in the upper part of Fig. 5.1a, and in the lower part of Fig. 5.1b). Mrk 538 is a Sdmp galaxy (Huchra 1977a; MB86) with a starburst nucleus (Balzano 1983); Mrk 325 is a clumpy irregular galaxy (Casini and Heidmann 1976) with violent star-formation, probably induced by tidal interaction with Mkr326 (Duflot-Augarde and Alloin 1982).

The mean $\log F_{60\mu}/F_{100\mu}$ of Markarian galaxies is -0.226 ± 0.013; the mean $\log F_{25\mu}/F_{60\mu}$ is -0.841 ± 0.014; and the mean $\log F_{12\mu}/F_{25\mu}$ is -0.508 ± 0.036. The last flux ratio has been derived using the Kaplan-Meier estimator (Schmitt 1985; Feigelson and Nelson 1985) which allows to take into account also the information content of upper limits.

The anti-correlation between $F_{12\mu}/F_{25\mu}$ and $F_{60\mu}/F_{100\mu}$ and the positive correlation between $F_{25\mu}/F_{60\mu}$ and $F_{60\mu}/F_{100\mu}$ exhibited by data points are successfully accounted for by our model.

The above mean FIR flux ratios are obtained for $I_w = 72 I_{local}$ and $R_{w/c} = 1$. Fig. 2 shows the corresponding average FIR spectrum (normalized to the flux at $60\mu m$). The error bars represent only the statistical errors around the mean.

In addition, we have used the data reported by Krügel et al. (1988a, 1988b) to derive the average $F_{1.3mm}/F_{60\mu}$ ratio for Markarians. Twenty-four

† Its upper limit $F_{12\mu}/F_{25\mu} < 1.86$ is the only one outside the scale of Fig. 5.1a.

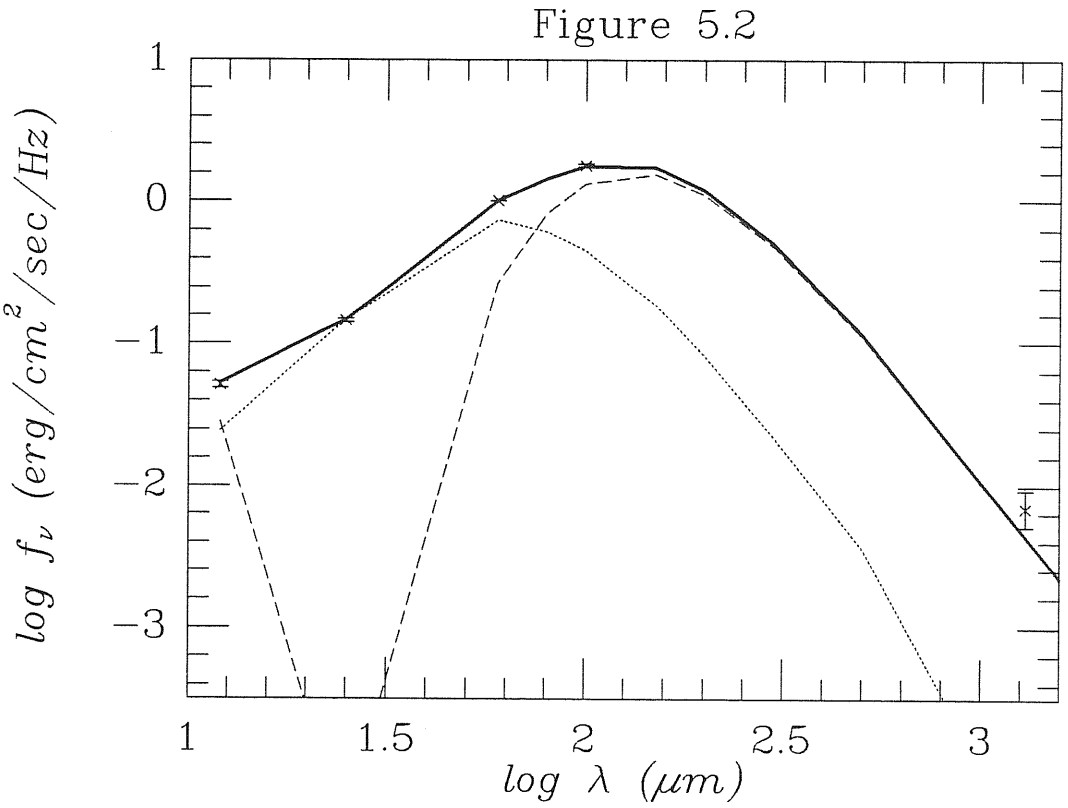

Fig. 5.2. *The average FIR spectrum of Markarian galaxies*

Heavy solid line: the global FIR spectrum of the best-fit model; dotted line: the warm component; dashed line: the cold component. Crosses with error bars: the average observed spectrum of Markarian galaxies.

Markarian galaxies brighter than 10 Jy at $100\mu m$ were observed with the 30m Millimeter Radio Telescope (MRT) (Baars et al. 1987) on Pico Veleta, Spain, using the bolometer system developed at the Max-Planck-Institut für Radioastronomie (MPIfR) (Kreysa 1985). The beam size was $11''$. The sample contains eight Seyferts or possible Seyferts and nine starburst galaxies, according to MB86. Since the aperture of mm observations is much smaller than both that of IRAS at $100\mu m$ ($3'.0 \times 5'.0$, Neugebauer et al. 1984) and of the optical sizes of the sources (H77a), we applied an aperture correction. To this end, the extent of the emitting region was assumed to match the photometric sizes (H77a), when available. Otherwise, the sizes reported by Markarian and collaborators were used (MB86 and references therein). The uncertainty introduced by the correction is not included in the error bar shown in Fig. 5.2.

$R_{w/c} = 1$ means that, on the average, warm dust associated to star-forming regions and cold dust associated to the galactic disk contribute equally to the FIR emission of Markarian galaxies. From Fig. 5.2 we can see that the warm component contributes dominantly at wavelength shorter than 80 micron, while cold dust dominates at longer wavelengths. The ratio between contributions from two components in the ranges 25—$100\mu m$ and 60—$100\mu m$ are $L^{wd}_{25-100}/L^{cd}_{25-100} = 1.2$, and $L^{wd}_{60-100}/L^{cd}_{60-100} = 0.54$, respectively, where L^{wd} denotes contribution from the warm component, L^{cd} from the cold component.

The above results may be biased in favour of warmer far–IR spectra, as a consequence of having included in our sample only those sources detected by IRAS at least at 25 μm, 60 μm, and 100 μm. As a check on this possibility, we have used the Kaplan-Meier estimator, which allows to take into account also the information content of upper limits, to estimate the average FIR spectrum of the complete Markarian galaxies' sample of Xu et al. (1988). No significant differences have been found. Furthermore, the mean FIR flux ratios reported here are in good agreement with the results of Franceschini et al. (1988) for the UGC starburst/interacting galaxies sample.

For Markarian starburst galaxies Sekiguchi (1987) finds the average spectral indexes $\alpha_{60\mu/25\mu} = 2.02 \pm 0.16$, $\alpha_{100\mu/60\mu} = 0.71 \pm 0.31$. The corresponding best-fit model has $I_w = 75 I_{local}$ and $R_{w/c} = 1.5$, and yields the following luminosity ratios between warm and cold components: $L^{wd}_{25-100}/L^c d_{25-100} = 1.6$, and $L^{wd}_{60-100}/L^{cd}_{60-100} = 0.66$. So, at variance with previous conclusions (see Soifer et al. 1987a and references therein), we find that *the FIR emission of Markarian galaxies (including those with starburst nuclei) at wavelengths longer than* $60\mu m$ *is dominated by the cold dust component associated with the galactic disk, rather than by the warm component associated with star-forming regions.*

In Figs. 5.3*a* and 5.3*b*, we show, for comparison, the IRAS data for other samples (triangles are always upper limits). Compact blue galaxies (open squares and open triangles) generally locate in the region where our model predicts relatively high $R_{w/c}$ and high I_w. It must be recalled, however, that compact blue galaxies usually are not disk galaxies. They have neither a conspicuous population of old stars, nor normal galactic disks (Searle and Sargent 1972, Searle, Sargent and Bagnuolo 1973, Thuan and Martin 1981). Thus our FIR model might not be straightforwardly applicable to them. In any case, our model results are consistent with their intrinsic properties. The high $R_{w/c}$ is compatible with the relative weakness of their old star population. The large I_w may be due, on one side, to their relatively high density of massive stars, and, on the other side, to their low metallicity (Thuan 1983) and consequent low extinction within their extended HII regions.

IRAS galaxies (starred squares, and starred triangles) have larger dispersions on FIR color-color diagrams than Markarian galaxies, consistent with being a mixture of widely different populations, ranging from extremely active interacting systems like Arp 220, to normal disk galaxies (see Soifer et al. 1987 for a review). Particularly noteworthy is the sub-group of galaxies located on the lower right–hand corner of the $F_{25\mu}/F_{60\mu}$ vs. $F_{60\mu}/F_{100\mu}$ diagram. Their

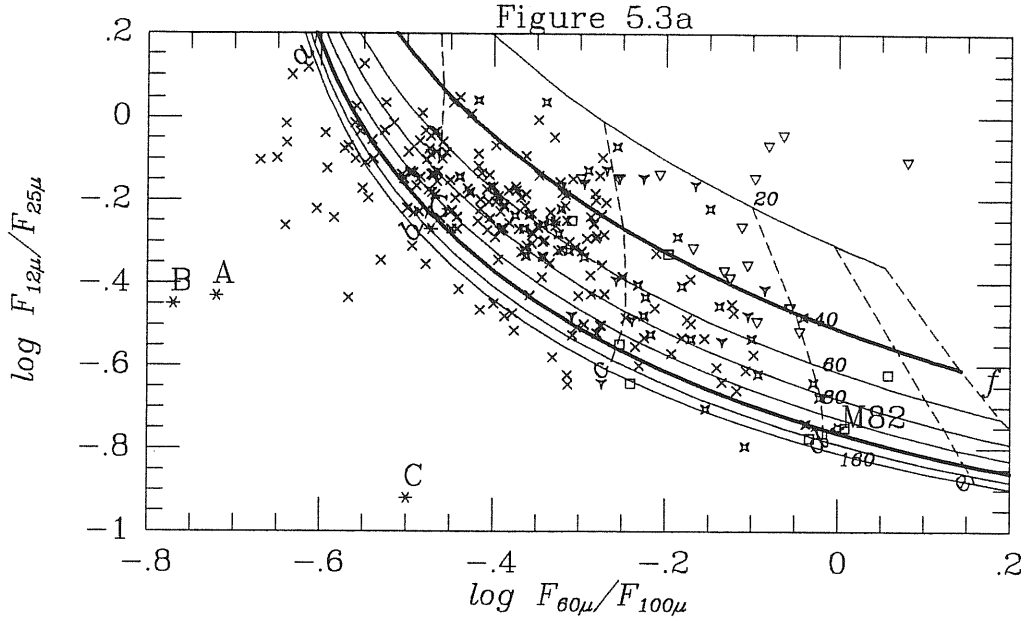

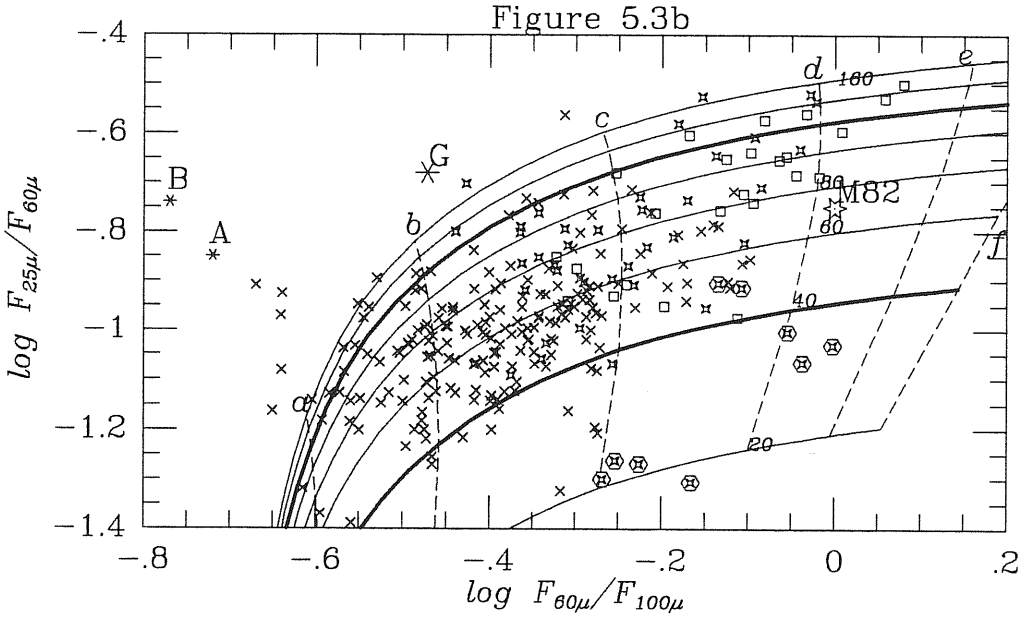

Fig. 5.3a. *The* $\log L_{12\mu}/L_{25\mu}$ vs. $\log L_{60\mu}/L_{100\mu}$ *diagram of other samples*

Fig. 5.3b. *The* $\log L_{25\mu}/L_{60\mu}$ vs. $\log L_{60\mu}/L_{100\mu}$ *diagram for other samples*

×: detected data of nearby disk galaxies; open squares: detected data of compact blue galaxies; open triangles: upper limtis of compact blue galaxies; starred square: detected data of IRAS selected galaxies; starred triangles: upper limits of IRAS selected galaxies; encircled starred squares: ultraluminous IRAS selected galaxies (see text). Star (G): data of the inner part of the Galaxy (Cox and Mezger 1987). Fat star (M82): data of M82 (Telesco and Harper 1980).

$F_{60\mu}/F_{100\mu}$ colors are relatively warm, but the $F_{25\mu}/F_{60\mu}$ colors are very cold. It turns out that the seven data points which are below the curve $I_w = 40\, I_{local}$ and rightward of the curve $R_{w/c} = 1$ (the dashed line c), together with the two other encircled squares which are a bit above them in the figure, are the nine galaxies with the largest L_{FIR}/L_{op} ratio in the IRAS selected sample. They are also among the brightest IRAS galaxies: their $L_{60\mu m}$ are higher than 4×10^{10} $L_\odot$ for $H_0 = 100$ (S87), or 1.6×10^{11} $L_\odot$ for $H_0 = 50$. Of the seven galaxies with $L_{60\mu m} \geq 10^{11}$ $L_\odot$ ($H_0 = 100$) in the sample of S87, six are in this sub-group.

There are evidences that almost all of the brightest FIR galaxies are interacting (Sanders et al. 1987), and their ultraluminous FIR emissions are very likely due to violent star-formations triggered by interactions (Soifer et al. 1987, Rieke 1988). It has been argued that the extinction in their star-forming region must be enormous ($A_V \gtrsim 30\, mag$, Rowan-Robinson 1986). If so, they may be optically thick even at MIR wavelengths (the local extinction at $10\mu m$ is about 1/15th of the visual extinction, and at $25\mu m$ about 1/70th: DL84). Then, the simple model considered in this work does not apply and a substantial fraction of the MIR emission may be absorbed and re-emitted at longer wavelengths.

On the other hand, Chini et al. (1987), based upon a compilation of IRAS data, together with near-IF data and 1.3 mm band data obtained by their own surveys (Chini et al. 1986b, 1986c), reported a set of average infrared spectra for compact galactic HII regions, ionized by different types of star: from early O's to early B's. In the wavelength range of our interest ($\geq 10\mu m$), no significant difference could be found between these spectra. Fig. 5.6 shows an example of them, superposed on the average far-IR spectrum of the nine ultraluminous IRAS galaxies mentioned above[†]. The two spectra indeed coincide with each other reasonably well, as is expected from the above discussion.

[†] The error bars only indicate the statistical uncertainties, no systematic error is taken into account

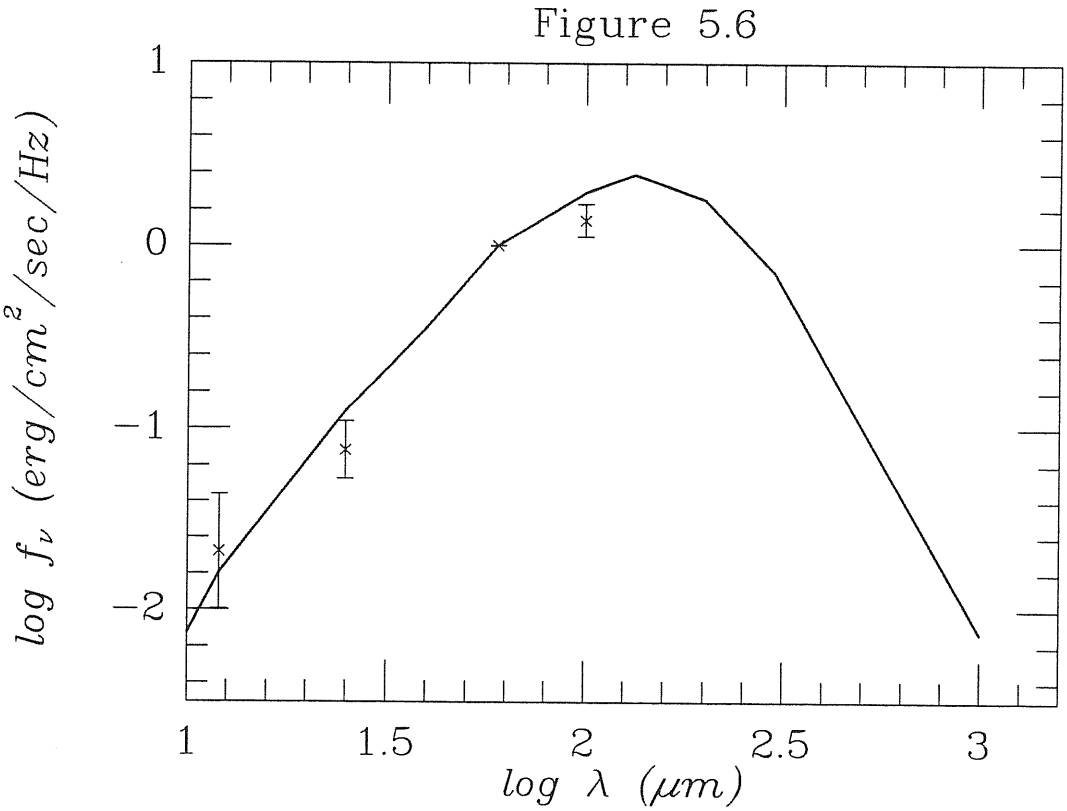

Fig. 5.6. *The average FIR spectra of compact HII regions and ultraluminous IRAS galaxies*
Solid line: the average observed FIR spectrum of compact HII regions (Chini et al. 1987). Crosses with error bars: the average observed spectrum of ultraluminous IRAS galaxies.

On FIR color-color diagrams, the data points of nearby disk galaxies apparently locate in a region of low $R_{w/c}$. Their warm component is usually smaller than the cold component ($R_{w/c} < 1$).

The FIR data for the inner part ($R < 8\,Kpc$) of our own Galaxy is taken from Fig. 2 of Cox and Mezger (1987). In the $(F_{25\mu}/F_{60\mu})$ vs. $(F_{60\mu}/F_{100\mu})$ diagram, it lies above the region of normal spirals. The FIR data for M82, a prototype star-forming galaxies (Rieke et al. 1980), is taken from Telesco and Harper (1980).

5.5. Discussions

(1) *Space density of massive stars*

As discussed in the previous section, our models are defined by two parameters: the intensity of the radiation field within HII regions I_w, and the ratio between the contributions from the warm component and from the disk component to the total galaxy FIR emission, $R_{w/c}$. It is important to investigate informations about the star-forming activity of galaxies carried by these two parameters.

Obviously I_w is a quantity related to the internal structure of star-forming regions. However, effects of the geometry of extended HII regions are unlikely to be important, since they are likely optically thick for UV photons. In the $\langle n_e^2 \rangle^{1/2}$ vs. d (the size of HII regions) diagram (their Fig. 2) of Habing and Israel (1979), all the giant and supergiant HII regions (type V and type VI in Israel's (1976) classification) lie above the line $\langle n_e^2 \rangle^{1/2} d = 300\ pc/cm^3$. For a normal dust/gas ratio, this indicates that the optical depths of giant and supergiant HII regions for UV photons are larger than two. Another evidence suggesting that star-forming regions are optical thick for UV photon can be found from the

sample of starburst nuclei by Balzano (1983): their median Balmer decrement is $L(H_\alpha)/L(H_\beta) = 5.3$, corresponding to a $\sim 7\ mag$ extinction in UV and to a $\sim 1.6\ mag$ extinction in the visual. Even if half of the extinction occurs in the disk, the UV extinction within HII regions is still substantial.

For an optically thick medium, the intensity of the radiation field I can simply be determined from the local energy balance

$$4\pi\epsilon = 4\pi I \cdot n \cdot \sigma_{_H}, \tag{5.30}$$

where ϵ is the emissivity, n is the H-atom density, $\sigma_{_H}$ is the specific absorption cross section of dust in units of cm^2/H-atom. Given the H-atom density and a starburst model, we can derive from I_w the massive star density within star-forming regions. The starburst model adopted here is described in Appendix A. With the conventional assumption of a power-law IMF with index p ranging from 2.5 to 1.5 (Sramek and Weedman 1986), and $n = 10$ H-atoms/cm^3 (Mezger et al. 1982; Habing and Israel 1979), we find that values of I_w/I_{local} in the interval 40—120 (encompassing essentially all non–Seyfert Markarians) correspond to massive star densities within star-forming regions in the range $8.7\cdot10^{-3}$—$2.6\cdot10^{-2}\ pc^{-3}$ (for the $p = 2.5$), or $1.8\cdot10^{-2}$—$5.5\cdot10^{-2}\ pc^{-3}$ (for the $p = 1.5$). The mean I_w ($\simeq 72 I_{local}$) of non-Seyfert Markarian galaxies corresponds to a massive star density of $\sim 1.5\cdot10^{-2}\ pc^{-3}$ for the $p = 2.5$, consistent with the estimate from data on starburst nuclei (see Sect. 5.2).

Again, the situation may be different for compact blue galaxies. There are evidences that CBG's are rather metal deficient (Thuan and Martin 1982; Thuan 1983): their metallicity is about a factor of five below normal, although with a large dispersion. Thus they are generally optically thin in the visual band. An average decimal reddening coefficient of H_β: $c(H_\beta) = 0.49$ with a dispersion of 0.33 can be found for the compilation of data on the 'most optically studied blue compact galaxies' by Kunth and Sévre (1985). It corresponds to

$A_V \simeq 0.5$ and $A_{UV} \sim 2$. The assumption that the star-forming regions are optically thick in the UV is only marginally applicable for CBG. On the other hand, if metals are underabundant by a factor of five, the deduced massive star density, if our FIR model is applicable to CBG, must be reduced by the same factor. In fact, as shown by equation (5.30), the emissivity (which is proportional to the massive star density) is a linear function of the specific absorption cross section, which, in turn, is proportional to the metal abundance, for normal dust-production efficiency.

(2) *L_{FIR}/L_{op} vs. $F_{60\mu}/F_{100\mu}$ diagram and starburst strength*

By definition $R_{w/c}$ should measure the strength of the starburst activity. Following Larson and Tinsley (1978), we define the starburst strength parameter, b, as follows:

$$b = \frac{\text{mass involved in starburst}}{\text{total mass of the galaxy}} \quad . \tag{5.31}$$

The starburst model can be used to estimate the mass to luminosity ratio of the warm component $(M/L)_w$. Adopting the local M/L for the disk component $(M/L)_c$, we can then relate the bolometric luminosity ratio $L^{wd}_{bol}/L^{cd}_{bol}$ to b. On the other hand, while L^{wd}_{bol} is easily estimated ($L^{wd}_{FIR}/L^{wd}_{bol} \sim 1$), to derive L^{cd}_{bol} we need to know the ratio L^{cd}_{FIR}/L^{cd}_{op}, which depends strongly on the the optical depth, τ, of the disk (de Jong and Brink 1986).

In Appendix B we conclude that the FIR to optical luminosity ratio of the disk, L^{cd}_{FIR}/L^{cd}_{op}, can be well approximated by

$$\frac{L^{cd}_{FIR}}{L^{cd}_{bol}} = \frac{\tau_0^{0.9}}{4} \tag{5.32}$$

where τ_0 is the optical depth at the center of the disk (see equation 5.5).

The inclination effect is taken into account, replacing τ_0 with $\tau = (a/b)\tau_0$, a and b being the major and minor axis of a galaxy, respectively. We adopt $(a/b) = 1.6$ as a representative value (de Jong and Brink, 1986). The local M/L ratio is about 0.97 $M_\odot$ $/L_\odot$ in the visible band (Mihalas and Binney 1981). Using data reported in Allen (1976), a bolometric correction of a factor of ~ 3 is found for a population of stars like that in the solar neighborhood.

Two different starburst models (model A and B), characterized by different power indexes for the IMF ($p = 2.5$ and $p = 1.5$) are used in this work. $(M/L)_w = 7.8e-4$ is found for model A ($p = 2.5$), and $(M/L)_w = 2.5e-4$ for model B ($p = 1.5$). To estimate the L^{wd}_{FIR}/L^{wd}_{op} ratio, the dust extinction of optical light is taken into account assuming that half of the reddening indicated by the median Balmer decrement of starburst galactic nuclei, $L(H_\alpha)/L(H_\beta) = 5.3$ (Balzano 1983), occurs in the starforming region. For both model A and model B, we find $(L^{wd}_{FIR}/L^{wd}_{op}) \simeq 0.02$.

In the framework of our model, the ratio L_{FIR}/L_{opt} for a galaxy can be derived from

$$\frac{L_{FIR}}{L_{opt}} = \frac{1 + R_{w/c}}{\left(\frac{L^{cd}_{opt}}{L^{cd}_{FIR}}\right) + R_{w/c}\left(\frac{L^{wd}_{opt}}{L^{wd}_{FIR}}\right)} \quad . \tag{5.33}$$

The starburst strength b is obtained from

$$b = R_{w/c}\frac{\left(\frac{L^{cd}_{FIR}}{L^{cd}_{tot}}\right)}{\left(\frac{L^{wd}_{FIR}}{L^{wd}_{tot}}\right)}\frac{\left(\frac{M}{L}\right)_{wd}}{\left(\frac{M}{L}\right)_{disk}}, \tag{5.34}$$

where $L_{tot} = L_{FIR} + L_{op}$.

Thus, given the starburst model, the FIR to optical luminosity ratio, L_{FIR}/L_{op}, of a model galaxy depends only on the optical depth of its disk

and on its $R_{w/c}$ parameter. So does its starburst strength b. In Fig. 5.4a and 5.4b, we plotted our model predictions on $\log L_{FIR}/L_{op}$ vs. $\log F_{60\mu}/F_{100\mu}$ diagrams. The starburst model A ($p = 2.5$) is used in Fig. 5.4a, whereas model B ($p = 1.5$) is used in Fig. 5.4b. The dashed and solid curves correspond to models with different values of disk extinctions τ or starburst strength b, respectively. Each curve is labelled with the appropriate values of τ or b.

As for data points, the optical fluxes are estimated from (Lang 1980)

$$F_{opt} = 2.52 \cdot 10^{-5} \cdot 10^{-0.4(B-(B-V)-B.C.)} \quad (erg/cm^2/sec), \tag{5.35}$$

where $B.C.$ is the bolometric correction for the stellar component of galactic light; the radiation from interstellar medium, like the FIR radiation by dust, is not taken into account. According to Soifer et al. (1986), for Markarian galaxies, $B - V = 0.5$, $B.C. = 1.2$; for normal disk galaxies, $B - V = 0.8$, $B.C. = 0.9$. For IRAS selected galaxies, we adopt the value $(B - V) + B.C. = 1.7$. The mean color index of compact blue galaxies is derived from the sample of Thuan (1983) as $B - V = 0.40 \pm 0.14$. The bolometric correction for their stellar light is estimated from the mean $V - K$ (Aaronson 1977; Soifer et al. 1986) of the same sample, which is 1.74 ± 0.94. The corresponding $B.C.$ (Johnson 1966) is ~ 0.1.

The FIR fluxes F_{FIR} are estimated from their $F_{60\mu}$ and $F_{100\mu}$ IRAS data (Soifer et al. 1986):

$$F_{FIR} = C \cdot 1.26 \cdot 10^{-11} \cdot (2.85F_{60\mu} + F_{100\mu}) \quad (erg/cm^2/sec) \quad . \tag{5.36}$$

Our model yields an average value of $C \simeq 1.8$, to be compared with the value 1.5 used by Soifer et al. (1986), 1.75 by Boulanger et al. (1985) and 1.8 by Kunth and Sévre (1985).

The mean value of the logarithm of the FIR to optical luminosity ratio, $\log L_{FIR}/L_{op}$, of Markarian galaxies is -0.11 ± 0.28. The ratio is about a factor

of 2.5 below the mean L_{FIR}/L_B of non-Seyfert Markarian galaxies found by Xu et al. (1988), mainly due to the difference between the definitions of L_{op} and L_B. For CBG's, $\log L_{FIR}/L_{op}$ is 0.56 ± 0.42; for IRAS selected galaxies, it is 0.35 with a dispersion of 0.52; for nearby disk galaxies, it is -0.54 with a dispersion of 0.46. The relatively large mean $\log L_{FIR}/L_{op}$ of CBG's is apparently due to their small $B-V$ and $B.C.$.

Our model prediction for the mean value of the visual extinction in the disks of Markarian galaxies is $\tau_0 \simeq 0.8$, with a dispersion of about a factor of 3. This value is consistent with the observed mean Balmar decrement. (Balzano 1983). The predicted values of starburst strengths are in the range 10^{-4}–3×10^{-3} for starburst model A ($p = 2.5$) and $3.\times10^{-5}$–10^{-3} for starburst model B ($p = 1.5$). These values are lower than those found from previous models for Markarian galaxies (Huchra 1977b; Belfort et al. 1987), because of the rather low M/L value of our starburst models: $M/L = 7.75\times10^{-4}$ for our model A, comparing to $M/L = 5\times10^{-3}$ for the Belfort et al.'s (1987) model with both the age and the duration of the starburst $= 2\times10^7\ yr$. This in turn is a consequence of the adopted high values for the upper and lower mass limits of the IMF. On the other hand, through kinematical studies, Augarde and Lequeux (1985) estimated that the starburst strength of Mkr 171 is $\lesssim 10^{-3}$, and Duflot-Augarde and Alloin (1982) found $b \simeq 3\times10^{-4}$ for NGC 7673=Mkr 325.

Figures 5.4a and 5.4b show clearly that Markarian galaxies have a significantly more active star-formation than normal disk galaxies: the mean starburst strength of Markarian galaxies is ~ 5 times higher than that of normal disk galaxies. These results are fully consistent with those of previous optical studies (Huchra 1977a, 1977b).

Let us recall once again that our model cannot be used for ultraluminous IRAS selected galaxies (represented by the starred squares laying at the top of

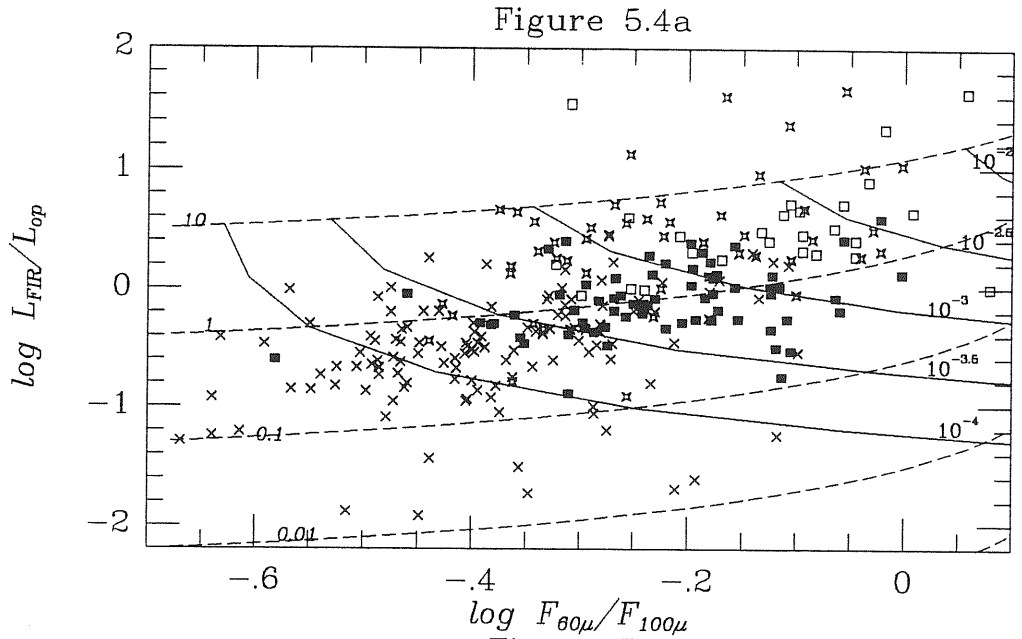

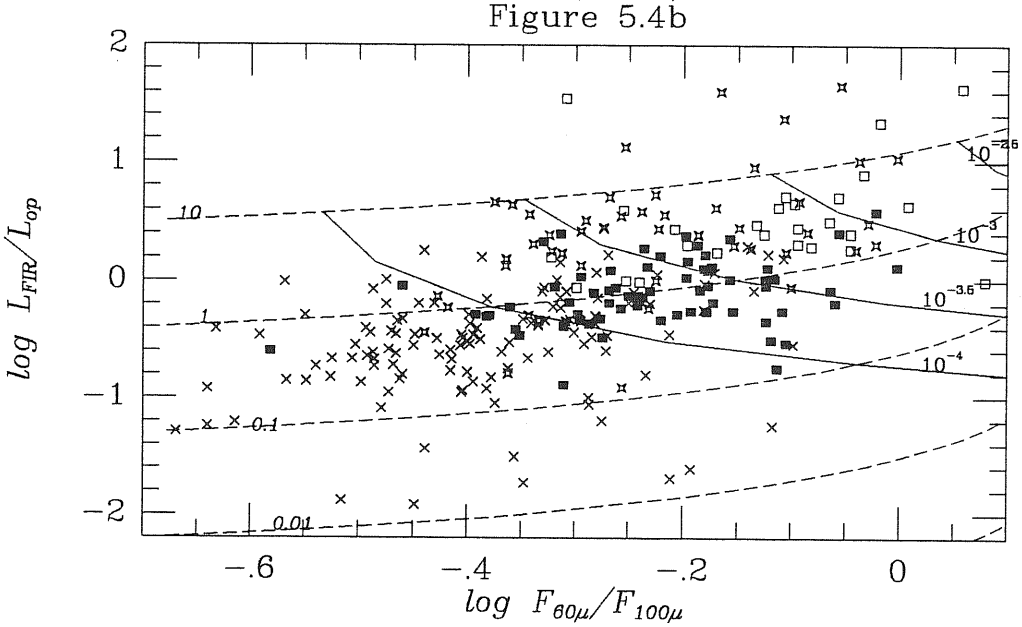

Fig. 5.4a. $\log L_{FIR}/F_{op}$ vs. $\log L_{60\mu}/L_{100\mu}$: *predictions of the starburst model A*

Fig. 5.4b. $\log L_{FIR}/F_{op}$ vs. $\log L_{60\mu}/L_{100\mu}$: *predictions of the starburst model B*

Marks have sames menings as those in Fig. 5.1 and Fig. 5.2. Full lines: models with constant staburst strength b (values marked on the lines). Dashed lines: models with constant τ (values marked on the lines).

both figures), and that in the case of compact blue galaxies, the meaning of the optical thickness of the disk is doubtful. Data for these galaxies are plotted only for sake of comparison with Markarian galaxies.

(3) *Comparison with other FIR models*

There are, in the literature, several theoretical models for the FIR emission from disk galaxies.

Rowan-Robinson and Crawford (1986) proposed a 3-component model comprising: (1) A disk which contains 2 sub-components at temperatures of 30K and 210K, mixed up empirically (see also Rowan-Robinson 1986). (2) A 'starburst' component based on the model for compact HII regions by Rowan-Robinson (1980, 1982a, 1982b) and Crawford and Rowan-Robinson (1986). (3) A 'Seyfert' component represented by an $\alpha = 0.7$ power-law continuum source embedded in a spherically symmetric dust cloud with density distribution $n(r) \propto r^{-1}$, $(r_1 \leq r \leq r_2)$. The model by Rowan-Robinson (1980, 1982a, 1982b) and Crawford and Rowan-Robinson (1986), however, is appropriate for 'compact HII regions', whose density is higher than 10^4 H-atoms/cm^3 and whose $A_v > 30\,mag$. However, as we discussed above, except for those galaxies where the starburst has been just turned on and only shine in the FIR (e.g. very bright IRAS galaxies with faint optical counterparts), the dust associated with compact HII regions shouldn't dominate the warm FIR emission. In fact, Rowan-Robinson and Crawford (1986) claimed that their 'starburst' component is able to fit the data of Telesco et al. (1984) for the 3 kpc ring in NGC 1068, and the average spectrum of the clouds of dust and molecules, which are believed to be associated with compact HII regions, in our own Galaxy (Rowan-Robinson, 1979). Besides, the FIR flux ratios of this component: $\log F_{12\mu}/F_{25\mu} = -0.07$, $\log F_{25\mu}/F_{60\mu} = 0.12$, $\log F_{60\mu}/F_{100\mu} = 0.43$, are very far from data on any known optically selected star-forming galaxy (cf. Fig. 5.3a, Fig. 5.3b), and

their model cannot account for the anti-correlation between $F_{12\mu}/F_{25\mu}$ and $F_{60\mu}/F_{100\mu}$.

The model by de Jong and Brink (1986) comprises two components: a warm and a cold component due to dust at temperatures $T_w \simeq 60K$ and $T_c \simeq 16K$, respectively. The warm component is associated to star-forming regions. They assume that only one half of the star-light from young massive stars contribute to heat the warm dust, while the cold dust is heated by disk stars as well as by light leaking out from star-forming regions. The L_{FIR}/L_B vs. $F_{100\mu}/F_{60\mu}$ diagrams for a sample of 120 RSA galaxies (Revised Shapley-Ames Catalog of Bright galaxies, Sandage and Tamman 1981) plus 20 optically studied mini-survey IRAS galaxies (Soifer et al. 1984) are fitted by sets of models with different L_2/L_1 ratios and disk opacities, τ, where L_2 is the total star light from massive stars, and L_1 is the total light from disk stars. The temperatures of warm and cold components have been determined empirically: T_w was chosen to be somewhat larger than the largest dust temperature as derived from the observed $F_{100\mu}/F_{60\mu}$ flux ratios, T_c was chosen so that the average face-on extinction derived from the model for RSA galaxies agrees with optically determined values. The model predicted that IRAS mini-survey galaxies generally have larger disk extinction and L_2/L_1 ratio than RSA galaxies. The difference between these two samples in the blue-FIR luminosity ratio versus the $F_{60\mu}/F_{100\mu}$ IRAS color diagram can also be explained by the models. However, as will be discussed below, the model is too simple to account for emissions of disk galaxies in all IRAS bands, i.e. when not only $60\mu m$ and $100\mu m$ bands, but also $12\mu m$ and $25\mu m$ fluxes are taken into account.

The two-component phenomenological model by Helou (1986) is essentially aimed at explaining the anti-correlation between $F_{12\mu}/F_{25\mu}$ and $F_{60\mu}/F_{100\mu}$. His starburst component hinges upon the dust emission model constructed by Désert (1986). In that model, grains, as well as molecules (PAH),

are heated by the ambient radiation field whose intensity ranges from the value appropriate to the solar neighborhood to values several hundreds times larger. The model for the cold component is based on observational data of galactic cirrus (Boulanger and Pérault, 1986). The model can explain the $F_{12\mu}/F_{25\mu}$ vs. $F_{60\mu}/F_{100\mu}$ diagram of normal galaxies quite well. However, judging from Fig. 1 of Désert (1986), it predicts a too steep $F_{25\mu}/F_{60\mu}$ when $F_{60\mu}/F_{100\mu}$ is in the reasonable range (not much larger than unit). For example, his $x = 100$ model (the radiation field is 100 times the local one) predicts $F_{60\mu}/F_{100\mu} \sim 3$ and $F_{25\mu}/F_{60\mu} \sim 0.03$, while the ratio $F_{25\mu}/F_{60\mu}$ of galaxies is usually larger than 0.1. Although it is possible to fit the $F_{25\mu}/F_{60\mu}$ color with higher values of x, even larger values of $F_{60\mu}/F_{100\mu}$ for the warm component would result. Then, contrary to Helou's (1986) conclusion, a big cold component is always needed to obtain a good fit to the $F_{60\mu}/F_{100\mu}$ color of galaxies which is usually smaller than 1. This difficulty arises from their assumption for the radiation field heating the warm component: a local-ISRF-like radiation field, i.e. mostly optical photons. Since the temperature of a grain is only determined by its energy balance (Section 5.2), and the absorption efficiency of grains in both the optical band and in the FIR band is approximately proportional to a, the grain size, all the grains with different sizes in the warm component of Helou (1986) have similar temperature (the heating radiation is uniform), and the component is essentially a single-temperature one. The emission spectrum is then too narrow to give a good fit to the $F_{25\mu}/F_{60\mu}$ ratio and a reasonable value of $F_{60\mu}/F_{100\mu}$ simultaneously, given the fact that the $F_{25\mu}/F_{60\mu}$ and the $F_{60\mu}/F_{100\mu}$ color temperatures of galaxies are very different: ~ 50—$60K$ and ~ 20—$30K$, respectively, for a ν^2 dependence of the grain absorption efficiency. Furthermore, Pajot et al. (1986) found a wide, smooth, power-law-like temperature distributions for interstellar dust in different environments within the Galaxy.

Our warm component is heated by a uniform radiation field, too. But we have assumed that the heating is mainly due to UV light from massive stars.

Figure 5.5

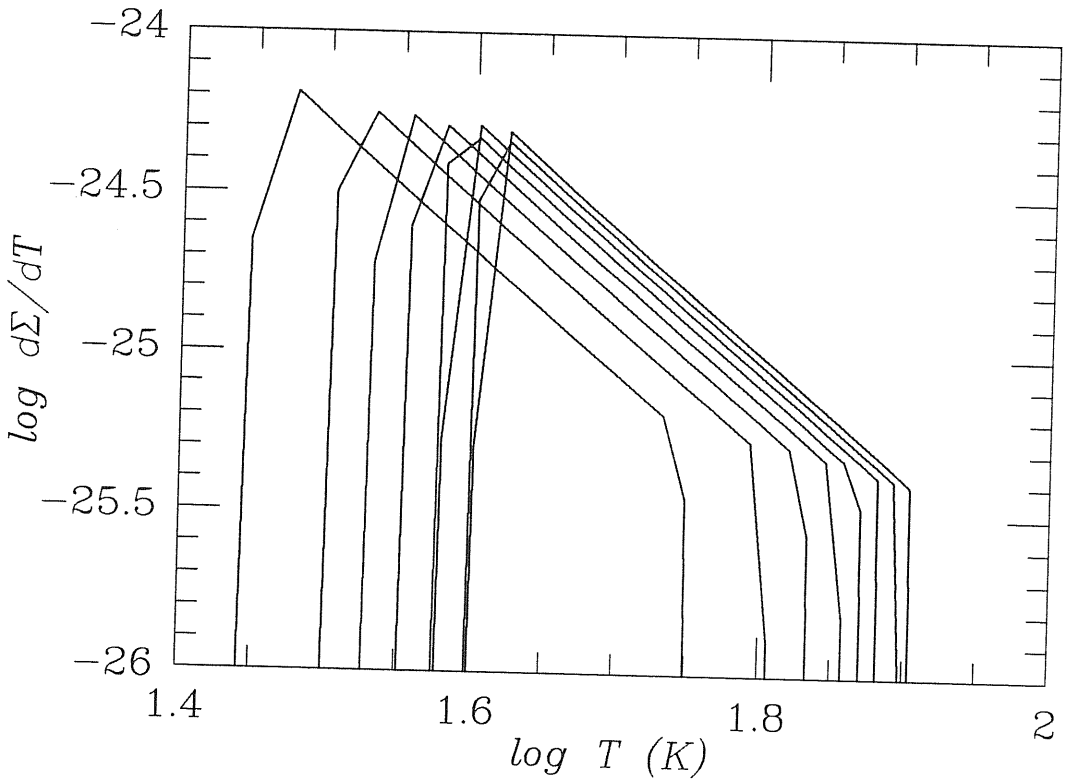

Fig. 5.5. *Temperature distribution of the warm component*

Σ: the integrated FIR absorption cross-section of the warm component in the unit of cm^2 (arbitrarily calibrated). The various lines correspond to models with different values of I_w. From left to right: I_w = 20, 40, 60, 80, 100, 120, 140, 160 × I_{local}.

Since the UV absorption efficiency of grains is very insensitive to the grain size and nearly unity (DL84), small grains heated by UV radiation are warmer than larger ones, because the later cool down faster than the former (due to the dependence of the FIR absorption efficiency Q_{FIR} on grain size a). Grain sizes range from 50 to 2500$\mathring{A}$, yielding a temperature distribution having a width of about a factor of $(2500/50)^{\frac{1}{6}} \simeq 2$ (see equation 5.20 and Fig. 5.5).

Since two-temperature models are very popular in the current literature (e.g. de Jong and Brink 1987; Sekiguchi 1987; Lonsdale Persson and Helou 1987; Chini et al. 1986a; Fitt et al. 1988; etc), it is probably useful to stress that, in the light of the above discussion, some of the results based on them are likely to be unreliable. In particular, they tend to over-estimate the cold component, since the narrow spectrum of the warm component always leaves a big dip in the wavelength range longer than $60\mu m$ that is usually, and arbitrarily, filled enhancing the strength of the cold component.

(4) *The cold component*

In principle, our cold component is in the same category of that of Cox et al. (1986, see also Cox and Mezger 1987). Judging from Fig. 2 of Cox and Mezger (1987), the flux ratios of $F_{25\mu}/F_{60\mu}$ and $F_{60\mu}/F_{100\mu}$ predicted by our cold component also agree very well with theirs. However, as reported by Cox and Mezger (1987), the model failed to give right prediction of the color temperature $T_c(60\mu$–$100\mu)$ of the Galactic disk as a function of galactic longitude. Cox and Mezger (1987) suggested that this could be due to the ignorance of the temperature fluctuations of grains smaller than 100Å, as were tentatively modeled by Draine and Anderson (1985). Meanwhile, Cox and Mezger argued that the nature of these small grains is still unknown, and the models by Draine and Anderson (1985) predicted $\simeq$ 20% of carbon cosmic abundance in grains <20Å, which is at odd with the local extinction curve. Moreover, the points

representing predictions by Draine and Anderson's models (points A and B in Fig. 5.3a and 5.3b, corresponding to their models of $x = 1$ and $x = 0.5$, respectively[†]) are away from the main trend of data points of disk galaxies.

Boulanger et al. (1985) reported detections of a 'warm cirrus' by IRAS at all four bands. The data is represented by point C in Fig. 5.1a and 5.1b. The 'cirrrus' is obviously warmer than many disk galaxies, and, thus, is likely to be an anomalous one selected by IRAS due to its very warm spectrum.

Nevertheless, the fact that some cold disk galaxies, whose FIR emission is presumably dominanted by the disk component, fall outside the region covered by our model predictions on FIR color-color diagrams, reveals some shortcomings of our simple models. Although we do not think the problem is serious for the case of Markarian galaxies, which are very well fitted by our models, further studies on the nature of cold dust, especially on that of small grains (< 100Å), are needed to work out models of more general validity.

Appendix A
Starburst model

Sramek and Weedman (1986) found that a power-law IMF with slope in

[†] x is a parameter specifying the intensity of the heating light (Draine and Anderson 1985)

the range 1.5 to 2.5 and with lower mass cut-off at 4 to 6 $M_\odot$ and upper mass cut-off at 30 to 40 $M_\odot$ is compatible with the results of their study on the thermal and non-thermal radio emission of starbursting regions. A similar IMF but with a smaller lower limit, 0.1 $M_\odot$, and higher upper cut-off, 120 $M_\odot$, was employed by Belfort et al. (1986) to account for the UBV colors and the L_{FIR}/L_B ratios of starburst galaxies. Although there have been evidences that the upper mass cut-off may be relatively low ($\sim$ 40 $M_\odot$) in some particular star-forming galaxies (e.g. M82), two arguments suggest that a higher upper mass cut-off, like that used by Belfort et al. (1986), may be preferable, in general. On one side, the study of Scalo (1986, see also Garmany and Conti 1982)) on the stellar luminosity function in the Galaxy led him to conclude that the upper-cut off could be very high and that previuos results (e.g. Miller and Scalo 1979) may well have under-estimated it. On the other hand, Campbell et al. (1986) argued that low metallicity, frequently found in star-forming galaxies (Huchra 1987), favours the formation of high mass stars.

In view of the above, our starburst population is specified by a power law IMF with lower mass cut-off of 4 $M_\odot$ and upper mass cut-off of 120 $M_\odot$. We will discuss a IMF with power index of $p = 2.5$ (model A), and a flatter IMF of $p = 1.5$ (model B). The mass, life-time, main-sequence averaged bolometric luminosity and *Lyc* production rate of different types of star are taken from Güsten and Mezger (1982, see also Cox et al. 1986). The ratio between *Lyc* luminosity and total stellar luminosity as a function of star type for massive ionizing stars is taken from Paragia (1973).

As for the starburst duration (or life-time, i.e. the time span from the beginning to the end of the burst), published estimates range from 1 to 10 $\times$ $10^7\,yr$ (cf. Balzano 1983, and references therein). We have chosen a fiducial value of $2 \times 10^7\,yr$. The same value has been adopted as the typical burst age (the time passed since the beginning of the burst). This means assuming

that we are seeing all bursts in their late phases. This assumption minimizes the M/L ratio of bursts (Belfort et al. 1987), as well as the estimated burst strength for a given IMF and underlying galaxy.

In the context of normal disk galaxies, $2 \times 10^7\ yr$ is the life time of star-forming clouds (Yorke 1986). After this time, stars formed within the cloud will move outside it, and, then, contribute to the general ISRF of the disk rather than to the heating of the warm dust.

Appendix B
The FIR to optical luminosity ratio of the cold component

The total luminosity of the disk is

$$L_{tot,d} = \int_0^\infty 4\pi\epsilon(r) \cdot Z(r) \cdot 2\pi r\, dr, \qquad (5B.1)$$

where $\epsilon(r)$ is the emissivity; $Z(r)$ is the thickness of the disk at radius r. Since

$$\epsilon(r) \cdot Z(r) + I(r) \cdot \tau_{sc}(r) = S(r) \cdot \tau(r), \qquad (5B.2)$$

where $S(r)$ is the source function, I the intensity of the radiation field, $\tau(r) = \tau_{ab}(r) + \tau_{sc}(r)$ is the opacity, $\tau_{ab}(r)$ is the opacity due to absorption, and $\tau_{sc}(r)$ the opacity due to scattering.

The relation between S and I can be approximated by (Mihalas 1978)

$$\langle I \rangle = \frac{1}{2\tau} \int_0^{\tau_1} d\tau \cdot \int_0^{\tau} S \cdot E_1(|t - \tau_1|)\, dt, \qquad (5B.3)$$

where $\langle I \rangle$ is the average intensity of the radiation field (averaged first over different directions at a particular point and then over all points along a particular vertical line within the disk), E_1 is the first order Schwarschild function. The definition of E_n is (Mihalas 1978)

$$E_n(x) = \int_1^{\infty} t^{-n} e^{-xt}\, dt = x^{n-1} \int_x^{\infty} t^{-n} e^{-t}\, dt \quad . \qquad (5B.4)$$

Suppose that S is insensitive to position, which is equivalent to assuming a similar r dependence of emissivity and absorbancy. Then S can be treated approximately as a constant, and eq. (5B.4) is solved†:

$$\begin{aligned} \langle I \rangle &= \frac{S}{2\tau} \int_0^{\tau} d\tau_1 \int_0^{\tau} E_1(|\tau_1 - t|)\, dt = \frac{S}{\tau} \int_0^{\tau} d\tau_1 \int_0^{\tau_1} E_1(x)\, dx \\ &= \frac{S}{\tau} \int_0^{\tau} (1 - E_2(\tau_1))\, d\tau_1 = S(1 - \frac{1}{\tau}(\frac{1}{2} - E_3(\tau))) \qquad (5B.5) \\ &= S(1 - \frac{1}{2\tau}(1 - e^{-\tau}) - \frac{1}{2} E_2(\tau)) . \end{aligned}$$

† The following derivations follow from the relations (Mihalas, 1978):

(1) $$E_n'(x) = -E_{n-1}(x),$$

(2) $$E_n(x) = (e^{-x} - x \cdot E_{n-1}(x))\ (n-1).$$

From numerical results (Fig. 5B.1), we can see that, for $\tau \geq 10^{-3}$, equation (5B.5) can be further approximated by:

$$\frac{\langle I \rangle}{S} = \frac{\tau^{0.9}}{0.6 + \tau^{0.9}} \quad . \tag{5B.6}$$

Thus,

$$\begin{aligned} L_{tot}^{cd} &= \int 8\pi^2 (S(r) \cdot \tau(r) - I(r) \cdot \tau_{sc}) r \, dr \\ &= 8\pi^2 \int I(r)(\tau_{ab}(r) + 0.6\tau^{0.1}(r)) r \, dr, \end{aligned} \tag{5B.7}$$

In our model of disk FIR emission, we have assumed (see equation 5.22 and 5.23)

$$I(r) = I_0 e^{-\frac{r}{r_0}} \quad ,$$

$$\tau(r) = \tau_0 e^{-\frac{r}{r_0}} \quad .$$

So

$$\begin{aligned} L_{tot,d} &= 8\pi^2 I_0 \int_0^\infty e^{-\frac{r}{r_0}} (\tau_{ab,0} e^{-\frac{r}{r_0}} + 0.6\tau_0^{0.1} e^{-\frac{0.1r}{r_0}}) r \, dr \\ &= 8\pi^2 I_0 \left(\frac{\tau_{ab,0}}{4} + \frac{\tau_0^{0.1}}{2.02} \right) \quad . \end{aligned} \tag{5B.8}$$

On the other hand,

$$L_{FIR}^{cd} = \int 4\pi I(r) \cdot \tau_{ab}(r) \cdot 2\pi r \, dr = 8\pi^2 I_0 \frac{\tau_{ab,0}}{4}. \tag{5B.9}$$

Hence, the FIR to optical luminosity ratio of the cold component of our model, $(L_{FIR}^{cd}/L_{opt}^{cd})$, is

$$\left(\frac{L_{FIR}^{cd}}{L_{opt}^{cd}} \right) \doteq \frac{\tau_{ab,0}}{2\tau_0^{0.1}}. \tag{5B.10}$$

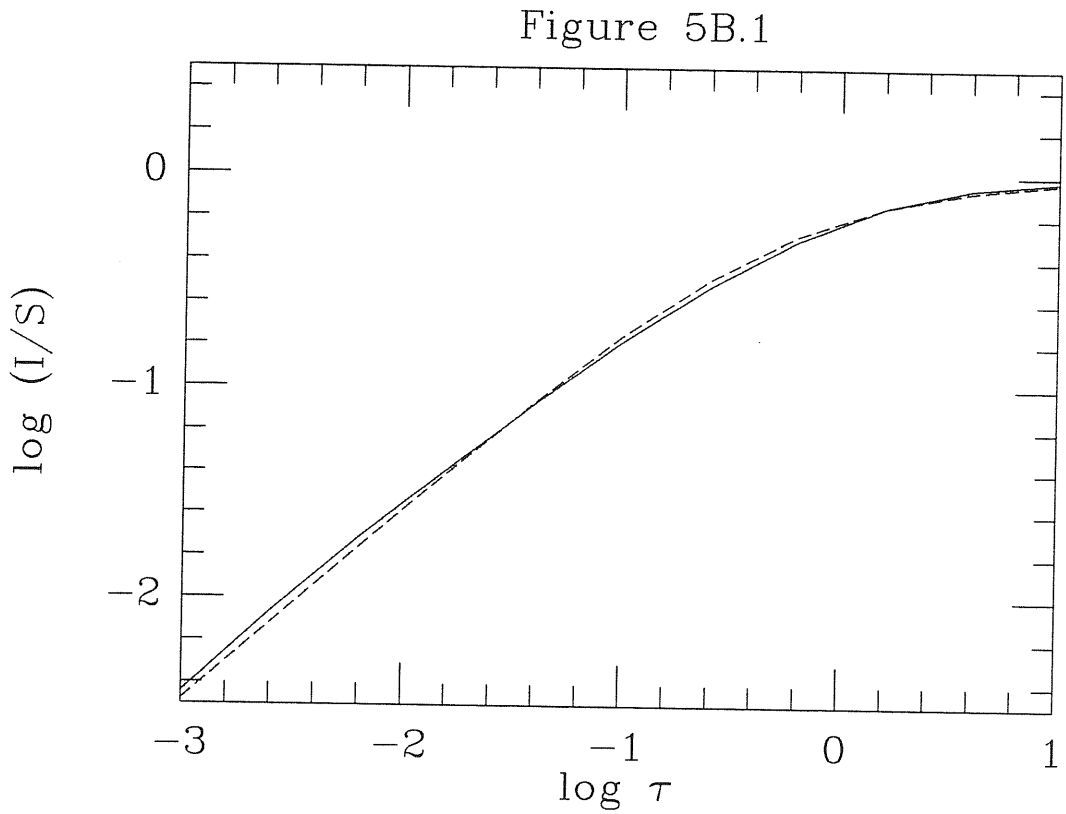

Fig. 5B.1 *The* $\log(I/S)$ vs. $\log\tau$ *relation for a geometrically thin configuration*
Solid line: numerical integration of equation (5B.5). Dashed line: $I/S = \tau^{0.9}/(.6 + \tau^{0.9})$ (see text).

The albedo of normal grains is about 0.5 in a wide wavelength range from optical to UV (DL84). Therefore we assume

$$\tau_{ab,0} = \frac{\tau_0}{2}, \tag{5B.11}$$

and $(L^{cd}_{FIR}/L^{cd}_{op})$, is

$$\left(\frac{L^{cd}_{FIR}}{L^{cd}_{opt}}\right) = \frac{\tau_0^{0.9}}{4}. \tag{5B.12}$$

Chapter 6
Luminosity Functions and Cosmic Evolution

6.1. Optical and FIR luminosity functions of Markarian galaxies

Included in the following (pp. 85—96) is a paper published in *Astron. Astrophys.* **196** (1988), pp. 59—70.

Astron. Astrophys. 196, 59–70 (1988)

ASTRONOMY AND ASTROPHYSICS

Optical and far-IR luminosity functions of Markarian galaxies

C. Xu[1], G. De Zotti[2], A. Franceschini[3], and L. Danese[3]

[1] International School for Advanced Studies, Strada Costiera 11, I-34014 Trieste, Italy
[2] Osservatorio Astronomico, Vicolo dell' Osservatorio 5, I-35122 Padova, Italy
[3] Dipartimento di Astronomia, Vicolo dell' Osservatorio 5, I-35122 Padova, Italy

Received August 13, accepted October 24, 1987

Summary. A new optical luminosity function of Markarian galaxies is presented, which improves on earlier determinations both because of the improved data situation (the sample is complete, Zwicky magnitudes and redshifts are available for essentially all objects) and for a more accurate treatment of several effects: Tully-Fisher distances have been used for low-z-galaxies; appropriate corrections have been applied to allow for binning and errors on apparent magnitudes; the results produced by the generalized Schmidt's estimator have been compared with those given by Turner's (1979) method, to investigate the effect of inhomogeneities in the galaxy distribution. The mean surface density of Markarian galaxies has been derived taking into account the non-uniform sky coverage of the survey; these objects are found to comprise $\simeq 11\%$ of galaxies brighter than $m_{zw} = 14.5$. Luminosity functions have been constructed both including and excluding Seyferts. The contributions of "stellar" and "diffuse" objects to the space densities of non-Seyfert Markarians have been computed. IRAS data have been used to derive, exploiting survival analysis techniques to take into account also upper limits, the far-IR luminosity function. We find that Markarian galaxies comprise an important fraction of IRAS galaxies above $L_{IR} \simeq 2\,10^{11}\ L_{\odot}$; yet, contrary to earlier claims, they are never the dominant component. Finally, we show that the far-IR to blue luminosity ratios of these sources increase with luminosity just as expected if the bulk of the energy comes from actively star-forming regions, cocooned by dust.

Key words: galaxies: active – luminosity function – infrared radiation

1. Introduction

The Markarian survey (Markarian et al., 1981 and references therein) is the main source of optically selected galaxies with enhanced star formation activity. These objects, referred to as "starburst" galaxies, are receiving increasing attention in the context of several astronomical problems. In particular, they are likely to play a key role in the interpretation of very deep Very Large Array (VLA) counts of radio sources (Condon and Mitchell, 1984; Fomalont et al., 1984; Partridge et al., 1986; Windhorst, 1984, 1986; Windhorst et al., 1987; Danese et al., 1987) and of Infrared Astronomical Satellite (IRAS) counts (Hacking and Houck, 1987; Franceschini et al., 1988b) and may also be significant contributors to the X-ray background (Weedman, 1987; De Zotti, 1987).

In view of the above, the importance of accurate determinations of the local space densities of these sources and of the comparisons with the densities of sources found in different frequency bands is obvious.

It is now possible to improve on the most accurate estimate of the optical luminosity function of Markarian galaxies available so far, due to Huchra (1977), in several respects.

Making use of all 15 Markarian lists we may pull together a sample of size comparable to Huchra's (based on the first seven lists), still confining ourselves to a bright enough limiting magnitude ($m_{zw} \leqslant 14.5$) for completeness to be ensured. In addition, redshift measurements are now available for all objects in the sample (while $\simeq 25\%$ of galaxies were rejected by Huchra because they lacked redshift). Also, all but four of our objects have Zwicky magnitudes, considerably more accurate than Markarian's estimates used for $\simeq 50\%$ of Huchra's objects.

Moreover, redshift-independent distance estimates, based on the Tully-Fisher (1977) relation, can be found for the majority of nearby galaxies ($z \leqslant 0.0075$) whose measured redshifts may have a substantial, or even a dominant, non-Hubble component. Further refinements over previous studies include a careful definition of the mean surface density of Markarian galaxies brighter than $m_{zw} = 14.5$ (allowing for inhomogeneities both in the sky coverage of the Markarian survey, and in the true spatial distribution of the objects), corrections for errors on magnitudes and for the effect of binning.

Previous determinations of the luminosity function of Markarian galaxies made use of Schmidt's estimator which holds on the assumption of a uniform distribution in space. As shown in Sect. 2, however, there is evidence of substantial clustering of these objects. As a check on the importance of this effect we have also applied the alternative method proposed by Turner (1979), which allows to derive the shape of the luminosity function for an arbitrary space distribution provided that such shape is the same in clusters and in the field.

Next, using IRAS data, we have constructed a fractional bivariate (optical, far-IR) function. Survival analysis techniques (Feigelson and Nelson, 1985; Schmitt, 1985) have been applied to exploit the information content of IR upper limits. The resulting

Send offprint requests to: G. De Zotti

far-IR luminosity function is presented and compared with previous estimates in Sect. 3. Sect. 4 contains a discussion of our main results.

2. The optical luminosity function

2.1. Definition of the sample

The sample comprises all Markarian galaxies fulfilling the following requirements:
i) $m \leqslant 14.5$. We used Zwicky magnitudes whenever possible; otherwise we took Markarian's magnitudes. The V/V_{max} test (Table 1) shows that Markarian's survey is increasingly incomplete for $m_{Zw} > 14.5$, as pointed out already by Sargent (1972) and Huchra and Sargent (1973). As is well known, the Markarian survey is also incomplete at the bright side, since some *nearby* galaxies brighter than 13 mag were left out (see Markarian, 1967), partly because of the difficulty in distinguishing abnormal from normal cases, and partly because a list of bright galaxies with anomalous spectral features was previously published by Markarian (1963). The latter list however does not obey the same selection criterion as the conventional Markarian lists, contains only galaxies of morphological type earlier than Sc (and thus misses active objects such as M82) and is anyway "far from being complete"; in view of the above we have chosen not to include it in our analysis. In practice, ignoring the incompleteness at bright magnitudes has a negligible effect on estimates of space densities of luminous objects ($M_{Zw} \leqslant -17$); for weak sources, on the other hand, the error is small in comparison to statistical uncertainties.
ii) $|b| \geqslant 30°$, to minimize the uncertainties related to the corrections for extinction within our own galaxy.
iii) $\delta \geqslant -2°$. This constraint has an operational meaning: in this region only four galaxies brighter than $m=14.5$ lack Zwicky magnitudes (Mkn 789, 205, 1239, and 1478; the first three of these are type 1 Seyferts).

Objects classified by Véron-Cetty and Véron (1985) as QSOs or BL Lacs (and, of course, the two stars Mkn 113 and Mkn 362) were excluded. The final sample comprises 176 non-Seyfert galaxies and 30 Seyferts; all have measured redshift. The relevant data are listed in Table 2; the reddening within our own galaxy, E(B−V), has been derived, for each source, from the maps of Burstein and Heiles (1982).

There is no indication of a correlation between apparent and absolute magnitudes of galaxies in the sample (correlation coefficient $=0.06$), consistently with the assumption that it is "homogeneous" (Neyman and Scott, 1961).

2.2. Determination of the mean surface density

Markarian and coworkers never defined clearly the boundaries of their survey. Also, the coverage of the surveyed region is admittedly far from uniform. Therefore the definition of the mean surface density of the sources brighter than any chosen magnitude limit requires some care.

We adopted the following procedure. First, we divided the region defined by conditions ii) and iii) into many subregions of equal effective area Ω_{eff}, defined as

$$\Omega_{eff} = \int 10^{-0.6 A_B} d\Omega \qquad (1)$$

to allow for the effect of galactic extinction on observed counts. The adopted extinction law, $A_B = 0.2(\mathrm{cosec}|b| - 1)$, is a good fit to the average extinction read on the maps of Burstein and Heiles (1982) (cf. Toffolatti et al., 1987; $A_B = 4E(B-V)$). Since the apparent magnitude limit is constant, this operation amounts to dividing our "sample space" into equal volumes. If the objects are uniformly distributed in space, the distribution of surface densities among subregions should be poissonian.

The effective area within the boundaries defined by the above conditions is 9699 deg^2; it was divided into 120 subregions plus some residuals, totalling 99 deg^2, which do not contain any object. This looked to be the finest subdivision with still reasonable numbers per region.

The surface density distribution is shown in Fig. 1. The expected excess of low surface density regions, associated to areas not, or only poorly, covered by the Markarian survey is clearly visible. The frequency of areas containing at least one galaxy can be fitted with a Poisson distribution with mean $\lambda = 2.4 \pm 0.4$ sources $(80\ \mathrm{deg}^2)^{-1}$, or 0.030 ± 0.005 sources deg^{-2}, brighter than $m_{Zw} = 14.5$. Excluding Seyferts we get $\lambda = 2.0 \pm 0.32$, i.e. a mean surface density of 0.025 ± 0.004 sources deg^{-2}. The total effective solid angle covered by the final sample is thus $\Omega \simeq 206/0.03 \simeq 6900 \pm 1100$ deg^2.

For comparison, the surface density of normal galaxies at the same limit is $\simeq 0.275$ deg^{-2} (Davis and Huchra, 1982); Markarians thus represent $\simeq 11\%$ of field galaxies.

2.3. Distances of nearby galaxies

Distances derived from the Tully-Fisher (1977) relation, scaled to an assumed distance of the Virgo cluster of 20 Mpc, have been adopted as far as possible for objects with $z \leqslant 0.0075$ (the uncertainties due to the dispersion around the mean relation are

Table 1. V/V_{max} test for Markarian galaxies

m_{Zw}	Seyfert included		non-Seyfert	
	$< V/V_{max} >$	N	$< V/V_{max} >$	N
13.0	0.633 ± 0.057	26	0.618 ± 0.058	25
13.5	0.588 ± 0.038	58	0.590 ± 0.038	57
14.0	0.555 ± 0.027	114	0.516 ± 0.030	99
14.5	0.513 ± 0.020	206	0.492 ± 0.022	176
15.0	0.497 ± 0.015	361	0.480 ± 0.017	305
15.5	0.464 ± 0.012	580	0.463 ± 0.013	496

Table 2. Data for galaxies in the sample. Most entries are self-explanatory. In Column 2, S1 or S2 denote type 1 or type 2 Seyferts, respectively. Column 7 gives the adopted distances (Mpc) for nearby objects (see text); for all other objects we have used redshift distances ($H_0 = 50$). Column 9 contains the absolute magnitudes, corrected for the galactic extinctions listed in Column 4. Column 10 gives the IRAS flux densities, or the adopted upper limits, at 60 μm, in Janskys

Mkn	Type	m_{Zw}	E(B-V)	z	Ref.	D(Mpc)	Notes	M_{Zw}	F_{60}(Jy)
10	S1	14.0	0.03	0.030	1			-22.40	0.84
12		12.7	0.03	0.014	1			-22.04	3.18
13		14.5	0.03	0.005	1	24.37	a	-17.55	0.48
14		14.4	0.03	0.011	1			-19.82	1.07
18		14.3	0.03	0.011	1			-19.92	2.07
25		14.2	0.01	0.009	1			-19.50	1.30
33		13.2	0.00	0.005	1	20.65	b	-18.37	4.73
35		12.9	0.00	0.004	1	20.65	b	-18.67	5.13
49		14.5	0.00	0.005	1	20.00	c	-17.00	0.74
52		12.4	0.01	0.007	1	11.25	d	-17.90	4.58
59		12.8	0.00	0.003	1	21.53	e	-18.86	1.82
84		13.6	0.03	0.020	1			-21.92	1.35
85		13.8	0.03	0.012	1			-20.61	<0.60
86		11.7	0.04	0.001	1	19.86	f	-19.95	3.15
87		13.4	0.03	0.010	1			-20.61	1.31
88		14.3	0.03	0.031	1			-22.17	1.27
90		13.9	0.03	0.015	1			-20.99	0.87
100		14.2	0.03	0.012	1			-20.21	1.39
101		13.6	0.02	0.016	1			-21.39	0.93
102		14.3	0.01	0.014	1			-20.36	0.69
111		13.9	0.04	0.013	1			-20.72	2.82
114		14.5	0.01	0.025	1			-21.42	1.52
119		14.1	0.03	0.010	1			-19.91	2.17
122		14.3	0.03	0.022	1			-21.42	1.07
131		13.8	0.01	0.004	1	21.48	g	-17.90	<0.60
133		12.8	0.03	0.007	1	58.48	h	-21.15	3.02
146		14.1	0.00	0.011	1			-20.00	0.89
149		14.4	0.01	0.006	1	16.68	i	-16.75	<0.60
155		13.2	0.00	0.006	1	31.60	a	-19.30	<0.60
156		14.5	0.00	0.004	1	23.58	a	-17.36	<0.60
157		14.0	0.00	0.005	1	25.49	a	-18.03	0.62
158		13.0	0.01	0.007	1	34.81	a	-19.75	8.40
161		13.4	0.00	0.020	1			-22.00	2.46
169		14.2	0.00	0.005	1	20.65	b	-17.37	3.59
171		11.8	0.00	0.010	1	20.65	b	-19.77	70.30
171A		12.7	0.00	0.011	1	20.65	b	-18.87	35.10
175		14.1	0.01	0.013	1			-20.40	<0.60
178		13.9	0.00	0.001	1	20.65	b	-17.67	<0.60
179		13.6	0.01	0.011	1			-20.54	0.99
181		13.9	0.00	0.020	1			-21.50	1.95
185		13.0	0.01	0.010	1			-20.93	2.47
186		13.2	0.00	0.003	1	16.89	d	-17.94	1.17
188		12.6	0.00	0.007	1	37.61	d	-20.28	4.76
190		13.1	0.00	0.003	1	20.65	b	-18.47	2.65
195		14.3	0.01	0.005	1	20.65	b	-17.31	1.79
201		13.0	0.00	0.009	1			-20.66	22.50
205	S1	14.5	0.02	0.072	1			-23.76	<0.40
207		13.5	0.01	0.008	1			-19.95	2.21
213		13.2	0.00	0.010	1			-20.69	3.89
220		14.1	0.00	0.017	1			-20.94	1.82
231	S1	14.1	0.01	0.041	1			-22.89	33.26
249		13.9	0.00	0.019	2			-21.38	<1.50
256		13.2	0.02	0.011	1			-20.98	2.87
266	S2	14.1	0.00	0.028	1			-22.03	7.20
270	S2	14.3	0.01	0.010	1			-19.63	<0.60
271		13.6	0.00	0.026	1			-22.36	1.50
279	S1	14.5	0.02	0.031	1			-21.93	1.08
281		12.5	0.00	0.008	1			-20.91	5.23
286		13.9	0.02	0.027	1			-22.23	4.40
297		14.1	0.03	0.016	1			-20.93	6.94
307		13.7	0.05	0.019	1			-21.78	1.83
313		13.3	0.04	0.007	1	23.59	j	-18.72	7.00
314		14.0	0.04	0.008	1			-19.57	1.29
319		14.0	0.06	0.028	1			-22.37	4.21
321		13.5	0.06	0.033	1			-23.22	2.67
323		13.7	0.06	0.015	1			-21.31	2.98
325		12.7	0.05	0.012	1			-21.79	5.18
326		13.9	0.05	0.013	1			-20.76	3.85
332		12.7	0.03	0.009	1			-21.08	4.98
333		14.3	0.05	0.016	2			-20.81	<1.50
334	S1	14.4	0.03	0.024	1			-21.51	4.19
335	S1	14.0	0.03	0.026	1			-22.08	0.45
341		13.3	0.01	0.017	1			-21.78	0.85
353		14.2	0.01	0.017	1			-20.88	3.89
359	S1	13.8	0.01	0.018	1			-21.41	1.24
363		13.9	0.02	0.010	1			-20.07	2.40
368		14.5	0.01	0.029	1			-21.74	0.71
370		13.5	0.09	0.003	1	11.88	a	-17.23	1.12
389		13.4	0.03	0.015	1			-21.49	0.74
391	S1	13.9	0.01	0.013	1			-20.60	1.28
394		14.3	0.01	0.031	1			-22.09	1.28
400		14.4	0.01	0.008	1			-19.05	1.22
401		13.6	0.00	0.005	1	76.03	f	-20.80	2.49
404		12.0	0.00	0.004	1	23.30	k	-19.84	11.66
409		14.2	0.00	0.005	1	23.30	k	-17.64	<0.60
418		13.2	0.00	0.006	1	28.87	l	-19.10	1.74
430		13.4	0.00	0.020	1			-22.00	0.83
431		14.3	0.00	0.010	2			-19.59	
432		14.0	0.00	0.011	1			-20.10	3.58
439		12.3	0.00	0.004	1	5.98	m	-16.58	5.91

Table 2 (continued)

Mkn	Type	m_{Zw}	E(B-V)	z	Ref.	D(Mpc)	Notes	M_{Zw}	F_{60}(Jy)
442		14.3	0.00	0.002	1	9.61	a	-15.61	<1.50
446		14.2	0.00	0.024	1			-21.59	1.45
449		13.5	0.00	0.004	1	21.53	e	-18.16	2.27
452		14.0	0.00	0.017	1			-21.04	<1.50
461	S2	14.5	0.00	0.016	1			-20.41	<1.50
470		14.5	0.00	0.015	1			-20.27	<1.50
471	S1	14.5	0.00	0.034	1			-22.05	0.64
479		13.9	0.01	0.021	1			-21.64	1.65
480		14.2	0.00	0.019	1			-21.08	1.80
489		14.2	0.00	0.032	1			-22.22	1.50
491		14.4	0.00	0.040	1			-22.50	<0.60
496		14.0	0.01	0.029	1			-22.24	6.43
518		14.3	0.07	0.032	1			-22.40	2.70
527		14.5	0.02	0.012	1			-19.87	4.37
530	S1	14.4	0.03	0.030	1			-22.00	0.82
531		13.5	0.03	0.013	1			-21.08	4.71
533	S2	13.6	0.03	0.030	1			-22.80	5.47
534		13.2	0.03	0.018	1			-22.09	7.29
538		13.1	0.01	0.010	1			-20.83	11.07
545		12.5	0.03	0.016	1			-22.53	8.98
547		14.5	0.00	0.018	1			-20.67	0.64
555		12.9	0.00	0.014	1			-21.72	3.89
562		14.2	0.00	0.009	1			-19.46	<1.50
565		13.8	0.00	0.022	1			-21.80	1.76
571		14.1	0.00	0.018	1			-21.07	1.48
573	S2	14.0	0.00	0.017	1			-21.04	1.25
575		14.0	0.03	0.018	1			-21.29	2.74
577		14.2	0.03	0.042	1			-22.93	<1.50
582		14.0	0.00	0.019	1			-21.28	4.94
587		14.5	0.01	0.015	1			-20.31	0.91
589		14.3	0.01	0.011	1			-19.84	2.66
590	S1	14.0	0.00	0.026	1			-21.96	0.53
602		13.2	0.06	0.010	1			-20.93	3.55
616		14.1	0.06	0.012	1			-20.43	<1.50
622	S2	14.4	0.04	0.023	1			-21.46	1.36
626		13.8	0.02	0.013	1			-20.74	1.00
649		14.3	0.00	0.024	1			-21.49	<1.50
656		13.7	0.00	0.023	1			-22.00	<1.50
665		14.3	0.00	0.026	1			-21.66	0.67
669		13.9	0.00	0.018	2			-21.27	<1.50
673	S2	14.2	0.00	0.036	1			-22.47	2.85
686	S2	13.9	0.00	0.014	1			-20.72	0.59
691		13.2	0.02	0.011	1			-20.98	4.06
703		13.3	0.03	0.012	1			-21.11	3.95
705	S1	13.9	0.01	0.028	1			-22.27	0.67
708		14.0	0.02	0.006	1	32.36	a	-18.63	5.37
710		13.5	0.00	0.005	1	25.06	a	-18.49	2.66
712		14.3	0.00	0.015	1			-20.47	0.84
718		14.5	0.00	0.027	3			-21.55	1.31
729		14.2	0.00	0.042	1			-22.81	

Mkn	Type	m_{Zw}	E(B-V)	z	Ref.	D(Mpc)	Notes	M_{Zw}	F_{60}(Jy)
731		13.4	0.01	0.004	1	27.18	a	-18.81	2.99
732		13.9	0.01	0.029	3			-22.34	1.91
736		13.0	0.00	0.008	1			-20.41	
741		14.5	0.00	0.011	3			-19.60	
743		13.1	0.02	0.003	1	20.61	a	-18.55	1.48
744	S1	13.0	0.00	0.009	1			-20.66	
747		14.5	0.02	0.002	1	9.32	a	-15.43	<1.50
752		14.4	0.01	0.020	1			-21.04	0.71
759		12.5	0.02	0.007	1	30.83	f	-20.02	4.13
761		14.3	0.01	0.014	1			-20.36	5.33
766	S1	13.7	0.01	0.013	1			-20.80	4.01
769		12.3	0.01	0.005	1	20.00	c	-19.24	8.53
773		14.1	0.00	0.003	3	5.98	m	-14.78	0.60
778		14.4	0.01	0.023	2			-21.34	<1.50
781		13.5	0.00	0.009	3	20.00	c	-18.00	1.82
789	S1	14.5	0.00	0.032	1			-21.92	3.79
799A		12.7	0.01	0.011	1			-21.44	10.64
800		13.8	0.00	0.014	1			-20.82	2.52
806		14.5	0.00	0.006	2	38.33	n	-18.42	<0.60
809		14.5	0.00	0.025	1			-21.38	1.80
814		14.4	0.01	0.013	3			-20.10	1.53
817	S1	14.3	0.01	0.032	1			-22.16	2.24
829		14.5	0.00	0.004	1	28.72	o	-17.79	0.71
839		13.8	0.06	0.013	3			-20.90	5.15
841	S1	14.0	0.00	0.036	1			-22.67	0.51
861		14.5	0.01	0.015	3			-20.31	1.34
874		14.5	0.01	0.014	7			-20.16	0.47
900		14.3	0.05	0.004	2	14.41	a	-16.69	<0.60
991		14.2	0.03	0.037	1			-22.65	1.42
993	S2	14.0	0.01	0.015	2			-20.81	<0.40
1002		13.5	0.02	0.011	2			-20.68	4.85
1003		14.4	0.02	0.010	5			-19.57	0.59
1007		14.2	0.03	0.017	1			-20.96	<1.50
1027		14.4	0.03	0.030	1			-22.00	5.28
1068		14.0	0.06	0.017	2			-21.28	1.16
1101		14.3	0.00	0.034	1			-22.25	1.86
1104		13.6	0.00	0.007	1	33.43	a	-19.02	1.46
1134		14.3	0.06	0.017	1			-20.98	4.76
1224		14.3	0.01	0.050	1			-23.12	4.35
1230		14.0	0.02	0.004	1	24.99	a	-18.07	1.12
1233		13.9	0.02	0.016	6			-21.09	2.79
1236		13.5	0.02	0.005	1	10.79	d	-16.74	2.28
1237		14.3	0.00	0.015	1			-20.47	<0.60
1239	S1	14.5	0.02	0.019	1			-20.86	1.39
1243	S1	14.5	0.02	0.036	1			-22.25	0.51
1260		14.2	0.01	0.025	1			-21.72	
1261		14.1	0.02	0.025	1			-21.86	
1264		14.4	0.01	0.002	2	10.82	a	-15.81	
1267		14.1	0.02	0.019	1			-21.26	
1288		14.4	0.00	0.023	2			-21.30	

Table 2 (continued)

Mkn	Type	m_{Zw}	E(B-V)	z	Ref.	D(Mpc)	Notes	M_{Zw}	F_{60}(Jy)
1301		14.5	0.00	0.005	2	33.16	p	-18.10	
1304		13.7	0.01	0.018	6			-21.51	3.81
1308		13.7	0.01	0.003	1	10.43	a	-16.43	<1.50
1325		13.6	0.00	0.024	1			-22.19	<1.50
1326		13.5	0.00	0.006	2	20.00	c	-18.00	0.97
1346		13.7	0.00	0.003	1	21.53	e	-17.96	0.88
1365		14.1	0.00	0.018	1			-21.07	3.84
1418		13.5	0.00	0.002	1	9.06	a	-16.28	0.56
1419		13.6	0.02	0.016	1			-21.39	0.76
1425		14.0	0.00	0.024	4			-21.79	1.00
1443		12.6	0.00	0.002	2	15.93	q	-18.41	1.22
1466		13.1	0.01	0.004	1	17.66	d	-18.17	5.88
1478		14.5	0.00	0.027	8			-21.55	0.98
1479		14.2	0.00	0.001	4	4.75	a	-14.18	<1.50
1485		12.4	0.00	0.008	1			-21.01	2.24
1496		14.5	0.02	0.008	2			-18.99	0.66

References for redshifts: 1. Palumbo et al. (1983) 2. Huchra et al. (1983) 3. Denisyuk and Lipovetskii (1983) 4. Markarian et al. (1983) 5. Markarian et al. (1984) 6. Dennefeld and Sevre (1984) 7. Karachentsev (1981) 8. Markarian et al. (1985)

References for distances of nearby galaxies:

a. Calculated from the model of Aaronson et al. (1982a).
b. Member of the Ursa Major cluster (Aaronson and Mould, 1983).
c. Member of the Virgo cluster (Huchtmeier and Richter, 1986).
d. Bottinelli et al. (1985).
e. Member of the NGC 5033 group (Aaronson and Mould, 1983).
f. Bottinelli et al. (1984).
g. Member of the NGC 3079 group (Turner and Gott, 1976); distance of the group estimated from data on NGC 3079 (Aaronson et al., 1982b).
h. Bottinelli et al. (1986).
i. Member of group 63 of Geller and Huchra (1983); distance from data on NGC 3359 (Aaronson et al., 1982b).
j. Member of group 163 of Geller and Huchra (1983); distance from data on NGC 7448 (Bottinelli et al., 1985) and the B-band Tully-Fisher relation by Bottinelli et al. (1984).
k. Member of group 50 of Geller and Huchra (1983); distance from data on NGC 3003 (Aaronson et al., 1982b).
l. Member of group 67 of Geller and Huchra (1983); distance from data on NGC 3430 (Aaronson et al., 1982b).
m. Member of the cluster CVnI (Aaronson and Mould, 1983).
n. Member of group 135 of Geller and Huchra (1983); distance from data on NGC 5676 and I1029 (Aaronson et al., 1982b).
o. Member of group 161 of Geller and Huchra (1983); distance of the group from the model of Aaronson et al. (1982).
p. Member of group 84 of Geller and Huchra (1983); distance from data on NGC 3755 and NGC 3813 (Aaronson et al., 1982b).
q. Member of group 75 of Geller and Huchra (1983); distance from data on NGC 3600 and NGC 3675 (Aaronson et al., 1982b).

Table 3. Estimates of the optical luminosity function of Markarian galaxies (Seyfert included) using both Schmidt's estimator and Turner's method. N is the number of galaxies in the bin, f_c is the correction factor for binning and errors on apparent magnitudes. Columns 3 and 4 give, for each bin, the values of $\langle V/V_{max} \rangle$ obtained including and excluding, respectively, the regions of the sky containing the Virgo and Ursa Major-Coma I clusters. $H_0 = 50$

M_{Zw}	N	$< V/V_{max} >$		f_c	ϕ_0 (Mpc^{-3} mag^{-1})	
					Schmidt	Turner
-14	1	.66 ± .29	.66 ± .29	.76	(.67 ± .67) 10^{-2}	(.63 ± .63) 10^{-1}
-15	2	.79 ± .20	1.0 ± .29	.98	(.53 ± .39) 10^{-2}	(.32 ± .32) 10^{-1}
-16	4	.55 ± .14	.48 ± .17	.92	(.28 ± .15) 10^{-2}	(.27 ± .21) 10^{-2}
-17	8	.62 ± .10	.70 ± .11	.92	(.13 ± .05) 10^{-2}	(.21 ± .14) 10^{-2}
-18	21	.43 ± .06	.50 ± .08	.92	(.88 ± .24) 10^{-3}	(.48 ± .19) 10^{-3}
-19	14	.32 ± .08	.39 ± .09	.91	(.16 ± .03) 10^{-3}	(.19 ± .09) 10^{-3}
-20	35	.61 ± .05	.69 ± .05	.89	(.92 ± .15) 10^{-4}	(.82 ± .33) 10^{-4}
-21	64	.45 ± .04	.45 ± .04	.79	(.37 ± .06) 10^{-4}	(.33 ± .13) 10^{-4}
-22	46	.57 ± .04	.58 ± .04	.48	(.43 ± .09) 10^{-5}	(.31 ± .16) 10^{-5}
-23	10	.53 ± .09	.53 ± .09	.14	(.85 ± .48) 10^{-7}	(.52 ± .52) 10^{-7}
-24	1	1.0 ± .29	1.0 ± .29	.02	(.31 ± .31) 10^{-9}	(.60 ± .60) 10^{-10}

Table 4. Optical luminosity of non-Seyfert Markarians and contributions of "stellar" and "diffuse" sources (Schmidt's estimator). $H_0 = 50$

M_{Zw}	ϕ_0 (Mpc^{-3} mag^{-1})		
	Total	"Stellar"	"Diffuse"
-14	(.68 ± .68) 10^{-2}	...	(.68 ± .68) 10^{-2}
-15	(.52 ± .38) 10^{-2}	...	(.52 ± .38) 10^{-2}
-16	(.28 ± .15) 10^{-2}	(.19 ± .10) 10^{-2}	...
-17	(.13 ± .05) 10^{-2}	(.52 ± .23) 10^{-3}	(.80 ± .43) 10^{-3}
-18	(.88 ± .24) 10^{-3}	(.45 ± .17) 10^{-3}	(.32 ± .13) 10^{-3}
-19	(.16 ± .03) 10^{-3}	(.76 ± .24) 10^{-4}	(.10 ± .03) 10^{-3}
-20	(.87 ± .14) 10^{-4}	(.40 ± .12) 10^{-4}	(.43 ± .12) 10^{-4}
-21	(.31 ± .05) 10^{-4}	(.19 ± .06) 10^{-4}	(.93 ± .21) 10^{-5}
-22	(.32 ± .07) 10^{-5}	(.17 ± .07) 10^{-5}	(.19 ± .06) 10^{-5}
-23	(.61 ± .35) 10^{-7}	(.27 ± .23) 10^{-7}	(.42 ± .28) 10^{-7}

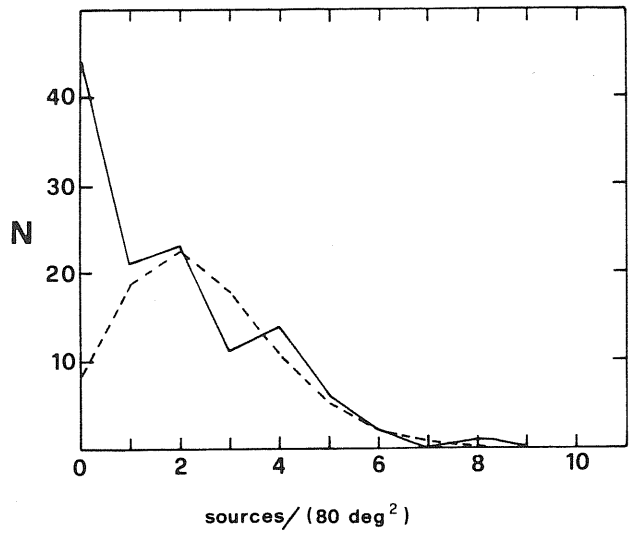

Fig. 1. Observed surface density distribution of Markarian galaxies in the area of the sky defined in sub-Section 2.1 (solid line). The dashed line shows the best fit Poisson distribution. The excess empty areas correspond to regions not, or only poorly, covered by the Markarian survey

probably larger than those due to random motions for higher redshifts). All members of the Virgo cluster (Huchtmeier and Richter, 1986) or of the Ursa Major cluster (Aaronson and Mould, 1983) have been given the same distance, irrespective of their redshifts (i.e. also if they are larger than 0.0075).

Distances based on IR magnitudes have been used preferentially; those given by Aaronson et al. (1982b) have been updated using the new IR magnitude/H I velocity-width relation of Aaronson et al. (1986). Galaxies which belong to a group have been assigned the mean distance of the group members (in several cases however the distance of only one member is available).

Tully-Fisher distances (or data to derive them) were found in the literature for 32 of the 52 galaxies with $z \leqslant 0.0075$ (cf. Table 2). The distances of the remaining 20 objects were estimated from redshifts after having corrected for the Virgocentric motion using the model by Aaronson et al., (1982a).

2.4. *The generalized Schmidt's estimator*

As far as the assumption of a uniform distribution of galaxies holds, the luminosity function can be efficiently derived using the generalized Schmidt's estimator, Φ_G, of the density of sources in the absolute magnitude range $M \pm \Delta M$ (Felten, 1976):

$$\Phi_G = \sum_i \frac{1}{V_m(M_i)}, \tag{2}$$

where the summation is over the objects in the chosen luminosity interval. Since our sample is "local" ($z \leqslant 0.07$ for the full sample; $z \leqslant 0.05$ for non-Seyfert galaxies) we can safely neglect K corrections as well as deviations from an Euclidean geometry. The accessible volume, V_m, then reads:

$$V_m = (\Omega/3)\,(cz_m/H_0)^3, \tag{3}$$

Ω being the effective solid angle covered by the survey and z_m the redshift at which a source of absolute magnitude M has an apparent magnitude equal to the survey limit. The variance of Φ_G (Eq. (18) of Felten, 1976) for sufficiently narrow absolute magnitude bins reduces to

$$\sigma^2 \simeq \phi_0(M)/V_m(M) \tag{4}$$

where ϕ_0 is the differential optical luminosity function.

Two corrections need to be applied to Φ_G in order to derive ϕ_0. First, we must recall that Φ_G is actually an estimator of the integral of ϕ_0 between $M-\Delta M$ and $M+\Delta M$ (correction for binning); second, we must correct for the effect of errors on nuclear magnitudes (Eddington, 1913). The latter were assumed to have a gaussian distribution with dispersion $\simeq 0.5$ mag (Fasano, 1985). In practice to obtain ϕ_0 we need to solve an integral equation (see Cheng et al., 1985, Eqs. (20) and (21)). This can be done with the iterative technique of Lucy (1974). The results are summarized in Tables 3 and 4 (cf. also Fig. 2).

Only 6 of the objects in our sample have no emission lines. Of the remaining 170 non-Seyfert Markarians, 94 are classified as "stellar", 76 as "diffuse". Their luminosity functions, listed in Table 4, are remarkably similar.

2.5. *Turner's (1979) method*

Although the value of $\langle V/V_{max} \rangle$ for the sample as a whole is consistent with that expected for a complete sample of uniformly distributed galaxies, significant deviations from 0.5, probably associated to inhomogeneities in the spatial distribution, show up when we decompose the sample into absolute magnitude bins (cf. Table 3). These fluctuations, however, cannot be ascribed to the 27 galaxies belonging to the two rich clusters (Virgo and Ursa Major – Coma I) contained into the explored volume (dropping them does not appreciably relieve the problem, see Table 3); they are most likely due to the clumpy distribution of galaxies in general. The assumption of homogeneity may then introduce systematic errors varying with absolute magnitude. (Note that there is indication of fluctuations of $\langle V/V_{max} \rangle$ for $M_{Zw} \geqslant -21$, suggesting the presence of significant structure on scales of up to $\simeq 100$ Mpc.)

As shown by Turner (1979), an estimate of the *form* of the luminosity function completely independent of spatial variations in the density of objects can be obtained, on the assumption that such form is constant throughout the sampled volume, and given a *complete* sample, from:

$$\phi_0(M) = A\, Y(M) \exp\left(\int_{-\infty}^{M} Y(M')\, dM' \right) \tag{5}$$

where $Y(M)dM$ is the ratio between the number $n(M)dM$ of objects in the sample having absolute magnitude M, within dM, and the total number of objects with absolute magnitude brighter than M, $N(\leqslant M)$:

$$Y(M)dM = n(M)dM/N(\leqslant M). \tag{6}$$

The normalization constant A can be straightforwardly obtained given the mean surface density (Subsect. 2.2). Again the results need to be corrected for the effects of binning and of errors on magnitudes.

As noted by Turner (1979), there is no simple way for assigning formal errors to the derived space densities because the

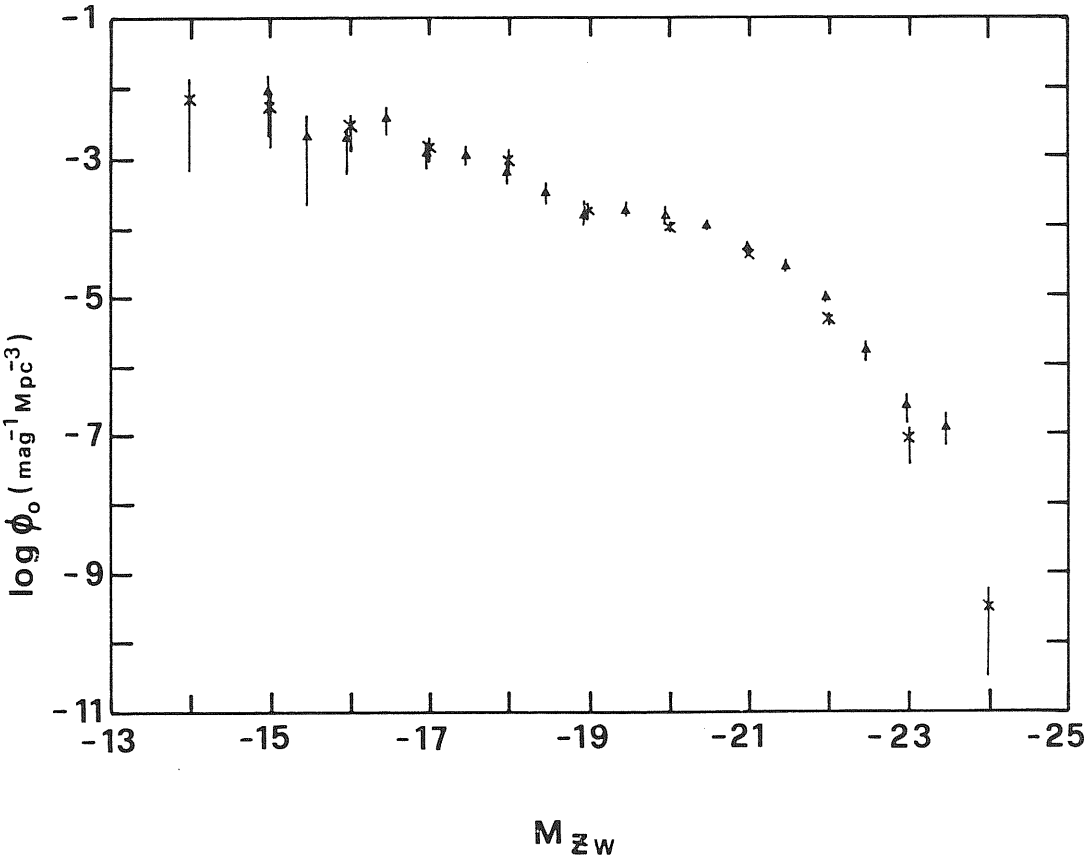

Fig. 2. Optical luminosity function of Markarian galaxies (Seyferts included). Crosses denote the present estimates; triangles, the results by Huchra (1977)

various points are not statistically independent. The estimates listed in Table 3 are obtained from a conventional error analysis; they are probably fairly reliable, because most of the statistical uncertainties are contributed by the terms $n(M)dm$, which *are* independent.

Since no statistically significant differences from the results of the generalized Schmidt's estimator are found, we may conclude that systematic errors originated by clustering of Markarian galaxies are not large.

3. Far-IR properties

Only 11 galaxies in our sample (including the type 2 Seyfert Mkn 744) fall in areas not covered by IRAS (IRAS Explanatory Supplement, 1985); 163 objects (including 24 Seyferts) were detected at 60 μm and upper limits are given for two more (Cataloged Galaxies and Quasars Observed in the IRAS Survey, 1985). The overestimation of fluxes for faint objects in the IRAS Point Source Catalog should not be a serious problem here since only 7 detected sources are fainter than 0.6 Jy at 60 μm. For only one source (Mkn 313 = UGC 12317) there is evidence of extended emission; the 60 μm flux given in the IRAS Small Scale Structure Catalog (1986) has been adopted for it.

Upper limits at 60 μm of 0.6 Jy or of 1.5 Jy were adopted (IRAS Explanatory Supplement, 1985) for undetected sources falling in areas covered with three or two confirming scans, respectively.

The fractional bivariate (optical, far-IR) luminosity function and the associated errors have been computed using the Kaplan-Meier estimator (Schmitt, 1985; Feigelson and Nelson, 1985), which exploits also the information content of upper limits. The results are shown in Table 5.

The far-IR luminosity function of Markarians is given in Table 6; the errors are the quadratic sum of uncertainties on the optical luminosity function and on the bivariate. As shown by Fig. 3, it is very similar to the optical one, as a consequence of the tight correlation between the emissions in the two bands (cf. Fig. 4): the linear correlation coefficient between luminosities at 0.43 μm (L_B) and at 60 μm (L_{60}) is $r = 0.85 \pm 0.03$ (L_B and L_{60} are defined as νL_ν; the former has been estimated using the relation between Zwicky and photographic magnitudes derived by Huchra (1976) and the absolute calibration of the blue magnitude given by Lang (1974)).

This correlation is, actually, much stronger than that found by Rieke and Lebofsky (1986) for normal galaxies. Such difference may be due to the fact that, in the case of Markarian galaxies, bursts of star formation account for most of both the blue and far-IR emissions, while, in normal galaxies, a substantial fraction of blue light may be contributed by older stars. On the other hand it is also possible that selection effects also play a role;

Table 5. Fractional bivariate function of Markarians (Seyfert included). L_{60} is in solar units. The first line gives the value, the second the error

M_z / $\log L_{60}$	-14	-15	-16	-17	-18	-19	-20	-21	-22	-23
7.25	1.00 .000	1.00 .000	.202 .000							
7.75			.798 .000							
8.25				.724 .724	.252 .252					
8.75				.265 .209	.631 .152	.255 .047				
9.25				.010 .010	.117 .073	.543 .172	.222 .146			
9.75						.155 .151	.597 .108	.364 .364	.034 .034	
10.25						.047 .045	.168 .096	.510 .094	.388 .043	.279 .279
10.75							.013 .013	.126 .043	.473 .104	.301 .229
11.25									.106 .046	.292 .232
11.75										.082 .082
12.25										.047 .044

Table 6. Local luminosity function of Markarian galaxies at 60 μm. L_{60} is defined as νL_ν (60 μm) and is in units of $L_\odot = 3.9\ 10^{33}$ erg s^{-1}. $H_0 = 50$

$\log(L_{60}/L_\odot)$	ϕ_{IR} (Mpc^{-3} $\log L_{60}^{-1}$)	
	Seyfert included	non-Seyfert
7.25	$(.31 \pm .19)\ 10^{-1}$	$(.31 \pm .19)\ 10^{-1}$
7.75	$(.55 \pm .29)\ 10^{-2}$	$(.55 \pm .30)\ 10^{-2}$
8.25	$(.30 \pm .26)\ 10^{-2}$	$(.30 \pm .26)\ 10^{-2}$
8.75	$(.24 \pm .09)\ 10^{-2}$	$(.24 \pm .09)\ 10^{-2}$
9.25	$(.58 \pm .20)\ 10^{-3}$	$(.57 \pm .20)\ 10^{-3}$
9.75	$(.23 \pm .08)\ 10^{-3}$	$(.23 \pm .08)\ 10^{-3}$
10.25	$(.11 \pm .03)\ 10^{-3}$	$(.10 \pm .03)\ 10^{-3}$
10.75	$(.20 \pm .05)\ 10^{-4}$	$(.19 \pm .05)\ 10^{-4}$
11.25	$(.12 \pm .05)\ 10^{-5}$	$(.51 \pm .35)\ 10^{-6}$
11.75	$(.18 \pm .18)\ 10^{-7}$	$(.20 \pm .20)\ 10^{-8}$
12.25	$(.99 \pm .99)\ 10^{-8}$	

for example, the Markarian survey may be biased in favour of galaxies with low internal extinction (Smith, 1985).

There is strong evidence that the optical and IR luminosities are not directly proportional: as shown by Fig. 5, more luminous objects tend to have relatively larger percentages of their output in the far-IR. The correlation coefficient between $\log(L_{60})/L_B)$ and $\log(L_{60})$ is 0.68 ± 0.04; the slope of the linear regression is 0.26 ± 0.02 (cf. Table 7). Qualitatively similar behaviors have been found by Deutsch and Willner (1986) for Balzano's (1983) starburst nuclei and, most recently, by Feigelson et al. (1987) for Markarian galaxies.

These results can be simply understood in terms of extinction by dust in star-forming regions. In the limiting case whereby such regions are more or less uniformly spread throughout the volume and only those that lie near the surface toward the observer emit blue light that can escape, we would have $L_{60}/L_B \propto L_{60}^{1/3}$ (Harwit et al., 1987).

Indeed, strong evidence for a significant dust content in Markarian galaxies comes out from Fig. 5. Most objects turn out to be more luminous in the far-IR than in the blue; the mean value of $\log(L_{60}/L_B)$ is 0.28 ± 0.027.

A close correlation between the far-IR excess L_{60}/L_B and the far-IR luminosity has also been found by Rieke and Lebofsky (1986) and by Smith et al. (1987) for IRAS galaxies. In this case, however, L_B and L_{60} turn out to be only weakly correlated and, as a consequence, the slope of the linear regression in the log $L_{60} - \log(L_{60}/L_B)$ plane is close to unity.

As noted by Smith et al. (1987), the IRAS survey preferentially selects galaxies within a relatively narrow range of absolute blue luminosity; it apparently undersamples galaxies of low and very high blue luminosity. A comparison with the results of recent analyses of large, optically selected samples (Franceschini et al., 1988a, b; Feigelson et al., 1987) shows that the deficiency of low L_B galaxies in IRAS samples (relative to optical samples) can be

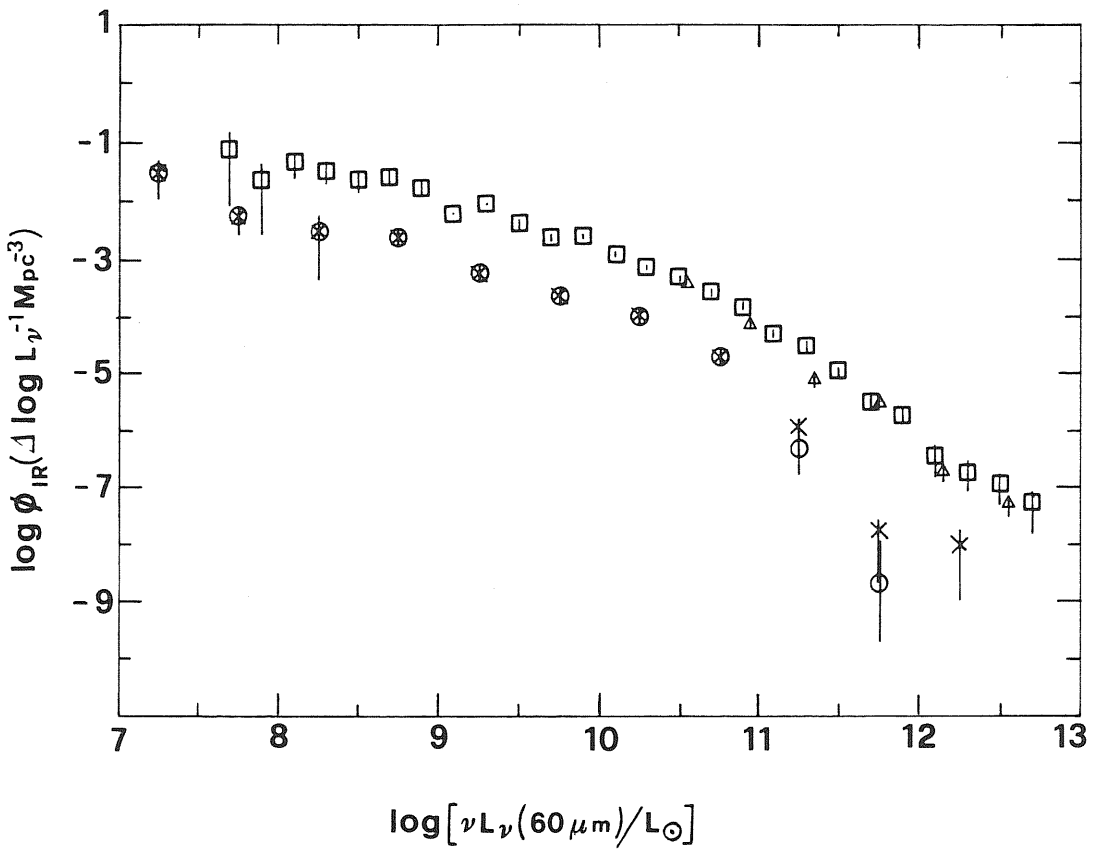

Fig. 3. Luminosity function of Markarian galaxies at 60 μm. Crosses and circles show our estimates including and excluding Seyferts, respectively. Also shown, for comparison, are the luminosity functions of IRAS galaxies derived by Lawrence et al. (1986; squares) and Soifer et al. (1986). Luminosities are defined as νL_ν and are in solar units ($L_\odot = 3.9\ 10^{33}$ erg s^{-1})

only partly understood as the consequence of the fact that they are relatively weaker far-IR emitters due to the effect of dust, as discussed above; optical samples of spiral and irregular galaxies appear to comprise a number of weak galaxies which are truly underluminous in the far-IR. The lack of very high L_B galaxies in the IRAS samples, on the other hand, demonstrates that the far-IR excess versus luminosity relation cannot be extrapolated to the most powerful sources.

Seyferts display a weaker correlation between far-IR and blue luminosities than non-Seyfert Markarians; correspondingly, the ratio L_{60}/L_B is closely correlated with L_{60} and the slope of the linear regression is relatively steep.

4. Discussion and conclusions

As shown by Fig. 2, the present estimate of the optical luminosity function of Markarian galaxies is in good agreement with that obtained by Huchra (1977). We stress, however, that our results are more "solid" since known sources of systematic errors have been accurately dealt with. In particular the application of Turner's method has allowed to quantitatively estimate the systematic uncertainties originated by clustering.

Several authors (cf. Smith, 1985, and reference therein) emphasized that the Markarian survey may be biased against discovering objects with even quite small amounts of dust extinction. In view of the evidence of a significant dust content in Markarian galaxies, we may expect that the derived space densities are severely underestimated. Since starburst galaxies are known to be overluminous in the far-IR, the IRAS survey would greatly help to settle the question.

As shown by Fig. 3, the contribution of Markarians to the luminosity function of galaxies at 60 μm is never dominant. This result is at variance with the claim by Soifer et al. (1986) that "the space density of infrared galaxies is quite similar to that of the starburst (non-Seyfert Markarian) galaxies" in the luminosity range from $\simeq 3\,10^{10}$ to $3\,10^{11}$ $L_\odot$. Soifer et al. (1986), however, have apparently compared the "bolometric" luminosity function of Markarians with the far-IR luminosity function of IRAS galaxies. For a meaningful comparison, the luminosity function of Markarians in Fig. 1 of Soifer et al. (1986) should be shifted towards lower luminosities by a factor of 3 (they estimate that, in the mean, far-IR luminosities of Markarians are one-third of the total luminosities).

On the other hand, there is evidence that most of infrared luminous galaxies are undergoing outbursts of star formation activity (Elston et al., 1985; Soifer et al., 1987). This demonstrates that the IRAS survey is far more efficient than optical techniques for finding starburst systems. The increasing difference between the space densities of infrared selected galaxies and those of Markarians suggests that either dust affects more and more the

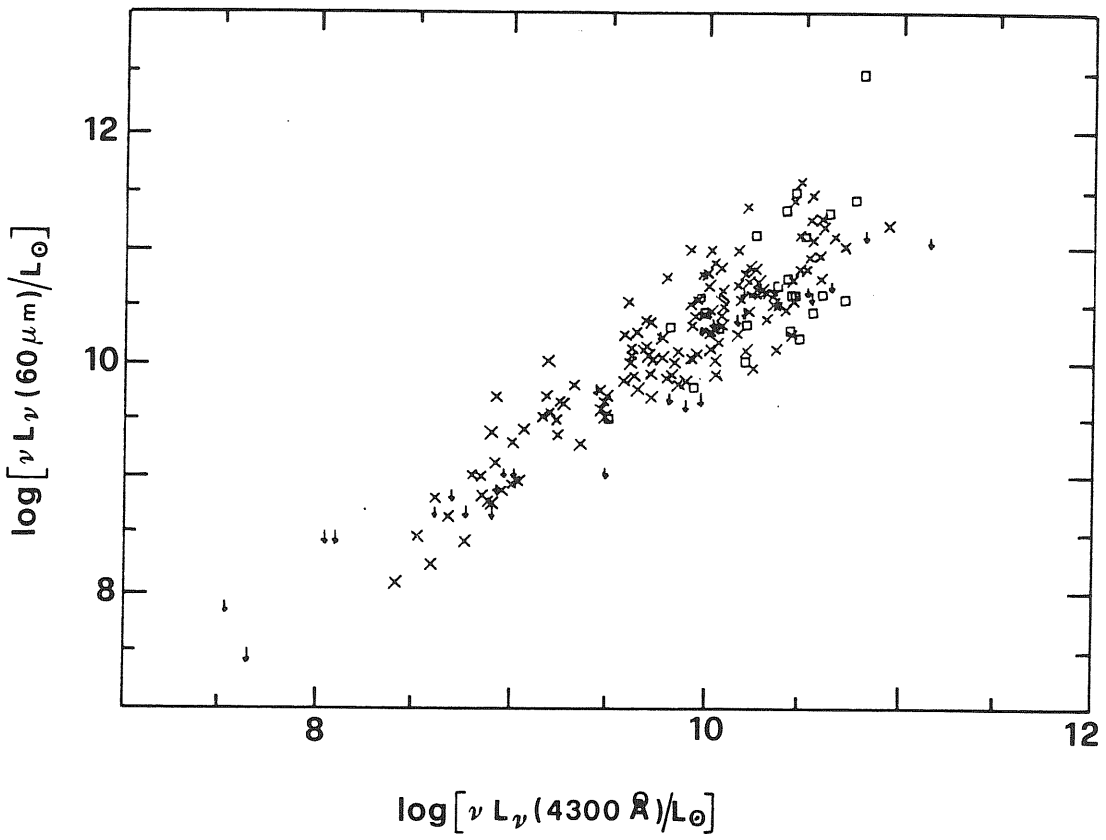

Fig. 4. Luminosities at 60 μm as a function of luminosities at 4300 Å. Crosses and squares refer to non-Seyfert Markarians and to Seyferts, respectively; arrows denote upper limits

Table 7. Best fit coefficients for relations between blue (0.43 μm) and far-IR (60 μm) luminosities. Both luminosities are defined as νL_ν and are in solar units ($L_\odot = 3.9\ 10^{33}$ erg s^{-1}). We consider linear relations of the form log Y = a + b·log X; r is the linear correlation coefficient

		a	b	r
$log\ L_{60} = a + b \cdot log\ L_B$	Sey. included	.02 ± .51	1.03 ± .05	.85 ± .02
	non-Seyf. only	-.39 ± .42	1.07 ± .05	.88 ± .02
	Sey. only	-1.47 ± 3.95	1.17 ± .39	.62 ± .15
$log\ \frac{L_{60}}{L_B} = a + b \cdot log\ L_{60}$	Sey. included	-2.3 ± .18	.26 ± .02	.68 ± .04
	non-Seyf. only	-2.17 ± .21	.25 ± .02	.66 ± .04
	Sey. only	-6.03 ± .88	.59 ± .08	.84 ± .08

optical selection as the IR luminosity increases (possibly because of the increase in the ratio L_{FIR}/L_B, cf. Sect. 3), or a new component becomes important at high luminosities.

Arguments in favor of the latter possibility are discussed by Harwit et al. (1987). On the other hand, Franceschini et al. (1988b) have shown that an evolving population comprising, in addition to Markarians, peculiar and interacting galaxies (in keeping with the notion that interactions play an important role in triggering starbursts), can easily account for all the available far-IR data as well as for the VLA counts of radio sources (Danese et al., 1987). In this framework the break in the far-IR luminosity function at $L \approx 10^{12}\ L_\odot$ noted by Lawrence et al. (1986) is interpreted as the trait of evolution rather than of the emergence of a new class of sources.

That the luminosity of actively star-forming galaxies evolves on a timescale shorter than the Hubble time is indeed expected on simple physical grounds. The increase in the far-IR to blue luminosity ratio with increasing luminosity, discussed in Sect. 3, implies that evolution is considerably milder in the optical than it is in the far-IR (and in the radio). The most spectacular bursts of star formation thus probably occur inside a cocoon of dust that obscures our view at optical wavelengths. Far-IR data may then

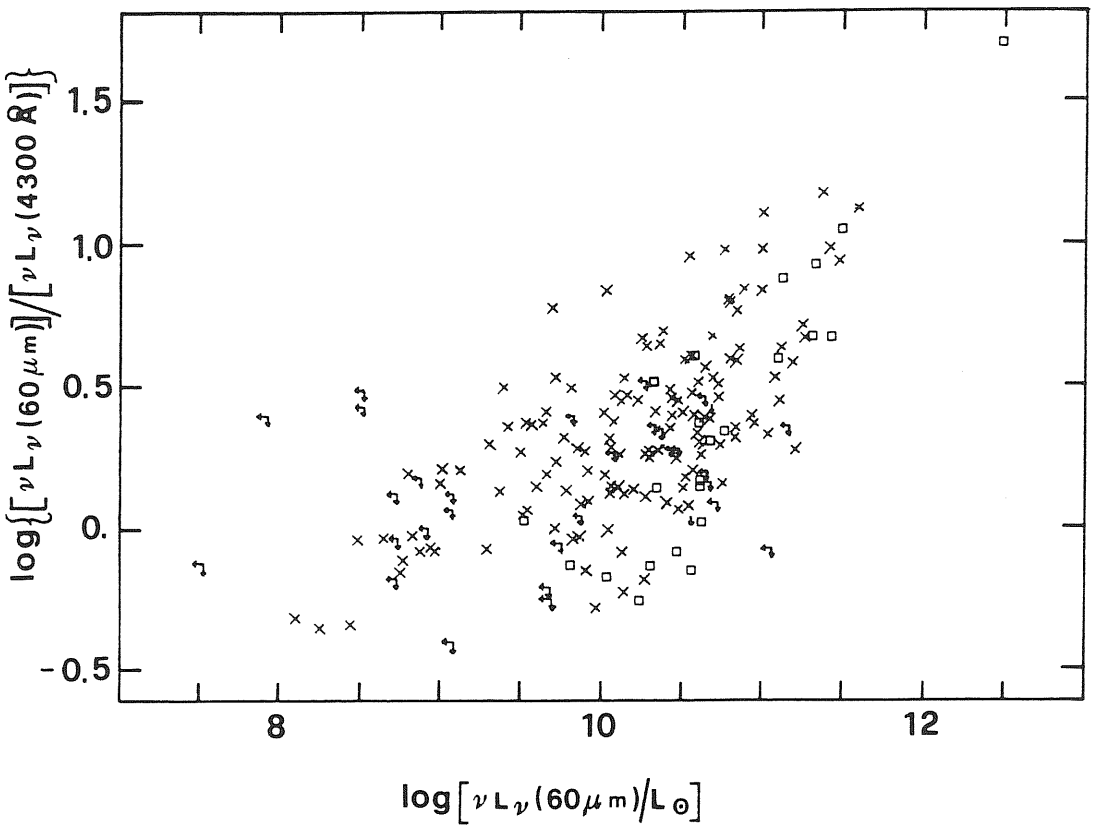

Fig. 5. Far-IR (60 μm) to blue (4300 Å) luminosity ratios as a function of 60 μm luminosity for non-Seyfert Markarians (crosses) and for Seyferts (squares). Arrows denote limits

represent the most powerful tool for investigating the early phases of galaxy evolution.

Acknowledgements. We wish to thank the referee for his useful comments. We also thank the Astronomical Data Center at the NASA Goddard Space Flight Center for providing copies of the IRAS data products. Work supported in part by MPI and CNR (through GNA and PSN).

References

Aaronson, M., Bothun, G., Mould, J., Huchra, J. Schommer, R.A., Cornell, M.E.: 1986, *Astrophys. J.* **302**, 536

Aaronson, M., Huchra, J., Mould, J.R., Schechter, P.L., Tully, R.B.: 1982a, *Astrophys. J.* **258**, 64.

Aaronson, M., Huchra, J., Mould, J.R., Tully, R.B., Fisher, J.R., van Woerden, H., Goss, W.M., Chamaraux, P., Mebold, U., Siegman, B., Berriman, G., Persson, S.E.: 1982b, *Astrophys. J. Suppl.* **50**, 241.

Aaronson, M., Mould, J.: 1983, *Astrophys. J.* **265**, 1.

Balzano, V.A.: 1983, *Astrophys. J.* **268**, 602

Bottinelli, L., Gouguenheim, L., Paturel, G., de Vaucouleurs, G.: 1984, *Astron. Astrophys. Suppl.* **56**, 381

Bottinelli, L., Gouguenheim, L., Paturel, G., de Vaucouleurs, G.: 1985, *Astron. Astrophys. Suppl.* **59**, 43

Burstein, D., Heiles, C.: 1982, *Astron. J.* **87**, 1165

Cataloged Galaxies and Quasars Observed in the IRAS Survey 1985, prepared by Lonsdale, C.J., Helou, G., Good, J.C., Rice, W., Jet Propulsion Laboratory

Cheng, F.-Z., Danese, L., De Zotti, G., Franceschini, A.: 1985, *Monthly Notices Roy. Astron. Soc.* **212**, 857

Condon, J.J., Mitchell, K.J.: 1984, *Astron. J.* **89**, 610

Danese, L., De Zotti, G., Franceschini, A., Toffolatti, L.: 1987, *Astrophys. J. Letters*, **318**, L15

Denisyuk, E.K., Lipovetskii, V.A.: 1983, *Astrofiz.* **19**, 229 [*Astrophys.* **19**, 134]

Dennefeld, M., Sèvre, F.: 1984, *Astron. Astrophys. Suppl.* **57**, 253

Deutsch, L.K., Willner, S.P.: 1986, *Astrophys. J. Letters* **306**, L11

De Zotti, G.: 1987, in Proc. 7th Italian Conference on *General Relativity and Gravitational Physics*, eds. U. Bruzzo, R. Cianci, E. Massa, World Scientific Press, p. 331

Eddington, A.S.: 1913, *Monthly Notices Roy. Astron. Soc.* **73**, 359

Elston, R., Cornell, M.E., Lebofsky, M.: 1985, *Astrophys. J.* **296**, 106

Fasano, G.: 1985, *Astron. Astrophys. Suppl.* **60**, 285

Feigelson, E.D., Isobe, T., Weedman, D.W.: 1987, *Astrophys. J. Letters* **319**, L51

Feigelson, E.D., Nelson, P.I.: 1985, *Astrophys. J.* **293**, 192

Felten, J.E.: 1976, *Astrophys. J.* **207**, 700

Fomalont, E.B., Kellermann, K.I., Wall, J.V., Weistrop, D.: 1984, *Science* **225**, 23

Franceschini, A., Danese, L., De Zotti, G., Toffolatti, L.: 1988a, *Monthly Notices Roy. Astron. Soc.* (in press)

Franceschini, A., Danese, L., De Zotti, G., Xu, C.: 1988b, *Monthly Notices Roy. Astron. Soc.* (in press)

Geller, M.J., Huchra, J.P.: 1983, *Astrophys. J. Suppl.* **52**, 61
Hacking, P., Houck, J.R.: 1987, *Astrophys. J. Suppl.* **63**, 311
Harwit, M., Houck, J.R., Soifer, B.T., Palumbo, G.G.C.: 1987, *Astrophys. J.* **315**, 28
Huchra, J.P.: 1976, *Astron. J.* **81**, 952
Huchra, J.P.: 1977, *Astrophys. J. Suppl.* **35**, 171
Huchra, J., Davis, M., Latham, D., Tonry, J.: 1983, *Astrophys. J. Suppl.* **52**, 89
Huchra, J.P., Sargent, W.L.W.: 1973, *Astrophys. J.* **186**, 433
Huchtmeier, W.K., Richter, O.G.: 1986, *Astron. Astrophys. Suppl.* **64**, 111
IRAS Catalogs and Atlases, Explanatory Supplement 1985, eds Beichman, C.A., Neugebauer, G., Haing, H.J., Clegg, P.E., Chester, T.J., Washington D.C. U.S. Government Printing Office
IRAS Small Scale Structures Catalog 1986, prepared by Helou, G., Walker, D., Washington D.C. U.S. Government Printing Office
Karachentsev, I.D.: 1981, *Pis'ma Astron. Zh.* **7**, 3 [*Sov. Astron. Lett.* **7**, 1]
Lang, K.R.: 1974, *Astrophysical Formulae*, Springer-Verlag, Berlin Heidelberg New York
Lawrence, A., Walker, D., Rowan-Robinson, M., Leech, K.J., Penston, M.V.: 1986, *Monthly Notices Roy. Astron. Soc.* **219**, 687
Lucy, L.B.: 1974, *Astron. J.* **79**, 745
Markarian, B.E.: 1963, *Soobcheniya Byur. Observatory* **34**, 3
Markarian, B.E.: 1967, *Astrofiz.* **3**, 55 [*Astrophysics.* **3**, 24]
Markarian, B.E., Erastova, L.K., Lipovetskii, V.A., Stepanian, D.A., Shapovalova, A.I.: 1985, *Astrofiz.* **22**, 215 [*Astrophys.* **22**, 127]
Markarian, B.E., Lipovetskii, V.A., Stepanian, D.A.: 1981, *Astrofiz.* **17**, 619 [*Astrophys.* **17**, 321]
Markarian, B.E., Lipovetskii, V.A., Stepanian, D.A.: 1983, *Astrofiz.* **19**, 221 [*Astrophys.* **19**, 129]
Markarian, B.E., Lipovetskii, V.A., Stepanian, D.A.: 1984, *Astrofiz.* **20**, 419 [*Astrophys.* **20**, 581]
Neyman, J., Scott, E.L.: 1961, *Proc. 4th Berkeley Symp. Mathematical Statistics and Probability* Vol. 3, Univ. Calif. Press, Berkeley, p. 261
Palumbo, G.G.C., Tanzella-Nitti, G., Vettolani, G.: 1983, *Catalog of Radial Velocities of Galaxies*, Gordon and Breach, New York
Partridge, R.B., Hilldrup, K.C., Ratner, M.I.: 1986, *Astrophys. J.* **308**, 46
Rieke, G.H., Lebofsky, M.J.: 1986, *Astrophys. J.* **304**, 326
Sargent, W.L.W.: 1972, *Astrophys. J.* **173**, 7
Schmitt, J.H.M.M.: 1985, *Astrophys. J.* **293**, 178
Smith, B.J., Kleinmann, S.G., Huchra, J.P., Low, F.J.: 1987, *Astrophys. J.* **318**, 161
Smith, M.G.: 1985, in *Active Galactic Nuclei*, ed. J.E. Dyson, Manchester University Press, p. 103
Soifer, B.T., Houck, J.R., Neugebauer, G.: 1987, *Ann. Rev. Astron. Astrophys.* **25**, 187
Soifer, B.T., Sanders, D.B., Neugebauer, G., Danielson, G.E., Lonsdale, C.J., Madore, B.F., Persson, S.E.: 1986, *Astrophys. J.* **303**, L41
Toffolatti, L. Franceschini, A., De Zotti, G., Danese, L.: 1987, *Astron. Astrophys.* **184**, 7
Tully, R.B., Fisher, J.R.: 1977, *Astron. Astrophys.* **54**, 661
Turner, E.L.: 1979, *Astrophys. J.* **231**, 645
Turner, E.L., Gott, J.R.: 1976, *Astrophys. J. Suppl.* **32**, 409
Veron-Cetty, M.-P., Veron, P.: 1985, ESO Scientific Report No. 4
Weedman, D.W.: 1987, in Proc. Conf. on *Star Formation in Galaxies*, Calif. Inst. Technology, Pasadena
Windhorst, R.A.: 1984, Ph.D. thesis, University of Leiden
Windhorst, R.A.: 1986, in *Highlights of Astronomy*, Vol. 7, ed. J.-P. Swings, Reidel, Dordrecht, p. 355
Windhorst, R.A., Dressler, A., Koo, D.C.: 1987, in Proc. IAU Symp. No. 124, *Observational Cosmology*, eds. G. Burbidge, L.Z. Fang, Reidel, Dordrecht, p. 573

6.2. Cosmic evolution of actively star-forming galaxies

As discussed in Chapter 2, most ($\sim 90\%$) of non-Seyfert Markarian galaxies are actively star-forming galaxies. The obvious expectation that objects of this kind experience a significant cosmological evolution appears to be borne out by recent observational evidence.

a. Very deep radio surveys

The first indication came from very deep radio source counts. VLA surveys, reaching flux densities as low as $\simeq 50$ —$100\mu Jy$, at 21 cm (Condon and Mitchell 1984; Windhorst 1984; Windhorst et al. 1985; Oort and Windhorst 1985; Oort 1987) and 6 cm (Fomalont et al. 1984; Partridge et al. 1986), revealed a significant steepening of the differential counts of radio sources below a few mJy.

Danese et al. (1987) pointed out that such steepening cannot be attributed to any of the canonical source populations which dominate the counts at high flux densities, given the observational constrains (in particular, the 408 MHz counts). A similar conclusion was also reached by Wall et al. (1986), who stressed that it is very difficult to produce pronounced features, such as the observed 'upturn', with sources dominating at high flux densities, given their extremely broad luminosity functions. The latter authors remarked that the space densities of low-luminosity radio sources are poorly known and suggested that they could be large enough to explain the sub-mJy counts without evolution. On the other hand, the detailed study of the local luminosity function of galaxies, carried out by Toffolatti et al. (1987), set strongest constraints on the density of weak sources. Using their results, Danese et al. (1987) concluded that the contribution to the observed counts of non-evolving sources with $\log P(400\,MHz;\, W/Hz/sr) \geq 20$ ($H_0 = 50$), must be small.

As noted by Franceschini et al. (1988b), if the upturn of the deep radio source counts is due to still weaker sources, they must be local: the median

redshift of sources with S(1.4 GHz) ≈0.5 mJy has to be $\leq 10^{-2}$. This latter prediction is strongly inconsistent with the results of direct redshift measurements, demonstrating that the mJy and sub-mJy radio source are at cosmological distances ($z_{median} \geq 0.25$; cf. Kron, Koo and Windhorst 1985; Windhorst, Dressler and Koo 1987; Donnelly, Partridge and Windhorst 1987). Thus the interpretation of the deep radio source counts in terms of a local population seems to be ruled out.

At the other extreme, Condon (1984a, b) interpreted the VLA counts as indicative of evolution of disc galaxies as a whole. However, as pointed out by van der Laan et al. (1986) and confirmed by Danese et al. (1987), evolving spirals can start contributing to the counts only below 1 mJy, as a consequence of their relatively low mean radio luminosity. Thus they cannot account for the significant fraction of blue galaxies observed up to $\simeq 10$ mJy (Windhorst et al. 1985).

Danese et al. (1987) then concluded that the simplest viable possibility for explaining the observed counts was to assume that galaxies with intense star formation activity evolve in radio luminosity on a time scale $\simeq$ 20–25% of the Hubble time. Their model accounts not only for the counts, but for all the data available so far, such as the optical colors, the radio to optical luminosity ratios, and the fraction of blue to red galaxies; it is also consistent with preliminary data on the redshift distribution, on the spectral index distribution, and on the source sizes (Windhorst et al. 1985; 1987).

Fig. 6.2.1 and Fig. 6.2.2 present their fit of source counts at 21 cm and 6 cm.

b. IRAS samples

Given the tight correlation between FIR and radio emissions and the high FIR to radio luminosity ratios for disk galaxies (de Jong et al. 1985; Helou et al.

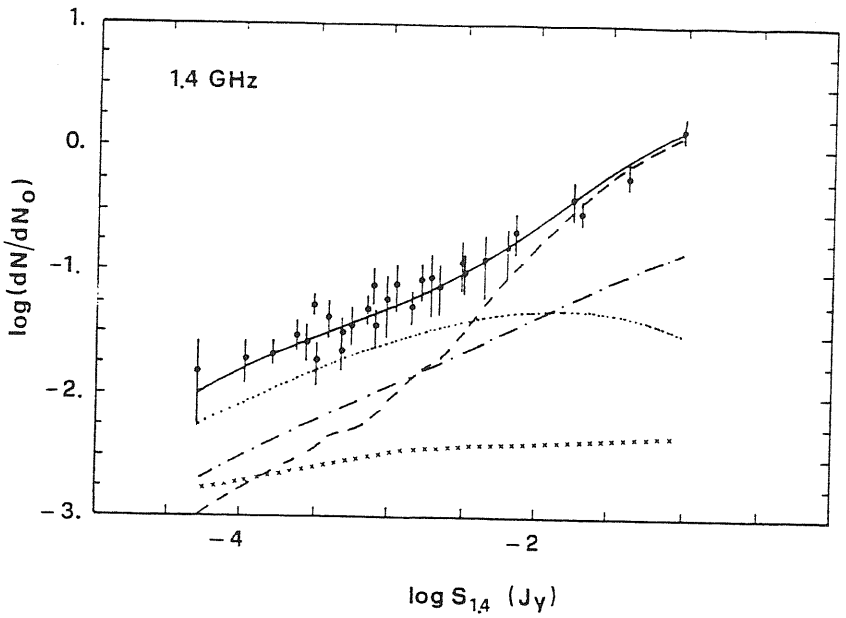

FIG. 2.—Deep counts at 1.4 GHz in relative differential form ($dN_0 = 150 S_{1.4}^{-2.5}$ sr^{-1} Jy^{-1}). The data points are those listed by Condon and Mitchell (1984) and Windhorst *et al.* (1985). The dashed and the dot-dashed lines show, respectively, the contributions of steep-spectrum and "flat"-spectrum ellipticals, S0's, and QSOs; the dotted line displays the expected counts from evolving starburst/interacting galaxies. All these results were obtained using the luminosity functions in Fig. 1 and the best-fit values of evolution parameters for $q_0 = 0.5$ listed in Table 1. The crosses display the counts of unevolving spirals and irregulars. The solid line is the sum of all the above contributions.

Fig. 6.2.1. Taken from Fig. 2. of Danese et al. (1987).

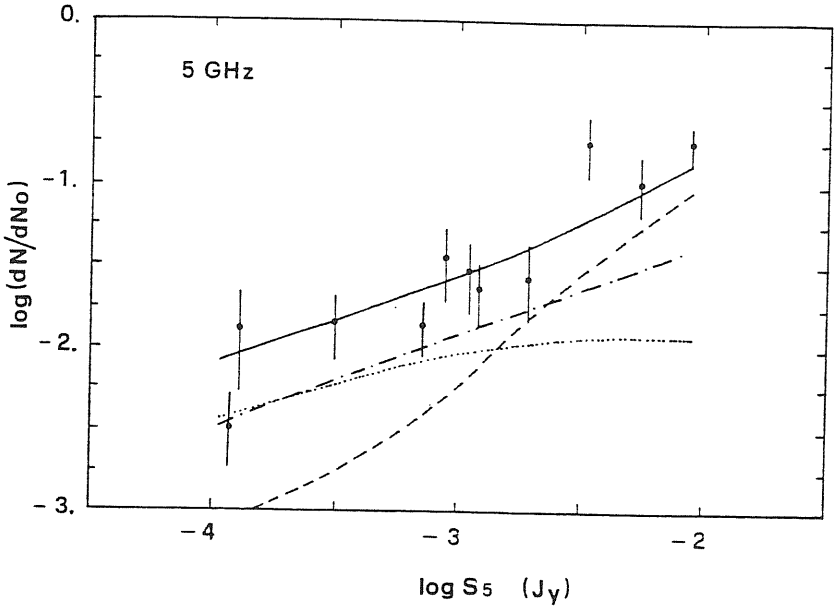

FIG. 3.—Deep counts at 5 GHz ($dN_0 = 150 S_5^{-2.5}$ sr^{-1} Jy^{-1}). The data are from Bennett *et al.* (1983), Fomalont *et al.* (1984), and Partridge, Hilldrup, and Ratner (1986). The lines have the same meaning as in Fig. 2. The (negligibly small) contribution of unevolving normal spirals and irregulars is not shown.

Fig. 6.2.2. Taken from Fig. 3. of Danese et al. (1987).

1985; Gavazzi et al. 1986), a direct test of the models by Danese et al. (1987) can be provided by applying them to IRAS data. To this purpose, Franceschini et al. (1988b) have directly translated the models fitted to the radio data into the FIR band, exploiting the observed distributions of FIR to optical luminosity ratios.

Separate $60\mu m$ local luminosity functions for classes of sources, in which basically different astrophysical processes are operating, were derived by Franceschini et al. (1988a). They have considered the following classes: (i) ellipticals+S0s; (ii) normal spirals+irregulars; (iii)star-burst/interacting (S/I) galaxies, comprising non-Seyfert Markarians and galaxies classified by Nilson (1973) as peculiar, eruptive, disrupted, interacting and blue compact; (iv) Seyfert galaxies.

The Kaplan-Meier estimator (Schmitt 1985; Feigelson and Nelson 1985; Isobe, Feigelson,and Nelson 1986) has been used to derive the bivariate (optical/FIR) distribution taking into account also the information content of upper limits.

In Fig. 6.2.3 (Fig. 1 of Franceschini et al. 1988b), the global FIR luminosity function of optically selected galaxies, sum of the contributions from the four populations, is compared with the luminosity function of IRAS galaxies derived by Lawrence et al. (1986) and Soifer et al. (1987b). The agreement is excellent up to $\log L_{60\mu} = 33$ ($L_{60\mu}$ is the monochromatic luminosity at 60 μm in erg/sec/Hz, hereafter $H_0 = 50$), implying that the space distribution of IRAS galaxies can be entirely accounted for by optical galaxies.

Note also that the data on the FIR local luminosity function strongly support our previous conclusion that the sub-mJy source counts cannot be understood in terms of local sources. Any population of low-luminosity sources contributing substantially to the deep radio counts should also show up in the

60-μm local luminosity function which is defined down to luminosities as low as $\approx 10^7 L_\odot$ (Lawrence et al. 1987), corresponding to $\log P(408MHz) \approx 18$ for disc galaxies. To account for the deep radio counts without evolution, one would need local space densities far in excess of those observed; in particular, the radio luminosity function used by Wall et al. (1986) for their illustrative calculation would translate in an increase of ϕ_{IR} by a factor ≈ 10 in the range $30 \leq \log L_{60\mu} \leq 31$, i.e. $10^9 \leq \nu L_\nu / L_\odot \leq 10^{10}$, where space densities are rather well defined by four independent samples. Increasing the space density of lower luminosity sources, where observational uncertainties on ϕ_{IR} are large, does not help much: we meet the constrains set by the counts, and by the luminosity distribution of bright IRAS galaxies, already with space densities well below those required by radio counts.

The UGC sample is not deep enough to allow a direct evaluation of space density of the highest luminosity sources. A rough estimate can, however, be obtained by combining the optical luminosity functions of galaxies with the observed distributions of $L_{60\mu}/L_{opt}$ (Franceschini et al. 1988a), which appears to be more or less independent of optical luminosity. The dominant contribution to the space density of galaxies with $\log L_{60\mu} = 32.5$ is found to come from S/I's and Seyferts, in agreement with the findings of Houck et al. (1985), Soifer et al. (1987b) and Smith et al. (1987), and corresponds to the high tail of the distribution of FIR to optical luminosity ratios. The result, shown by the cross in Fig. 6.2.3, agrees with the estimates by Soifer et al. (1987b) and Smith et al. (1987), but falls below the points of Lawrence et al. (1986). While the samples of Soifer et al. (1987b) and Smith et al. (1987) are truly local ($z_{max} = 0.08$ and $= 0.07$, respectively), the average redshift for the three highest luminosity bins of Lawrence et al (1986) is $= 0.2$, so the evolution may come into play (see also Soifer et al. 1987b).

Indeed, the models by Danese et al. (1987), fitting the data from deep VLA surveys of radio sources, do predict an increase with red shift of the

space density of ultra-luminous IRAS galaxies, fully consistent with the data by Lawrence et al. (1986), as shown by Fig. 6.2.3.

These models assume that shape of the radio luminosity functions of S/I and Seyfert galaxies does not change with cosmic time

$$\phi_R[L_R(z), z] = \phi_R[L_R(0), 0], \tag{6.2.1}$$

while their radio luminosity increases with redshift according to

$$L(z) = L(0)\exp(\kappa_R \times \tau(z)), \tag{6.2.2}$$

$\tau(z)$ being the look-back time and κ_R^{-1} the evolution time-scale, both in units of the Hubble time; κ_R^{-1} is obtained essentially by fitting the data on mJy and sub-mJy radio sources.

The data on brighter sources determine the parameters characterizing the evolution properties of elliptical + S0 galaxies and of QSO's. The models imply that objects of these classes evolve only if their radio power exceeds some threshold $[P(408\,MHz) > 10^{23.5}\,W/Hz/sr]$. The contribution to the far-IR counts of the evolving portion of the luminosity function, however, is small and will be neglected here.

Normal spiral and irregular galaxies are assumed not to evolve.

Exploiting the radio survey by Dressel and Condon (1978) and the IRAS data on the sample, we can construct the conditional far-IR luminosity function, $\psi_{IR}(L_{60\mu}|z, P_{2.4})$, describing the distribution of $L_{60\mu}$, given the redshift z and the radio power at 2.4 GHz, $P_{2.4}$ (in $W/Hz/sr$). Using the method developed by Schmitt (1985), which takes into account data censored in both variables, Franceschini et al. (1988b) found the following best-fitting linear regressions:

$$\log L_{60\mu} = 7.44 + 0.82 \log P_{2.4} \qquad \text{for S/I galaxies} \tag{6.2.3}$$

and

$$\log L_{60\mu} = 13.54 + 0.61 \log P_{2.4} \qquad \text{for Seyferts.} \tag{6.2.4}$$

Then, assuming that ψ_{IR} is independent of redshift and that the quantity $\log(L_{60\mu}/P_{2.4})$ has a Gaussian distribution with a dispersion = 0.4 around the mean given, as a function of $P_{2.4}$, by equations (6.2.3) and (6.2.4), the 60μ luminosity functions of S/I galaxies at any cosmic time can be derived directly from $\phi_R(P_{2.4}, z)$:

$$\phi_{IR}(L_{60\mu}, z) = \int \phi_R(P_{2.4}, z)\psi(L_{60\mu}, P_{2.4})d(\log P_{2.4}). \tag{6.2.5}$$

Analytical fits to the results of Franceschini et al. (1988) have been adopted to represent the local radio luminosity functions ($X = \log P_{2.4} - 24$):

$$\log \phi_{24}(P_{2.4}, 0) = -7.46 - 1.359X^2 - \exp(X + 1) \tag{6.2.6}$$

for S/I galaxies, and

$$\log \phi_{2.4}(P_{2.4}, 0) = -7.36 - 0.985X - 0.0478X^2 \tag{6.2.7}$$

for Seyferts.

For non-evolving spirals+irregulars and ellipticals+S0s, we need only the 60μ local luminosity functions derived by Franceschini et al. (1988a).

In this framework the space densities (Fig. 6.2.3) and the luminosity distribution (Fig. 6.2.4) of the highest luminosity sources of Lawrence et al. (1986) are accounted for by evolution of S/I and Serfert galaxies.

c. Deep FIR counts

Franceschini et al. (1988b) exploited their model to predict $60\mu m$ counts down to $F_{60\mu} = 1\ mJy$. Predictions were tested against the observed IRAS

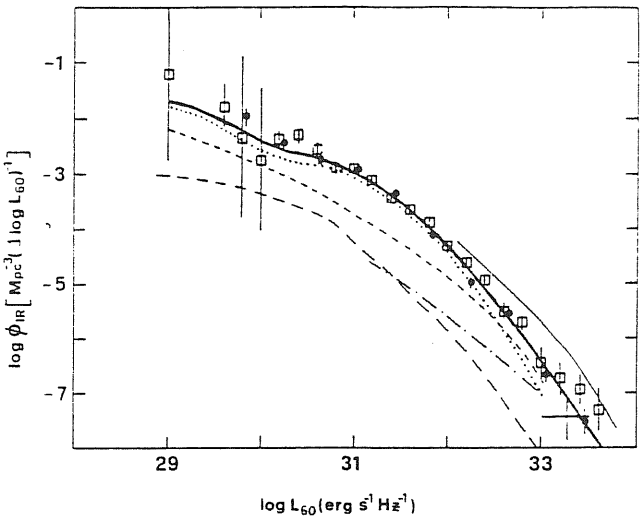

Figure 1. Local luminosity functions at 60 μm of optically selected galaxies. The heavy solid line shows the adopted global space densities, sum of contributions of spirals + irregulars (dotted line), S/Is (short dashes), ellipticals + S0s (long dashes) and Seyferts (dot-dashed line). The cross shows the estimate of the space density of high-luminosity sources obtained as described in the text. Also plotted, for comparison, are the local luminosity functions of *IRAS* galaxies derived by Lawrence *et al.* (1986; open squares) and by Soifer *et al.* (1987) excluding the Virgo cluster galaxies (filled circles). The results of Smith *et al.* (1987) are not shown to avoid overcrowding the figure; they are in excellent agreement with those of Soifer *et al.* (1987). The thin continuous line shows the predicted luminosity function at $z = 0.25$ (the mean redshift of the galaxies in the highest luminosity bin of Lawrence *et al.*), allowing for evolution of S/I and Seyfert galaxies.

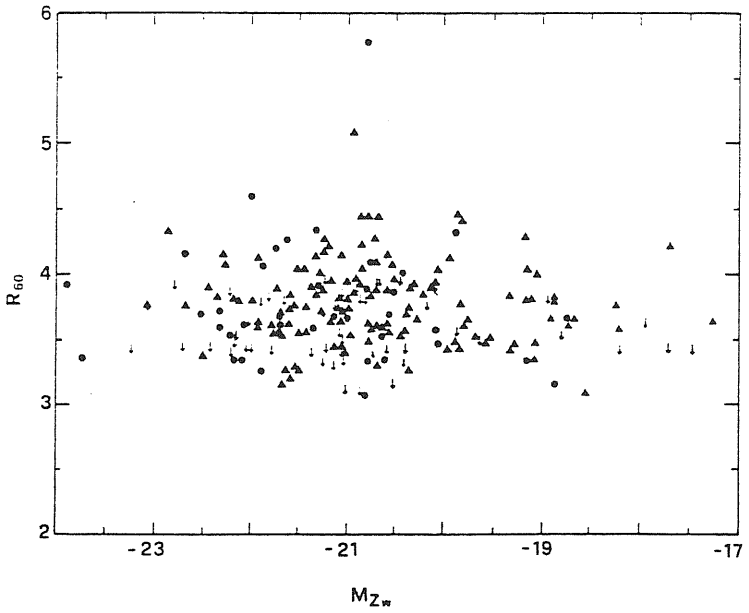

Figure 2. Logarithmic ratios of far-IR to optical fluxes as a function of the absolute Zwicky magnitude for S/I galaxies (triangles) and Seyferts (circles). Arrows denote upper limits. $R_{60} = \log S_{60} + (m_{Z_w} - 12.5)/2.5$; S_{60} in mJy.

Fig. 6.2.3. Taken from Fig. 1. of Franceschini et al. (1988b).

Fig. 6.2.4. Taken from Fig. 2. of Franceschini et al. (1988b).

we have done the analysis for sources detected at both wavelengths (taking into account the limits at the other); the results are very similar (cf. Table 6.2.1).

The spectral index $\alpha_{60/25}$ has been assumed to be independent of luminosity (see e.g. Rieke and Lebofsky 1986).

The predicted contributions to the $60\mu m$ counts are shown in Fig. 6.2.6. Note that although the radio evolution time-scale of S/I galaxies is comparable to that of QSO's and of powerful radio galaxies, the far-IR counts are never very steep: actually, they are slightly flatter than Euclidean for $F_{60\mu} > 0.1$ Jy and decline significantly at fainter fluxes.

Three factors contribute to keep the $\log N$–$\log S$ quite flat:

(i) non-evolving spirals and irregulars outnumber S/I galaxies over the flux density range where the counts of the latter are steeper.

(ii) The evolution rate in the far-IR is, in the present framework, slower than in the radio: it is easily seen from equations (6.2.1) to (6.2.5) that the evolution times-scale in the far-IR, κ_{IR}^{-1}, is $\simeq (0.82\kappa_R)^{-1}$ and $\simeq (0.61\kappa_R)^{-1}$ for S/I and Serfert galaxies, respectively.

(iii) The very strong K-correction flattens down effectively the $\log N$–$\log S$ of S/I galaxies themselves. In order to emphasize the more efficiently evolving S/I galaxies, surveys at longer wavelengths ($\approx 300\mu m$), such as those that could be carried out with the Multiband Imaging Photometer planned for the *Far-IR and Submillimeter Space Telescope (FIRST)*, would be needed.

(2) PRIMEVAL GALAXIES

To obtain an order-of-magnitude estimate of the possible contribution of primeval disc galaxies to the $60\mu m$ counts down to 1 mJy, we have adopted the following simple approach.

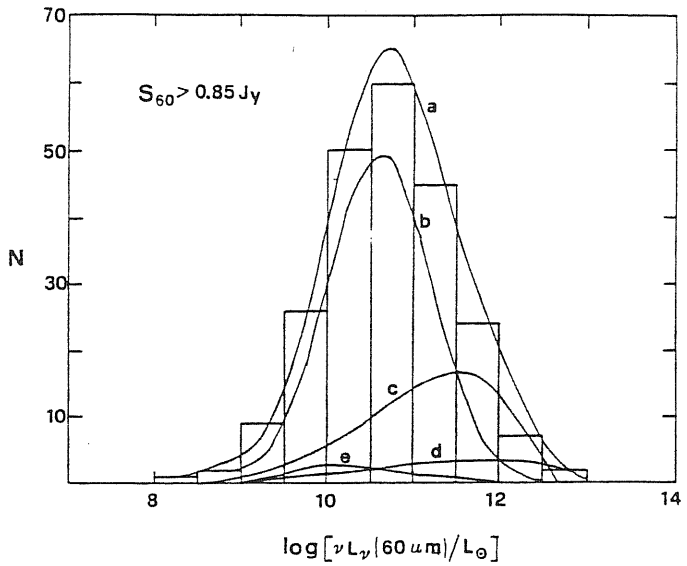

Figure 3. Comparison between predicted and observed luminosity distributions of *IRAS* galxies brighter than $S_{60}=0.85$ Jy. Luminosity is νL_ν at 60 μm, in units of $L_0=3.9\times10^{33}$ erg s^{-1}. The curve a represents the sum of the contributions of spiral + irregular galaxies (curve b), of evolving S/I galaxies (curve c), of evolving Seyferts (curve d), and of non-evolving Ellipticals + S0s (curve e). The data (histogram) are from Lawrence *et al.* (1986).

Fig. 6.2.5. Taken from Fig. 3. of Franceschini et al. (1988b).

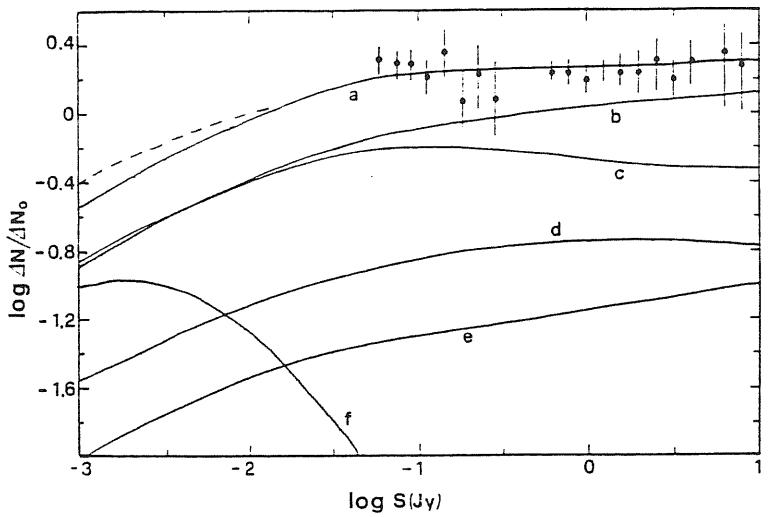

Figure 4. Differential log N–log S at 60 μm, normalized to $\Delta N_0=600\,S^{-2.5}$ (Jy^{-1} sr^{-1}). The data for S_{60} above or below 0.5 Jy are from Rowan-Robinson *et al.* (1986) and from Hacking & Houck (1987), respectively. Curve a shows the predicted counts, sum of the contributions from non-evolving spirals + irregulars (curve b), evolving S/I galaxies (curve c) and Seyferts (curve d), non-evolving E + S0s (curve e). Curve f displays the estimated contribution from primeval disc galaxies shining for a time $\Delta t=2\times10^8$ yr at $z_f=2.5$; the dashed line shows the total counts including them.

Fig. 6.2.6. Taken from Fig. 4. of Franceschini et al. (1988b).

We assume that primeval disc galaxies emit in the far-IR, with a spectrum similar to that S/I galaxies, the bulk of energy released in the production of a solar metal abundance. If the luminosity function of primeval galaxies has the same form as that of normal spirals, and their bright phase occurs at $z_f = 2.5$ and lasts $\Delta t = 2 \times 10^8\ yr$ (consistent with the study of the chemical history of the disc of the Galaxy by Shore, Ferrini and Palla 1987), we obtain the counts shown by curve 'f' in Fig. 6.2.6. In this case, primeval galaxies would be about 100 times brighter than at present, and would start showing up at $S_{60\mu} \simeq 10mJy$: The Infrared Space Observatory, *ISO*, to be launched in the early 1993, should be able to detect a large number of them.

Obviously, higher values of z_f would make primeval galaxies fainter: if $z_f \geq 4$ and $\Delta t \approx 10^8\ yr$, their effect on the $60\mu m$ counts above 1 mJy would be negligible. Note, however, that the evidence of dark haloes around galaxies, extending out to $\geq 100\ kpc$, implies that the disc formation cannot be completed before $z \simeq 2$ or 3 (Rees 1986); direct evidence of low heavy-element abundances in a system at $z = 3.1723$ has been reported by Hunstead et al. (1987).

(3) QSO'S AND POWERFUL RADIO GALAXIES

A crude estimate indicates that radio-loud and radio-quiet QSO's, and powerful radio galaxies, comprise only a small fraction of sources brighter than 1 mJy at $60\mu m$.

Miley and de Grijp (1986) found that only nine (including two doubtful identifications) QSO's ($M_B < -23$) from the Bright Quasar Survey (BQS; Schmidt and Green 1983) have IRAS counterparts (positional coincidence within 30 arcsec); their median apparent magnitude is $B = 15$. Since the BQS covers 3.26 sr, the surface density of QSO's brighter than the IRAS survey limit, $F_{60\mu} \simeq 0.5$ Jy, can be roughly estimated to be $\approx 2.8\, sr^{-1}$, very close

to the surface density of QSO's with $B < 15$ (Schmidt and Green 1983). A very similar result is obtained by combining the optical counts with the distribution of far-IR to optical luminosity ratios of radio-quiet QSO's measured by Neugebauer et al. (1986).

The optical counts of QSO's are very steep (slope of the integral $\log N - \log S \simeq 2.15$) for $B \leq 19.5$, and turn over sharply at fainter magnitudes (Boyle et al. 1987). For a constant mean far-IR to optical luminosity ratio, we would then expect that the QSO contribution to the surface density of extragalactic sources at $60\mu m$ increases from ≈ 0.1 per cent at 0.5 Jy to a maximum of a few per cent at $\simeq 8$ Jy.

The above estimate ignores differences between radio-loud and radio-quiet QSO's. However, if quasars with flat radio spectra have significantly higher far-IR to optical luminosity ratios than radio-quiet ones (Neugebauer et al. 1986), the latter have steeper counts, implying a stronger evolution (cf. e.g. Danese, De Zotti and Franceschini 1985). Thus, radio-loud QSO's are likely to remain a minor fraction of IR-selected quasars, as is the case for $F_{60\mu} > 0.5$ Jy: only one of the 7–9 QSO's detected by IRAS in the region covered by the BQS is radio-loud. This conclusion is confirmed by an extrapolation to $60\mu m$ of the radio counts of QSO's at 1.4 GHz (Windhorst et al. 1985) using a mean ratio between the flux densities at the two frequencies $\langle S_{1.4}/F_{60\mu} \rangle = 30$ found, using both detections and limits, from data on radio-loud QSO's given by Neugebauer et al. (1986).

Powerful radio galaxies [$P(408\,MHz) > 10^{23.5}\,W/Hz/sr$] are weak far-IR emitters. None of the ten such objects in Dressel and Condon's (1978) sample has been detected at $60\mu m$, but the ensuing constraints on the mean far-IR to radio luminosity ratio are uninterestingly weak. The detection rate is very low also for radio galaxies in the bright sample of Wall and Peacock (1985) even if we confine ourselves to those with $S(1.4\,GHz) > 10$ Jy. For the latter objects, an

inspection of *Cataloged Galaxies in the IRAS Survey* (1985), taking into account the completeness limits described in the *IRAS Explanatory Supplement* (1985), yields a conservative upper limit $L_{60\mu}/L_{\nu}(1.4\,GHz) < 0.04$, implying that the contribution of these sources to the $60\mu m$ counts is negligible.

d. Discussion

As already noted above (see 6.2.c.(1)), the predicted number of normal spirals and irregulars is found to exceed that of evolving S/I galaxies at least for $F_{60\mu} > 1\ mJy$, although the relative importance of the latter steadily increases with decreasing flux density: the radio $\Delta N(S/I)/\Delta N(spirals)$ is $\simeq 0.33$ at $10\,Jy$, $\simeq 0.44$ at $1\,Jy$, $\simeq 0.66$ at $0.1\,Jy$, $\simeq 0.93$ at $1\,mJy$. This result may appear strikingly at odd with the result for the radio band, where the contribution of the former class to the counts is found to be always small (Danese et al. 1987).

This apparent discrepancy arises from the combined action of the two effects already mentioned in 6.2.c.(1) [points(ii) and (iii)], i.e. of the slower evolution rate in the far-IR in comparison to the radio, and of the steep far-IR K-correction, which efficiently counters the effect of evolution. Both effect are illustrated by Fig. 6.2.7, which shows how the far-IR counts of S/I galaxies would look if κ_{IR} were equal to κ_R and if the spectral indices in the two bands were equal; the effect of the K-correction is obviously much stronger for the evolving populations than for non-evolving spirals and irregulars.

The present estimates of the counts of Seyfert galaxies are admittedly crude. The assumption of a radio evolution rate equal to that of S/I galaxies is somewhat arbitrary, since the origin of the radio emission may be different in the two classes if objects and, in the case of Seyferts, may be directly related to the nuclear activity (cf. Wilson 1983). On the other hand, for both classes the radio power is well-correlated with the far-IR luminosity (cf. Franceschini et

al. 1988a) and most of the latter, in essentially all type 2 and in a substantial fraction of type 1 Seyferts, is extended and appears to come from dust warmed in actively star-forming regions (Edelson, Malkan and Rieke 1987; Rodriguez Espinosa, Rudy and Jones 1986).

A detailed discussion of the evolution of Seyferts in the far-IR, allowing for a different behaviour of the 'starburst' and of the 'nuclear' components, however, is only of marginal interest here since, as shown by Fig. 6.2.6, the contribution of these objects to the $60\mu m$ counts can be important only in the case of an exceedingly strong cosmological evolution. In the present framework the fraction of Seyferts in the $60\mu m$ counts is ≤ 10 per cent. If these sources do not evolve in the far-IR, they never exceed a few per cent of galaxies (Fig. 6.2.8).

The assumption that the bulk of the ultraviolet light of primeval galaxies is absorbed by dust and re-radiated in the far-IR is probably not too unrealistic. Koo (1986) estimated that the average optical depth may become ≈ 1 when the fraction of metals in the star-forming gas is $\simeq 1/100$th solar; the time-scale for reaching such metal abundance may be only a few million years.

e. Conclusions

The hypothesis that actively star-forming galaxies have undergone significant cosmic evolution is strongly supported by the fact that a model, assuming that their radio luminosities evolve on a time scale $\simeq$ 20–25% of the Hubble time, can account not only for all the data available from the very deep radio surveys so far, but also for all available far-IR data (see Fig. 6.2.5 and Fig. 6.2.6).

We caution, however, that, although encouraging, this fact must not conceal the significant degree of uncertainty inherent in extrapolations from radio

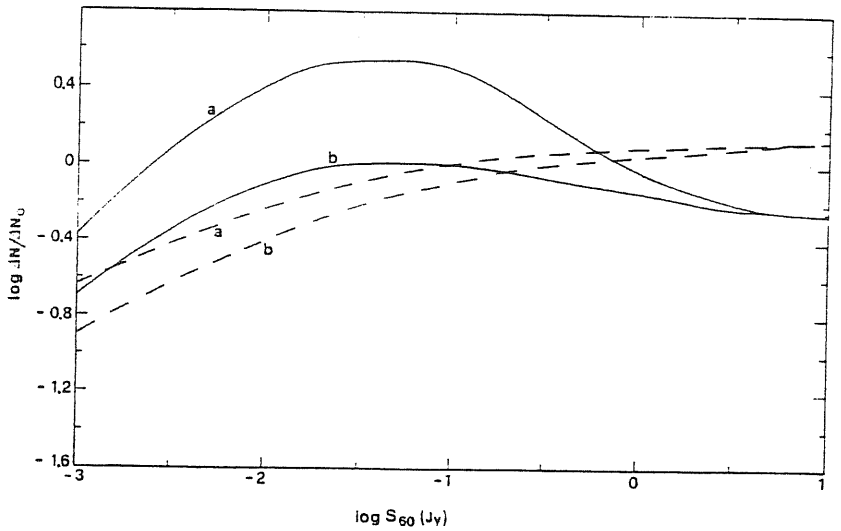

Figure 5. Effects of varying the evolution rate and of the K-correction on the differential $\log N$–$\log S$ relation at $60\,\mu$m. The solid lines show the expected counts of S/I galaxies if they were evolving at the same rate as in the radio band ($\alpha_{1R} = 4.35$) and had a far-IR spectral index $\alpha_{60/25} = 0.7$ [i.e. equal to the radio spectral index: curve (a) or $\alpha_{60/25} = 2.4$ (curve b)]. The dashed lines refer to non-evolving spiral + irregular galaxies and correspond to the same values of $\alpha_{60/25}$ as above.

Fig. 6.2.7. Taken from Fig. 5. of Franceschini et al. (1988b).

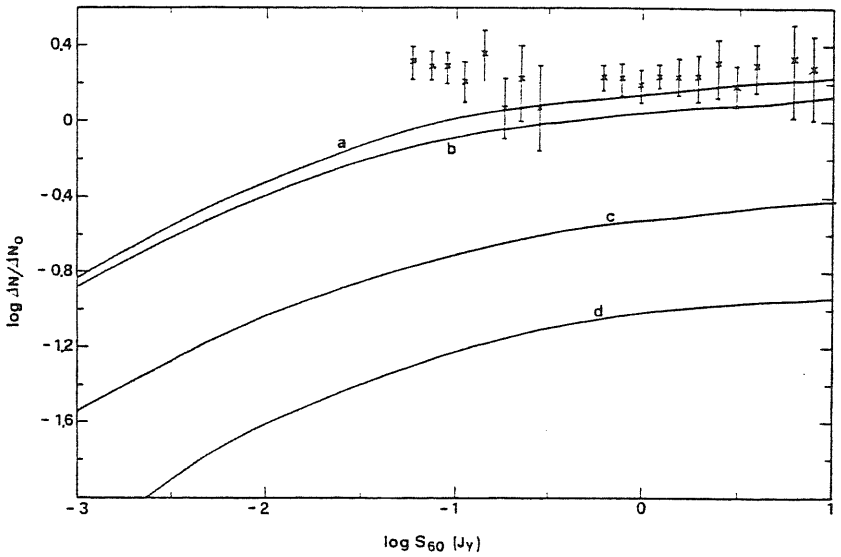

Figure 6. Predicted differential $\log N$–$\log S$ relation without evolution. Curve a gives the total counts, sum of the contributions of unevolving spirals + irregulars (curve b), S/I galaxies (curve c), Seyferts (curve d) and ellipticals + S0s (not shown). The data points are the same as in Fig. 4.

Fig. 6.2.8. Taken from Fig. 6. of Franceschini et al. (1988b).

to far-IR, as a consequence of errors in the local radio luminosity functions and of uncertainties in the relations between far-IR and radio emissions (equations 6.2.3 and 6.2.4). In particular, there are indications that equation (6.2.3) may overestimate the far-IR to radio luminosity ratio at the highest radio luminosities. Also, the predicted counts at faint flux levels depend to some extent on the assumed far-IR spectra: slight differences are expected when replacing the rather crude K-corrections adopted here with more refined ones based on detailed spectral shapes at $\lambda \leq 60\mu m$ (Xu and De Zotti 1988).

The discussion in Section 6.2.d sheds some light on why the available radio and FIR data, taken together, favour a model assuming evolution, but only for a subclass of disc galaxies, not for all of them. A key point is the steepness of the FIR spectra of these sources which entails that the counts of objects at cosmological distances converge faster at $60\mu m$ than at radio frequencies. Such faster convergence is absolutely needed to reconcile radio and FIR data: without it any extrapolation of the radio counts would over-predict by a substantial factor the $60\mu m$ counts. Of course, this requires that the typical redshifts of mJy and sub-mJy radio sources are not too small. Note that this argument works not only against non-evolving models, but also against models letting all disc galaxies evolve. In fact, the latter models obviously minimize (for a given local luminosity function) the amount of evolution needed to match the observed radio counts and, hence, the characteristic redshifts of sources. The K-corrections are , thus, less important, and the predicted FIR counts tend to be too high.

The steepness of the FIR spectra implies that the $60\mu m$ counts of unevolving galaxies are bound to converge quickly, while the observed counts keep a roughly Euclidean slope down to 50mJy: it is, in fact, easy to check that the deep IRAS counts, taken at face value, do entail some cosmological evolution. On the other hand, such counts are liable to systematic errors due, e.g. to confusion or to strong clustering in the small area covered by the survey of

Hacking and Houck (1987). The correlation between radio and FIR emissions of disc galaxies, however, implies that IRAS and radio data cannot be dealt with independently of each other. As discussed above, a consistent picture appears to be possible only in the framework of cosmological evolution.

A powerful test on the model would be provided by redshift distributions of weak sources (Fig. 6.2.9 and Fig. 6.2.10). We expect that evolving S/I and Seyfert galaxies clearly show up in the high-z tail of such distributions. On the other hand, our model predicts that the median redshift of IRAS galaxies brighter than 50 mJy at $60\mu m$ is ≈ 0.1, i.e. substantially lower than that of blue radio sources brighter than ≈ 0.5 mJy at 1.4 GHz, which is probably around 0.75 (Donnelly et al. 1987). By contrast, if the sub-mJy radio source counts could be accounted for by a simple extrapolation of the deep IRAS counts using a FIR luminosity ratio ≈ 100 (cf. e.g. Kellermann and Wall 1987), the two redshift distributions would be very similar.

As shown by Fig. 6.2.6, far-IR surveys might provide important insights on the early evolution of disc galaxies. Simple arguments do indeed suggest that these objects are likely to be cocooned by dust (except for the early phase lasting only a few million years), re-radiating the bulk of their luminosity in the far-IR. There are also good reasons to believe that discs formed at rather low redshifts ($z \simeq 2$ or 3; cf. Section 6.2.c.(2)), so that they could be detectable at flux levels that can be reached by *ISO*.

The source counts discussed in Section 6.2.c allow us also to estimate the contributions to the diffuse far-IR background. At $60\mu m$ we obtain $\simeq 0.02$ MJy/sr from both S/I and spiral+irregular galaxies and $\simeq 0.005$ MJy/sr from Seyferts. If the duration of the bright phase is $\approx$ a few times $10^8\,yr$, the contribution of primeval galaxies ranges from 0.01 MJy/sr for $z_f = 2.5$, to 0.004 MJy/sr for $z_f = 4$. The contributions of 'normal' ellipticals and S0's, of radio galaxies and of quasars are negligibly small.

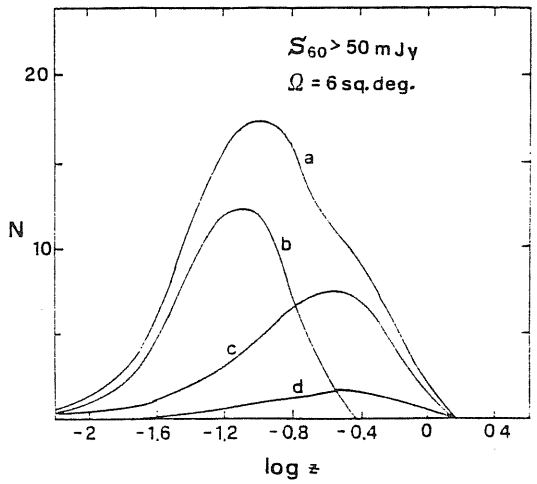

Figure 7. Predicted redshift distribution of sources with S_{60}>50 mJy (curve a). Also plotted are the contributions of unevolving spirals + irregulars (curve b), evolving S/I (curve c) and Seyfert (curve d) galaxies. The ordinates are the expected number of sources in an area of 6 square degrees.

Fig. 6.2.9. Taken from Fig. 7. of Franceschini et al. (1988b).

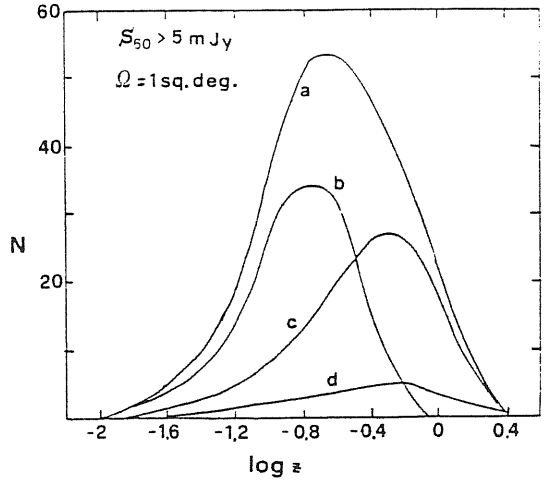

Figure 8. Predicted redshift distribution of sources with S_{60}>5 mJy in an area of 1 square degree. The labels of the curves have the same meaning as in Fig. 7.

Fig. 6.2.10. Taken from Fig. 8. of Franceschini et al. (1988b).

Using the mean spectral index between 100 and $60\mu m$ or between 60 and $25\mu m$ (Table 6.2.1) for non-evolving and for evolving populations, respectively, and assuming that primeval galaxies have a far-IR spectrum similar to S/I galaxies, we obtain an overall contribution at $100\mu m$ of $\approx$ 0.15 MJy/sr, i.e. of only a few per cent of the background intensity (5—6 MJy/sr) tentatively estimated by Rowan-Robinson(1986b). An extragalactic background flux of several MJy/sr may imply energy sources more efficient than thermonuclear reactions in stars.

References

Aaronson, M.: 1977, Ph.D. thesis

Aaronson, M., Cohen, J. G., Mould, J.,Malkan, M.: 1978, *Astrophys. J.* **223**, 824

Allamandola, L. J.: 1984, in *Galactic and Extragalactic IR Spectroscopy*, eds. M. F. Kessler, J. P. Philips

Allen, C. W.: 1976, *"Astrophysical Quantities"*, the Athlone Press

Alloin, D., Bergeron, J., Pelat, D.: 1977, *Astron. Astrophys.* **70**, 141

Arp. H.: 1966, *"Atlas of Peculiar Galaxies"* (Pasadena: California Institute of Technology); also *Astrophys. J. Suppl.* **14**, 123

Augarde, R., Lequeux, J.: 1985, *Astron. Astrophys.* **147**, 273

Baars, J., Hooghoudt, B., Mezger, P. G., de Jonge, M.: 1987, *Astron. Astrophys* **175**, 326

Baldwin, J. A., Phillips, M. M., Terlevich, R.: 1981, *Pub. A. S. P.* **93**, 5

Balkowski, C.: 1973, *Astron. Astrophys.* **29**, 43

Balkowski, C., Chamaraux, P., Weliachew, L.: 1978, *Astron. Astrophys.* **69**, 263

Balzano, V. A.: 1983, *Astrophys. J.* **268**, 602 (B83)

Balzano, V. A., Weedman, D. W.: 1981, *Astrophys. J.* **243**, 756

Barbaro, G., Bertelli, G., Chiosi, C., Nasi, E.: 1973, *Astron. Astrophys.* **29**, 185

Barbaro, G., Chiosi, C., Nobili, L.: 1972, *Astron. Astrophys.* **18**, 186

Belfort, P., Mochkovitch, R., Dennefeld, M.: 1987, *Astron. Astrophys.* **176**, 1

Benvenuti, P., Casini, C., Heidmann, J.: 1979, *Nature* **282**, 272

Benvenuti, P., Casini, C., Heidmann, J.: 1980, *2nd Europ. IUE Conf., Tübingen*, pp.263

Benvenuti, P., Casini, C., Heidmann, J.: 1982, *Monthly Notices Roy. Astron. Soc.* **198**, 825

Bieging, J. H., Biermann, P., Fricke, K. J., Pauliny-Toth, I. I. K., and Witzel, A.: 1977, *Astron. Astrophys.* **60**, 353

Biermann, P.: 1976, *Astron. Astrophys.* **53**, 295

Biermann, P., Clarke, J. N., Fricke, K. J., Pauliny-Toth, I. I., Schmidt, J., Witzel, A.: 1980, *Astron. Astrophys.* **81**, 235

Biermann, P., Fricke, K.: 1977, *Astron. Astrophys.* **54**, 461

Bookbinder, J., Cowie, L. L., Krolik, J. H., Ostriker, J. P., Rees, M. J.: 1980, *Astrophys. J.* **237**, 647

Bottinelli, L., Duflot, R., Gouguenheim, L., Heidmann, J.: 1975, *Astron. Astrophys.* **41**, 61

Bottinelli, L., Gouguenheim, L., Heidmann, J.: 1973, *Astron. Astrophys.* **22**, 281

Boulanger, F., Baud, B., van Albada, G. D.: 1985, *Astron. Astrophys.* **144**, L9

Boulanger, F., Perault, M.: 1986, preprint

Boyle, B. J., Fong, R., Shanks, T., Peterson, B. A.: 1987, *Monthly Notices Roy. Astron. Soc.* **227**, 717

Brinks, E., Klein, U.: 1985, in *Star-forming Dwarf Galaxies*, eds. D. Kunth, T. X. Thuan, J. Tran Thanh Van, pp. 281

Brown, R., Mathews, W.: 1970, *Astrophys. J.* **160**, 939

Burki, G.: 1977, *Astron. Astrophys.* **57**, 135

Caldwell, J. Gott, R., Hart, M.: 1974, unpublished

Campbell, A., Terlevich, R., Melnick, J., Moles, M: 1986, *Monthly Notices Roy. Astron. Soc.* **223**, 811

Casini, C., Heidmann, J.: 1976a, *Astron. Astrophys.* **47**, 371

Casini, C., Heidmann, J.: 1976b, *Astron. Astrophys. Suppl.* **24**, 473

Cataloged Galaxies and Quasars Observed in the IRAS Survey: 1985, prepared by C. J. Lonsdale, G. Helou, J. C. Good, W. L. Rice (Washington: U. S. Government Print Office)

Chini, R., Kreysa, E., Krugel, E.: 1986a, *Astron. Astrophys.* **157**, L1

Chini, R., Krugel, E., Kreysa, E.: 1986b, *Astron. Astrophys.* **166**, L8

Chini, R., Krugel, E., Kreysa, E.: 1986c, *Astron. Astrophys.* **167**, 315

Chini, R., Krugel, E., Wargau, W.: 1987, *Astron. Astrophys.* **181**, 378

Chiosi, C., Summa, C.: 1970, *Astrophys. Sp. Sci.* **8**, 478

Clark, D. H., Caswell, J. L.: 1976, *Monthly Notices Roy. Astron. Soc.* **174**, 267

Clark, D. H., Stenphenson, F. R.: 1982, in *Supernovae: A Survey of Current Research*, eds. M. J. Rees, R. J. Stoneham, pp.355

Condon, J. J., Condon, M. A., Gisler, G., Puschell, J. J.: 1982, *Astrophys. J.* **252**, 102

Condon, J. J., Mitchell, K. J.: 1984, *Astron. J.* **89**, 610

Cox, P., Krugel, E., Mezger, P.G.: 1986, *Astron. Astrophys.* **155**, 380

Cox, P., Mezger, P. G.: 1987, preprint

Crawford, J., Rowan–Robinson, M.: 1986, *Monthly Notices Roy. Astron. Soc.* **221**, 53

Cutri, R.M., Mcalary, C. W.: 1985, *Astrophys. J.* **296**, 90

Danese, L., De Zotti, G., Franceschini, A.: 1985, *Astron. Astrophys.* **143**, 277

Danese, L., De Zotti, G., Fraceschini, A., Toffolatti, L.: 1987, *Astrophys. J.* **318**, L15

de Jong, T., Brink, K.: 1986, in *Star Formation in Galaxies*, ed. C. J. Lonsdale Persson, pp.323

de Jong, T., Clegg, P.E., Soifer, B. T., Rowan-Robinson, M., Habing, H. J., Houck, J. R., Aumann, H. H., Raimond, E.: 1984, *Astrophys. J.* **278**, L67

de Jong, T., Klein, U., Wielebinski, R., Wunderlich, E.: 1985, *Astron. Astrophys.* (Letter) **147**, L6

Dennefeld, M., Karoji, H., Belfort, P.: 1985, in *Star-forming Dwarf Galaxies*, eds. D. Kenth, T. X. Thuan, J. T. Thanh Van, pp.351

Dennefeld, M., Sévre, F.: 1984, *Astron. Astrophys. Suppl.* **57**, 253

de Vaucouleurs, G., de Vaucouleurs, A.: 1964, *Reference Catalogue of Bright Galaxies* (Austin: University of Texas Press).

de Vaucouleurs, G., de Vaucouleurs, A.: 1972, *Monthly Notices Roy. Astron. Soc.* **77**, 1

de Vaucouleurs, G., de Vaucouleurs, A., Corwin, H. G. Jr.: 1976, " *Second Reference Catalogue of Bright Galaxies"*, University of Texas Press

Désert, F. X.: 1986, in *Light on Dark Matter*, ed. F.P. Isreal, pp.213

Deutsch, L. K., Willner, S. P.: 1986, *Astrophys. J. (letter)* **306**, L11

Deutech, L. K., Willner, S. P.: 1987, *Astrophys. J. Suppl.* **63**, 803

Donnelly, R. H., Partridge, R. B., Windhorst, R. A.: 1987, *Astrophys. J.* **321**, 94

Draine, B. T., Anderson, N.: 1985, *Astronphys. J.* **292**, 494

Draine, B. T., Lee, H. M.: 1984, *Astronphys. J.* **285**, 89 (DL84)

Dressel, L. L., Condon, J. J.: 1978, *Astrophys. J. Suppl.* **36**, 53

Duflot-Augarde, R., Alloin, A.: 1982, *Astron. Astrophys.* **112**, 257

Edelson, R. A., Malkan, M. A., Rieke, G. H.: 1987, *Astrophys. J.* in press.

Fabbiano, G., Feigelson, E., Zamorani, G.: 1982, *Astrophys. J.* **256**, 397

Fasano, G.: 1985, *Astron. Astrophys. Suppl.* **60** 285

Feigelson, E. D., Isobe, T., Weedman, D. W.: 1987, *Astrophys. J.* (Letter) **319**, L51

Feigelson, E. D., Nelson, P. I.: 1985, *Astrophys. J.* **293**, 192

Feldman, F. R., Weedman, D. W., Balzano, V. A., Ramsey, L. W.: 1982, *Astrophys. J.* **256**, 427

Fitt, A. J., Alexander, P., Cox, M. J.: 1988, *Monthly Notices Roy. Astron. Soc.* **233**, 907

Fomalont, E. B., Kellermann, K. I., Wall, J. V., Weistrop, D.: 1984, *Science*, **225**, 23

Franceschini, A., Danese, L., De Zotti, G., Toffolatti, L.: 1988a, *Monthly Notices Roy. Astron. Soc.* **233**, 157

Franceschini, A., Danese, L., De Zotti, G., Xu, C.: 1988b, *Monthly Notices Roy. Astron. Soc.* **233**, 175

French, H. B.: 1980, *Astrophys. J.* **240**, 41

Frogel, J. A., Persson, S. E., Aaronson, M., Matthews, K.: 1978, *Astrophys. J.* **223**, 824

Garmany, C. D., Conti, P. E.: 1982, *Astrophys. J.* **263**, 777

Gavazzi, G., Cocito, A., Vettolani, G.: 1986, *Astrophys. J.* **305**, L15

Gehrz, R. D., Sramek, R. A., Weedman, D. W.: 1983 *Astrophys. J.* **267**, 551

Ghosh, S. K., Drapatz, S.: 1987, in *Polycyclic Aromatic Hydrocarbons and Astrophysics*, eds. A. Léger, L. d'Hendecourt, N. Boccara, pp.317

Giaconni, R., et al.: 1979, *Astrophys. J.* **230**, 540

Gioia, I. M., Gregorini, L., Klein, U.: 1982, *Astron. Astrophys.* **116**, 164

Gott, J. R., Turner, E. L.: 1977, *Astrophys. J.* **213**, 309

Gottesman, S. T., Weliachew, L.: 1972, *Astrophys. Letters* **12**, 63

Gull, S. F.: 1973, *Monthly Notices Roy. Astron. Soc.* **161**, 47

Güsten, R. Mezger, P.G.: 1982, *Vistas in Astronmy*, **26**, 159

Habing, H. J., Israel, F. P.: 1979, *Ann. Rev. Astron. Astophys.* **17** 345

Hacking, P., Houck, J. R.: 1987, *Astrophys. J. Suppl.* **63**, 311

Harris, G. H.: 1976, *Astrophys. J. Suppl.* **30**, 415

Hartmann, W.: 1970, *Mém. Soc. Roy. Sci. Liége* 19, 49

Hawarden, T. G., Mountain, C. M., Leggett, S. K., Puxley, P. J.: 1986, *Monthly Notices Roy. Astron. Soc.* **221**, 41

Heidmann, J., Klein, U.,Wielebinski, R.: 1982, *Astron. Astrophys.* **105**, 188

Helou, G.: 1986, *Astrophys. J.* **311**, L33

Helou, G., Soifer, B. T., Rowan-Robinson, M.: 1985, *Astrophys. J.* **298**, L7

Henning, K., Wendker, H. J.: 1975, *Astron. Astrophys.* **44**, 91

Houck, J. R., Schneider, D. P., Danielson, G. E., Beichman, C. A., Lonsdale. C. J., Neugebauer, G., Soifer, B. T.: 1985, *Astrophys. J.* **290**, L5

Huchra, J. P.: 1977a, *Astrophys. J. Suppl.* **35**, 171 (H77a)

Huchra, J. P.: 1977b, *Astrophys.J.* **217**, 928

Huchra, J. P.: 1987, preprint.

Huchra, J. P., Davis, M., Latham, D., Tonry, J.: 1983a, *Astrophys. J. Suppl.* **52**, 89

Huchra, J. P., Geller, M. J., Gallagher, J., Hunter, D., Hartmann, L., Fabbiano, G., Aaronson, M.: 1983b, *Astrophys. J.* **274**, 125

Iben, I.: 1965, *Astrophys. J.* **142**, 1447

Iben, I.: 1966a, *Astrophys. J.* **143**, 483

Iben, I.: 1966b, *Astrophys. J.* **143**, 505

Iben, I.: 1966c, *Astrophys. J.* **143**, 516

Iben, I.: 1967a, *Astrophys. J.* **142**, 624

Iben, I.: 1967b, *Astrophys. J.* **147**, 650

"IRAS Catalogues and Atlas Explanatory Supplement": 1985, eds. C. A. Beichman, G. Neugebaur, H. J. Habing, P. E. Clegg, T. J. Chester (Washington: U.S. Government Printing Office)

"IRAS Point Source Catalog": 1985, Joint IRAS Science Working Group, (Washington: U.S. Government Printing Office)

Israel, F. P.: 1976, Ph. D. thesis

Isobe, T., Feigelson, E. D., Nelson, P. I.: 1986, *Astrophys. J.* **306**, 490

Johnson, H. L.: 1966, *Ann. Rev. Astron. Astrophys.* **4**, 193

Joseph, R. D., Meikle, W. P. S., Robertson, N. A., Wright, Q. S.: 1984, *Monthly Notices Roy. Astron. Soc.* **157**, 309

Jura, M.: 1982, *Astrophys. J.* **254**, 70

Keel, W. C.: 1980, *Astron. J.* **85**, 198

Keel, W. C., Kennicutt, R. C. Jr., Hummel, E., Yan den Hulst, J. M.: 1985, *Astron. J.* **89**, 708

Kellermann, K. I., Wall, J. V.: 1987, in *Observational Cosmology, IAU Symp. No. 124*, eds. A. Hewitt, G. Burbidge, L. Z. Fang, pp.545 (Reidel, Dordrecht, Holland)

Kennicutt, R. C.: 1983, *Astrophys. J.* **272**, 54

Kennicutt, R. C. Jr., Keel, W. C.: 1984, *Astrophys. J. (Letters)* **279**, L5

Kinman, T. D., Davidson, K.: 1981, *Astrophys. J.* **243**, 127

Klein, U., Wielebinski, R., Thuan, T. X.: 1984, *Astron. Astrophys.* **141**, 241

Kojoian, G., Tovmassian, H. M., Deckinson, D. F., Dinger, A.: 1980, *Astron. J.* **85**, 1462

Koo, D. C.: 1986, in *Spectral Evolution of Galaxies*, eds. C. Chiosi, A. Renzini, pp.419 (Reidel, Dordrecht, Holland)

Kreysa, E.: 1985, in *Proc. URSI Symp. on mm and submm wave radio astronomy*, (Granada 11.-14. 9. 84) pp.153

Kron, R. G., Koo, D. C., Windhorst R. A.: 1985, *Astron. Astrophys.* **146**, 38

Krügel, E., Chini, R., Kreysa, E., Sherwood, W. A.: 1988a, *Astron. Astrophys.* **190**, 47

Krügel, E., Chini, R., Kreysa, E., Sherwood, W. A.: 1988b, *Astron. Astrophys.* **193**, L16

Kunth, D., Martin, J. M., Maurogordato, S., Vigroux, L.: 1985, in *Star-forming Dwarf Galaxies*, eds. D. Kunth, T. X. Thuan, J. T. Thanh Van, pp.89

Kunth, D., Sévre, F.: 1985, in *Star-forming Dwarf Galaxies*, eds. D. Kunth, T. X. Thuan, J. T. Thanh Van, pp.331

Lang, K.: 1980, *Astrophysical Formulae*, Springer–Verlag Berlin Heideberg

Larson, R. B., Tinsley, B. M.: 1978, *Astrophys. J.* **219**, 46 (LT78)

Lawrence, A., Rowan-Robinson, M., Saunders, W., Efastathiou, G., Kaiser, N. Ellis, G., Frenck, C.: 1987, Preprint.

Lawrence, A., Walker, D., Rowan-Robinson, M., Leech, K. J., and Penston, M. V.: 1986 *Monthly Notice Roy. Astron. Soc.* **219**, 687

Lawrence, A., Ward, M., Elvis, M., Fabbiano, G., Willner, S. P., Carleton, N. P., Longmore, A.: 1985, *Astrophys. J.* **291**, 117

Lawrence, C. J., Persson, S. E., Matthews, K.: 1984, *Astrophys. J.* **287**, 95

Léger, A., Puget, J. L.: 1984, *Astron. Astrophys.* **137**, L5

Léger, A., d'Hendecourt, L.: 1987, in *Polycyclic Aromatic Hydrocarbons and Astrophysics*, eds. A. Léger, L. d'Hendecourt, N. Boccara.

Lequeux, J., Peimbert, M., Rayo, J. F., Serrano, A., Torres-Peimbert, S.: 1979, *Astron. Astrophys.* **80**, 155

Lequeux, J., Viallefond, F.: 1980, *Astron. Astrophys.* **91**, 269

Lonsdale Persson, C. J., Helou, G.: 1987, *Astrophys. J.* **314**, 513

Lonsdale, C. J., Persson, E. S.,Matthews, K.: 1984, *Astrophys. J.* **287**, 95

Loose, H-H., Thuan, T. X.: 1985, in *Star-forming Dwarf Galaxies*, eds. D. Kunth, T. X. Thuan, J. Tran Thanh Van, pp.73

Markarian, B. E.: 1963, *Soob. Byur. Obs.* **34**, 3

Markarian, B. E.: 1967, *Astrofizika* **3**, 55

Markarain, B. E.: 1969, *Astrofizika* **5**, 443; 581

Markarain, B. E.: 1972, *Astrofizika* **8**, 165

Markarian, B. E., Lipovetskii, V. A.: 1971, *Astrofizika* **7**, 511

Markarain, B. E., Lipovetskii, V. A.: 1972, *Astrofizika* **8**, 155

Markarain, B. E., Lipovetskii, V. A.: 1973, *Astrofizika* **9**, 487

Markarain, B. E., Lipovetskii, V. A.: 1974, *Astrofizika* **10**, 307

Markarain, B. E., Lipovetskii, V. A.: 1976a, *Astrofizika* **12**, 389

Markarain, B. E., Lipovetskii, V. A.: 1976b, *Astrofizika* **12**, 687

Markarian, B. E., Lipovetskii, V. A., Stepanyan, D. A.: 1977a, *Astrofizika* **13**, 225

Markarian, B. E., Lipovetskii, V. A., Stepanyan, D. A.: 1977b, *Astrofizika* **13**, 397

Markarain, B. E., Lipovetskii, V. A., Stepanyan, D. A.: 1979a, *Astrofizika* **15**,

201

Markarain, B. E., Lipovetskii, V. A., Stepanyan, D. A.: 1979b, *Astrofizika* **15**, 363

Markarain, B. E., Lipovetskii, V. A., Stepanyan, D. A.: 1979c, *Astrofizika* **15**, 549

Markarian, B. E., Lipovetskii, V. A., Stepanian, D. A.: 1981, *Astrofizika* **17**, 619

Mathis, J. S., Rumpl, W., Nordsieck, K. H.: 1977, *Astrophys. J.* **217**, 425 (MRN77)

Mathis, J. S., Mezger, P. G., Panagia, N.: 1983, *Astron. Astrophys.* **128**, 212 (MMP83)

Mazzarella, J. M., Balzano, V. A.: 1986, *Astrophys. J. Suppl.* **62**, 751 (MB86)

Melnick, J.: 1985, in *Star-forming Dwarf Galaxies*, eds. D. Kunth, T. X. Thuan, J. Tran Thanh Van, pp.171

Mezger, P. G.: 1978, *Astron. Astrophys.* **70**, 565

Mezger, P. G., Mathis, J. S., Panagia, N.: 1982, *Astron. Astrophys.* **105**, 372

Mihalas, D.: 1978, *Stellar Atmospheres*, W. H. Freeman and Company.

Mihalas, D., Binney J.: 1981, *Galactic Astronomy–Structure and Kinematics*, W. H. Freeman and Company.

Miley, G., de Grijp, R.: 1986, in *Light on Dark Matter*, ed. F. P. Israel, pp.471 (Reidel, Dordrecht, Holland)

Miller, G. E., Scalo, J. M.: 1979, *Astrophys. J. Suppl.* **41**, 533

Mochkovitch, R., Rocca-Volmerange, B.: 1984, *Astron. Astrophys.* **32**, 269

Neugebauer, G., Becking, E. E., Oke, J. B., Searle, L.: 1976, *Astrophys. J.* **205**, 29

Neugebauer, G., Habing, H. J., van Duinen, R., Aumann, H. H., Baud, B., Beichman, C. A., Beintema, D. A., Boggess, N., Clegg, P. E., de Jong, T., Emerson J. P., Gautier, T. N., Gillett, F. C., Harris, S., Hauser, M. G., Houck, J. R., Jennings, R. E., Low, F. J., Marsden, P. L., Miley, G., Olnon, F. M., Pottasch, S. R., Raimond, E., Rowan-Roninson, M., Soifer, B. T., Walker, R. G., Wesselius, P. R., Young E.: 1984, *Astrophys. J.* **278**, L1

Neugebauer, G., Miley, G. K., Soifer, B. T., Clegg, P. E.: 1986, *Astrophys. J.* **308**, 815

Nilson, P.: 1983, *Uppsala General Catalogue of Galaxies*, Uppsala Astronomical Observatory, Uppsala.

Nordsieck, K. H.: 1973, *Astrophys. J.* **184**, 735

O'Connell, R. W., Thuan, T. X., Goldstein, S. J.: 1978, *Astrophys. J.* (Letters) **226**, L11

Oort, M. J. A.: 1987, *Astron. Astrophys.* **188**, 266

Oort, M. J. A., Windhorst, R. A.: 1985, *Astron. Astrophys.* **145**, 405

Pajot, P., Boissé, P., Gispert, R., Lamasse, J. M., Puget, J. L., Serra, G.: 1986, *Astron. Astrophys.* **157**, 393

Panagia, N.: 1973, *Astron. J.* **78**, 929

Partridge, R. B., Hilldrup, K. C., Ratner, M. I.: 1986, *Astrophys. J.* **308**, 46

Persic, M., De Zotti, G., Danese, L., Palumbo, G., Franceschini, A., Boldt, E. A., Marshall, F. E.: 1988, submitted to Astrophys. J.

Puget, J. L., Léger, A., Boulanger, F.: 1985, *Astron. Astrophys.* **142**, L19

Puget, J. L.: 1987, in *Polycyclic Aromatic Hydrocarbons and Astrophysics*, eds. A. Léger, L. d'Hendecourt, N. Boccara, pp.303

Puxley, P. J., Hawarden, T. G., Mountain, C. M.: 1988, *Monthly Notices Roy. Astron. Soc.* **231**, 465

Reddish, V. C.: 1976, *"Star Formation"*, Pergamon Press

Rees, M.: 1986, in *Quasars, IAU Symp. No. 119*, eds. G. Swarup, V. K. Kapahi, Reidel, Dordrecht, Holland, pp.1

Rees, M. J.: 1984, *Ann. Rev. Astr. Astrophys.* **22**, 471

Rieke, G. H.: 1988, *Astrophys. J.* **331**, L5

Rieke, G. H., Lebofsky, M. J.: 1979, *Ann. Rev. Astr. Astrophys.* **17**, 477

Rieke, G. H., Lebofsky, M. J.: 1980, in *Objects of High Redshift*, Proc. IAU Symp. No. 92, eds. G. O. Abell, P. J. E. Peebles

Rieke, G. H., Lebofsky, M. J.: 1986, *Astrophys. J.* **304**, 326

Rieke, G. H., Lebofsky, M. J., Thompson, R. I., Low, F. J., Tokunaga, A. T.: 1980, *Astrophys. J.* **238**, 24

Rieke, G. H., Low, F. J.: 1972, *Astrophys. J.* (Letters) **176**, L95

Rieke, P. J., Low, F. T.: 1975, *Astrophys. J.* **197**, 17

Robertson, J. W.: 1972, *Astrophys. J.* **177**, 473

Rodriguez Espinosa, J. M., Rudy, R. J., Jones B.: 1986, *Astrophys. J.* **309**, 76

Rowan-Robinson, M.: 1979, *Astrophys. J.* **234**, 111

Rowan-Robinson, M.: 1980, *Astrophys. J. Supp.* 44, 403

Rowan-Robinson, M.: 1982a, in *Submilimeters Astronomy*, eds. Philips and Beckman.

Rowan-Robinson, M.: 1982b, *Monthly Notices Roy. Astron. Soc.* **200**, pp.197

Rowan-Robinson, M.: 1986a, in *Star Formation in Galaxies*, ed. C. J. Lonsdale Persson, pp.507

Rowan-Robinson, M.: 1986b, *Monthly Notices Roy. Astron. Soc.* **219**, 737

Rowan-Robinson, M., Clegg, P. E., Beichman, C. A., Neugebauer, G., Soifer, B. T., Aumann, H. H., Beintema, D. A., Boggess, N., Emerson, J. P., Gautier, T. N., Gillett, F. T., Hauser, M. G., Houck, J. T., Low, F. J., Walker, R. G.: 1984 *Astrophys. J.* **278**, L7

Rowan-Robinson, M., Crawford, J.: 1986, in *Ligt on Dark Matter*, eds. F.P. Israel, pp.421

Rowan- Robinson, M., Walker, D., Chester, T ., Fairclough, J.: 1986, *Monthly Notices Roy. Astron. Soc.* **219**, 273

Sandage, A., Tammann, G. A.: 1981, *"A Revised Shapley-Ames Catalog of Bright Galaxies"*, Carnegie Institution of Washington Publication, No. 635

Sanders, D. B., Soifer, B. T., Elias, J. H., Madore, B. F., Matthews, K., Neugebauer, G., Scoville, N. Z.: 1988, *Astrophys. J.* **325**, 74

Sanders, D. B., Soifer, B. T., Neugebauer, G., Svovill, N. Z., Madore, B.: 1987, in *Star Formation in Galaxies*, ed. C. J. Lonsdale Persson, pp.411 (Washington, DC: US Govt. Print. Off.)

Sargent, W. L. W.: 1970, *Astrophys. J.* **159**, 765

Sargent, W. L. W.: 1972,*Astrophys. J.* **173**, 7

Sargent, W. L. W., Searle, L.: 1970, *Astrophys. J. (letters)* **162**, L115

Scalo, J. M.: 1986, *Fund. Cos. Phys.* **11**, 1

Schechter, P.: 1973, *unpulished*

Schlesinger, B.: 1972, *Astron. J.* **77**, 584

Schmidt, M., Green, R. F.: 1983, *Astrophys. J.* **269**, 352

Schmitt, J. H. M. M.: 1985, *Astrophys. J.* **293**, 178

Searle, I.: 1971, *Astrphys. J.* **168**, 327

Searle, I., Sargent, W. L. W.: 1972, *Astrphys. J.* **173**, 25

Searle, L., Sargent, W. L. W., Bagnuolo, W. G.: 1973, *Astrophys. J.* **179**, 427

Sekiguchi, K.: 1986, in *Star Formation in Galaxies*, ed. C. J. Lonsdale Persson, pp.507

Sellgren, K.: 1984, *Astrophys. J.* **277**, 623

Shore, S. N., Ferrini, F., Palla, F.: 1987, *Astrophys. J.* **316**, 663

Shuder, J. M., Osterbrock, D. E.: 1981, *Astrophys. J.* **250**, 55

Smith, L. F., Biermann, P., Mezger, P. G.: 1978, *Astron. Astrophys.* **66**, 65

Smith, B. J., Kleinmann, S. G., Huchra, J. P., Low, F. J.: 1987, *Astrophys. J.* **318**, 161

Sodroski, T. J., Dwek, E., Hauser, M. G., Kerr, F. J.: 1987, *Astrophys. J.* **322**, 101

Soifer, B. T., Houck, L. R., Neugebauer, G.: 1987a, *Ann. Rev. Astron. Astrophys.* **25**, 187

Soifer, B. T., Rowan-Robinson, M., Houck, J. R., de Jong, T., Neugebauer, G., Aumann, H. H., Beichman, C. A., Boggess, N., Clegg, P. E., Emerson, J. P., Gillet, F. C., Habing, H. J., Hauser, M. G., Low, F. J., Miley, G., Young, E.: 1984 *Astrophys. J.* **278**, L71

Soifer, B. T., Sanders, D. B., Madore, B. F., Neugebauer, G., Danielson, G. E.,

Elias, J. H., Persson, C. J., Rice, W. L.: 1987b, *Astrophys. J.* **320**, 238

Soifer, B. T., Sanders, D. B., Neugebauer, G., Danielson, G. E., Lonsdale, C. J., Madore, B. F., Persson, S. E.: 1986, it Astrophys. J. **303**, L41

Sramek, R. A., Tovmassian, H. M.: 1975, *Astrophys. J.* **196**, 339

Sramek, R. A., Tovmassian, H. M.: 1976, *Astrophys. J.* **207**, 725

Sramek, R. A., Weedman, D.: 1986, *Astrophys. J.* **302**, 640-649

Struck-Marcell, C., Tinsley, B. M.: 1978, *Astrophys. J.* **221**, 562-566

Sulentic, J. W.: 1976,*Astron. J.* **81**, 582

Telesco, C. M., Becklin, E. E., Wynn-Willims, C. G., Harper, D. A.: 1984, *Astrophys. J.* **282**, 427

Telesco, C. M., Harper, D. A.: 1980, *Astrophys. J.* **235**, 392

Thuan, T. X.: 1983, *Astrophys. J.* **268**, 667

Thuan, T. X., Martin, G. E.: 1981, *Astrophys. J.* **247**, 823

Tinsley, B: 1972, *Astron. Astrophys.* **20**, 383

Toffolatti, L., Franceschini, A., De Zotti, G., Danese, L.: 1987, *Astron. Astrophys.* **184**, 7

Toomre, A., Toomre, J.: 1972, *Astrophys. J.* **178**, 623

Ulvestad, J. S.: 1982, *Astrophys. J.* **259**, 96

van der Laan, H., Katgert, P., Oort, M. J. A.: 1986, in *Structure and Evolution of Active Galactic Nuclei*, eds. G. Giuricin, F. Mardirossian, M. Mezzetti, M. Ramella (Dordrecht: Reidel), pp.437

ven den Bergh, S. 1975, *Ann. Rev. Astr. Astrphys.* **13**, 217

ven den Heuvel, E. P. J.: 1980, *X-ray Astronomy*, Proc. NATO Advanved Study Institute, Erice, Sicily, July 1-14, 1979; eds. R. Giancconi, G. Setti (Dordrecht: Riedel), p.119

Veron-Cetty, M. -P., Veron, P.: 1985, *ESO Scientific Report* No. 4.

Viallefond, F., Thuan, T. X.: 1983, *Astrophys. J.* **289**, 444

Wall, J. V., Benn, C. R., Grueff, G., Vigotti, M.: 1986, *Highlts Astron.*, **7**, 355

Wall, J. V., Peacock, J. A.: 1985, *Monthly Notices Roy. Astron. Soc.* **216**, 173

Wasilewski, A. J.: 1983, *Astrophys. J.* **272**, 68-83

Weedman, D. W.: 1972, *Astrophys. J.* **171**, 5

Weedman, D. W.: 1973, *Astrophys. J.* **183**, 29

Weedman, D. W.: 1983, *Astrophys. J.* **266**, 479

Weedman, D. W.: 1985, *Bull. A. A. S.* **17**, 846

Weedman, D. W., Feldman, F. R., Balzano, V. A., Ramsey, L. W.: 1981, *Astrophys. J.* **248**, 105

Whitemore, B. C., Kirshner, R. P.: 1981, *Astrophys. J.* **250**, 43

Whitemore, B. C., Kirshner, R. P., Schechter, P. L.: 1979, *Astrophys. J.* **234**, 68

Wielen, R.: 1974, in *Highlights of Astronomy*, Vol.3, ed: G. Contopoulos (Dordrecht: Reidel), p.395

Willner, S. P.: 1984, *Galactic and Extragalactic IR Spectroscopy*, eds. M. F. Kessler, J. P. Philips

Wilson, A. S.: 1983, *Highlts Astron.* **6**, 467

Windhorst, R. A.: 1984, Ph.D. thesis, University of Leiden

Windhorst, R. A., Dressler, Koo, D. C.: 1987, in *Cosmology, IAU Symp. No. 124*, eds. A. Hewitt, G. Burbidge, L. Z. Fang, pp.573

Windhorst, R. A., Miley, G. K., Owen, R. N., Kron, R. G., Koo, D. C.: 1985, *Astrophys. J.* **289**, 494

Windhorst, R. A., van Heerde, G. M., Katgert, P.: 1984, *Astron. Astrophys. Suppl.* **58**, 1

Wood, K. S., et al.: 1984, *Astron. Astrophys. Suppl.* **56**, 507

Wright, A. E.: 1972, *Monthly Notices Roy. Astron. Soc.* **157**, 309

Xu, C., De Zotti: 1988, in preparation.

Xu, C., De Zotti, G., Franceschini, A., Danese, L.: 1988, *Astro. Astronphys.* **196**, 59

Yorke, H. W.: 1986, *Ann. Rev. Astron. Astrophys.* **24**, 49

Ziólkowski, J.: 1972, *Acta. Astron.* **22**, 327

Zwicky, F.: 1971, *Catalogue of Selected Compact Galaxies and of Posteruptive Galaxies* (Guemligen, Switzerland: F. Zwicky)

Zwicky, F., Herzog, E., Wild, P., Karpowicz, M., Kowal, C.: 1961-1968, *"Catalogue of Galaxies and of Clusters of Galaxies"* (Pasadena: California Institute of Technilogy)